Aalborg University

Master's Thesis

Mathematics-Economics

A study of the Danish economy during the Covid-19 pandemic and the socioeconomic conditions that influence the severity of the pandemic

Jens K.R. Jensen • Mads Hovaldt • Qi Yao

FIN Group 1.204c

June 2, 2022

AALBORG UNIVERSITET
STUDENTERRAPPORT

Title:

A study of the Danish economy during the Covid-19 pandemic and the socioeconomic conditions that influence the severity of the pandemic

Topics:

Time Series Analysis
Panel Data Study

Project period:

February 1st, 2022 - June 3rd, 2022

Project group:

FIN Group 1.204c

Participants:

Jens Kramer Rold Jensen

Mads Hovaldt

Mads Hovaldt

Qi Yao

Supervisor: Esben Høg

Fifth year w/
Department of Mathematical Sciences
Mathematics-Economics
Skjernvej 4A
9220 Aalborg Ø
http://www.studerende.math.aau.dk/

Abstract:

This thesis evaluates the effects the Covid-19 pandemic has had across Denmark in two primary categories.
The first category uses a panel data framework to make an evaluation of how the spread rate of the virus has been affected by certain socioeconomic conditions and policy interventions. We find that regions with higher percentages of service oriented jobs, populations with many children and regions with low square meters per citizen in urbanized areas suffer are bigger increase in spread rate. Additionally, we find that policy interventions to prevent the spread of the virus have a better effect on regions with high percentages of service oriented jobs and populations with many children.
The second category uses a regime-switching GARCH framework to evaluate the Danish economy before and during the pandemic, the study uses the OMX C25 index as an indicator for the Danish economy. We find that the there is a 32% increase in mean conditional volatility during the pandemic.
Additionally, we make capitalization-weighted indices for each Danish region to evaluate if their volatility increase is similar to the general increase in the OMX C25 and to assess if the increase is homogeneous across regions. We find that all regional indices are affected by the pandemic, some more than others.

Page count: 89
Appendix pages: 76 - 89

By signing this document, each member of the group confirms participation on equal terms in the process of writing the project. Thus, each member of the group is responsible for the all contents in the project.

Preface

The following programs was used in the writing of this report

- **Overleaf** - Writing.
- **R** - Statistical calculations and data analysis.

Noticable **R** packages used in this project include: `tidyverse`, `MSGARCH`, `splm` and `plm`. Other packages has been used in lesser extent.

The bibliography on page 75 presents the literature used in the project. The sources in the bibliography are given in the following format:

[Author][Year][Title](Institution)(URL)

Where fields in [square brackets] are mandatory, while regular parenthesis only are relevant for certain formats (e.g. books or web pages). The bibliography entries are sorted after the appearance in the text.

Appendices can be found following the bibliography.

Reader's Guide:

On page vi, a table of contents is given. When viewing this report as a PDF, hyperlinks in the table of content will allow fast navigation to the desired section.

Due to the nature of this study the project can be read in to ways, from start to finish or topic-wise. Section 2.1, 3 and 5.1 focuses on panel data while section 2.2, 4 and 5.2 focuses on regime switching time series modeling.
So the project can be read either from start to the end or by topic, this is illustrated by the flowchart seen in figure 1 on the next page.

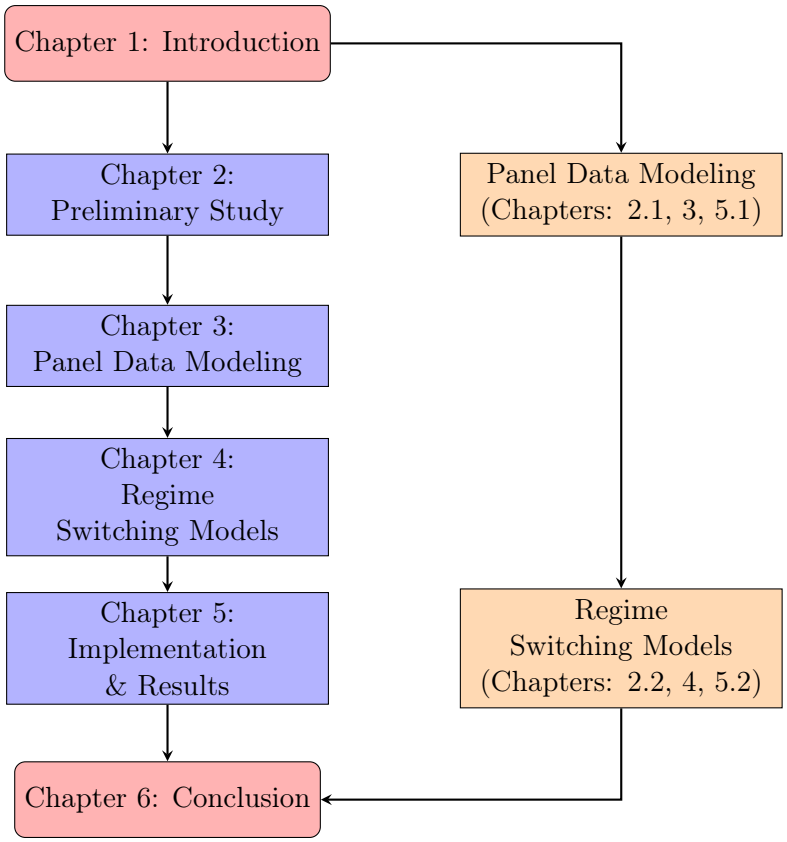

Figure 1. Reading flowchart.

Contents

Chapter 1

Introduction

Since the start of the Covid-19 pandemic, governments across the globe have been deploying countermeasures to prevent exacerbation of public health and their national economies. The disruptive nature of the pandemic has caused specialists with different areas of expertise and nations to collaborate in spectacular ways; nations continuously broadcasting Covid-19 related statistics worldwide, scientists developing proactive and reactive therapies to limit the spread of the virus and severity of the illness in record time and epidemiologists developing models to improve the understanding of the virus's characteristics.

The World Health Organization (WHO) has throughout the pandemic encouraged nations to take action against the spread of the virus through stringency policies; fitting degrees of lockdown, banning social events, setting up sanitary facilities in public places, etc. In addition to exercising these measures, nations have employed economically stimulating measures like salary compensation, subsidizing cost of canceled events, etc. to prevent their economies from exacerbating. KPMG [2020] and Li and Kapri [2021] investigates two key figures of Covid-19, the spread and death rate of the virus, by analyzing the effects of these political interventions and other relevant socioeconomic indicators in 183 different nations.
Oxford University has created the Oxford Covid-19 Government Response Tracker (OxCGRT) database that contains 18 standardized variables that measure degrees of policy interventions, additionally, using the 18 variables they have created various indices that each capture specific characteristic of the policy responses, e.g. their stringency index is made by aggregating various policies that aims to reduce spread of the virus, the economic support index is made by aggregating policies that stimulate the economy [Oxford, 2022].

The status quo after 2 years with the pandemic is looking bright as nations are recovering from the stagnant fiscal year of 2020. However, the pandemic has also brought daunting socioeconomic issues; decrease in public mental health, health systems under critical pressure or failing altogether, social and political polarization, etc. So by achieving a deeper understanding of the relation of socioeconomic indicators and political interventions on the Covid-19 key figures, it becomes easier to understand and prevent some of these issues.

Even for a small country, such as Denmark, within country specific variables such as population density causes different rates of spread, figure 1.1 and 1.2 below emphasizes this, they show the amount of people and the amount of people per million citizens admitted to the hospital due to Covid-19 related health problems in each region of Denmark.

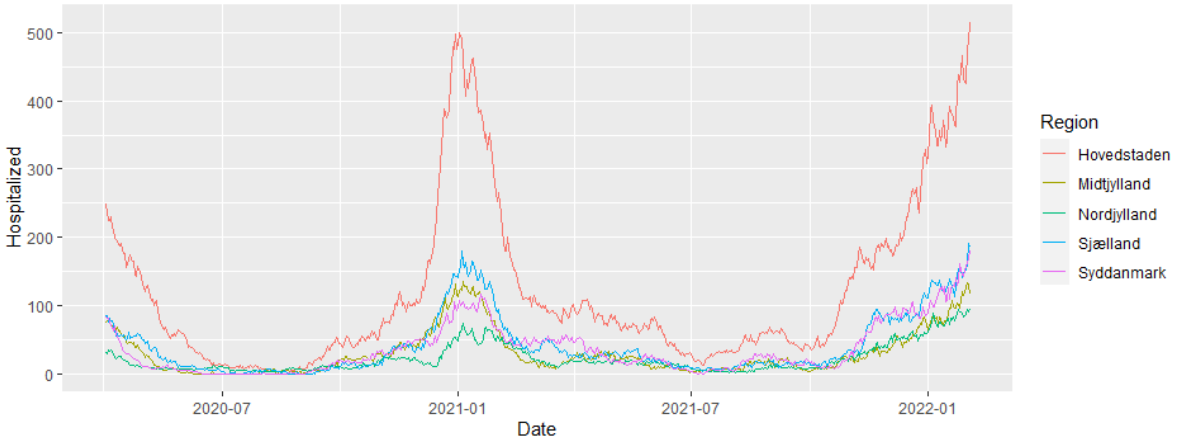

Figure 1.1. Hospitalized per region.

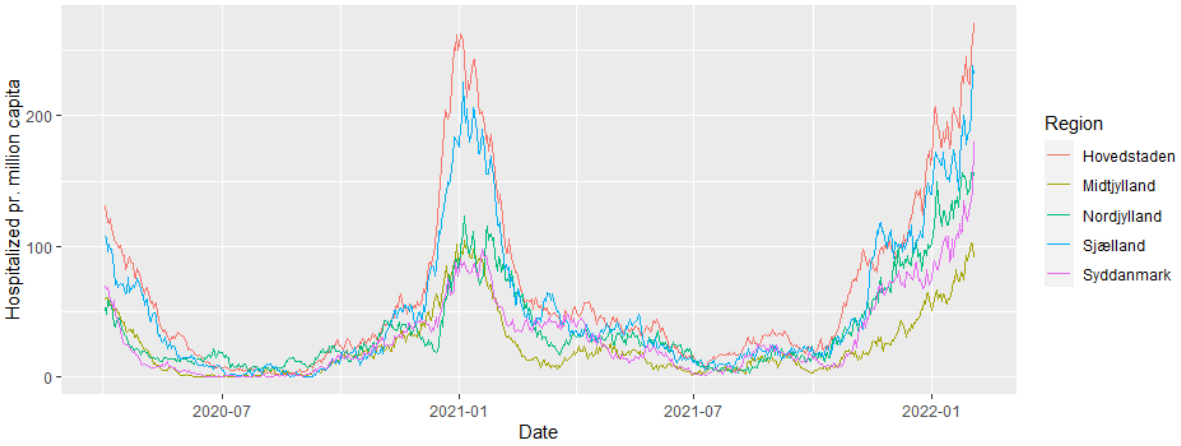

Figure 1.2. Hospitalized per capita per region.

Comparing the two figures it is clearly seen that even when accounting for the different population size for each region, as seen in figure 1.2, there is a clear difference between the regions. These findings emphasizes that while the entirety of Denmark has been affected by the Covid-19 pandemic, not all regions have been equally affected.

Denmark has several levels of divisions including the regional- and municipality-vise levels, where each region is a collection of municipalities. Figure 1.3 below shows divisions of Denmark.

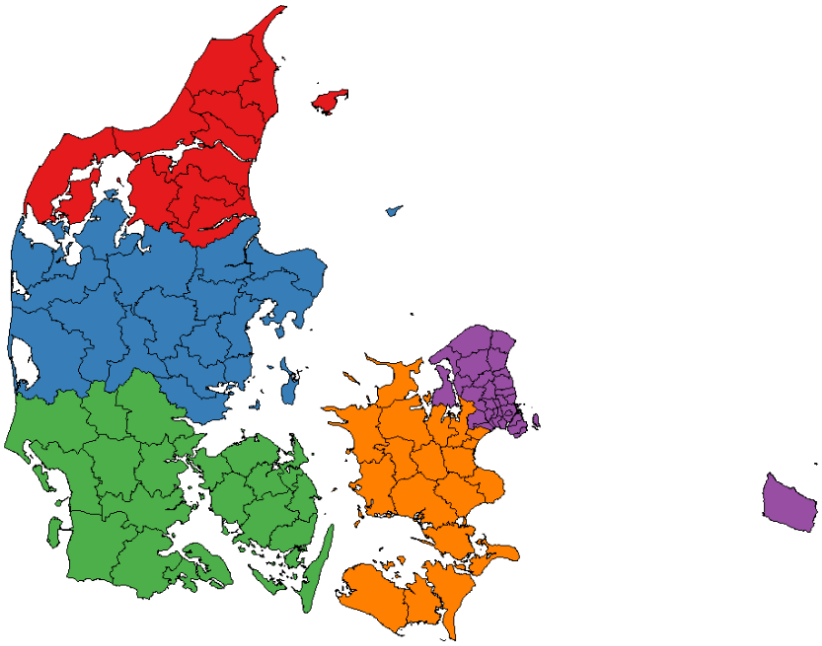

Figure 1.3. Divisions of Denmark. The black lines separate the municipalities and the colors indicate regional divisions.The red region is Nordjylland, blue is Midtjylland, green is Sønderjylland, orange is Sjælland and purple is Hovedstaden.

The regions' primary function is to operate the health system in Denmark, and they also maintain certain regional welfare tasks.
The municipalities maintain most welfare related tasks like kindergarten and primary schools, and each municipality has their own authority and politics which is maintained by the citizens. Every four years the municipalities have an election to either conserve or make structural changes to the municipality, be it the welfare system or infrastructure. So each municipality has their own set of structural qualities that might affect the spread rate of Covid-19 as well. Figure 1.4 below shows how the pandemic has had a differing impact on each municipality. Note that the relative growth rate is equivalent to *growth per citizen*, normalized with respect to the population in each municipality.

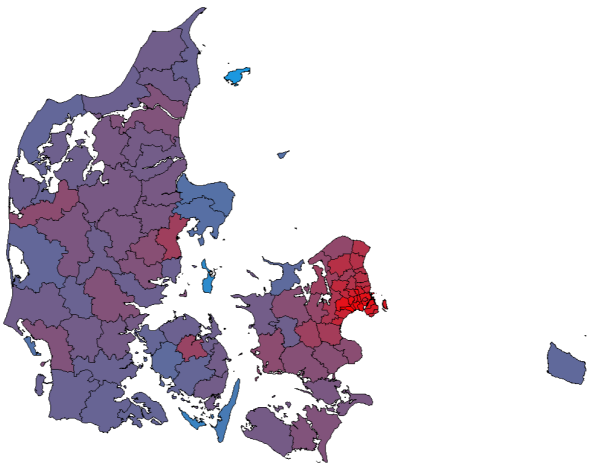

Figure 1.4. Covid-19 mean relative growth rate across municipalities. Blue indicates a low mean value and red indicates a high mean value.

Figure 1.4 shows the mean relative growth rate throughout the pandemic in each municipality. The calculation of the growth rates is explicitly presented in equation (2.1) in section 2.1. It is clear that even when normalized with respect to population sizes, the municipalities have differing spread rates of the virus.

As the Danish government executes strict policies to prevent the spread of the virus it also tries to alleviate the uncertainty of the economical health by applying economically stimulating policies. With all the uncertainty following the pandemic and with these political interventions, some level of imposed uncertainty on the financial markets is expected.

A casual inspection of the log return of the OMX C25 index, or simply OMXC25, below shows that the financial market sees an increase in volatility during the pandemic.

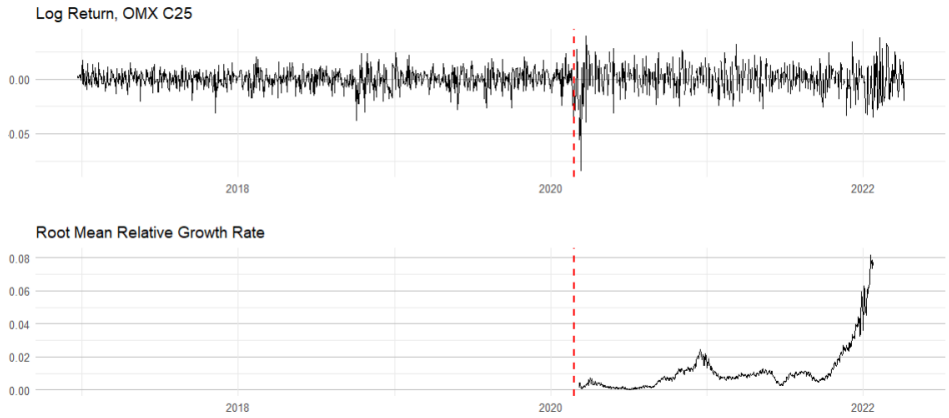

Figure 1.5. First plot: Logarithmic return of OMX C25, the red dashed line illustrates the first case of Covid-19 in Denmark at the 27th February of 2020. The log return standard deviation is 0.008 before and 0.013 after the first case.
Second plot: Root mean relative growth rate of Covid-19 across Danish Municipalities.

1.1 Literature Review

As mentioned, Li and Kapri [2021] investigated the spread and death rate by analyzing the effects of political intervention and relevant socioeconomic indicators on these key figures. They use a generalized regression modeling framework on weekly observations, they use these weekly observations to smooth out any errors that might be present in daily data. Additionally, they hypothesize that countries with a big service industry and those with energetic international trade have worse Covid-19 key figures than countries that do not exhibit these features.

Oshinubi et al. [2022] also worked on modeling socioeconomic and epidemiological data, using machine learning and deep learning. The paper put a great deal of thought into establishing a mathematical relationship between the Theil and Gini indices and how they effect theses key figures. Their methodology included use of neural network, regression analysis, multivariate analysis, prediction and clustering. The methods were used on a number of different socioeconomic and epidemiological variables, comparing the relationship between these variables for developing and developed countries. Their results showed no clear significance for the indices during the first wave of Covid-19 outbreaks, however, developed

countries reacted much better on the second Covid-19 outbreak than developing countries, mainly due to fast deployment of isolation and vaccination.

Bennedsen et al. [2020] comments on a number of challenges the Danish labor force have been facing during the Covid-19 pandemic. The paper analyzes the effects, implemented by the Danish government, to minimize unemployment by looking at the effect of some economically stimulating policies, like expense aid and tax aid. The paper found that while expense aid and tax aid have very little effect on preventing an increase in unemployment, work aid on the other hand, which is a government subsidy designated for companies paying salaries, was a strong incentive for companies to keep their employees on the payroll. This naturally is a win-win for the companies and the employees as it relieves the economical stress on the company and it promotes well-being of the employees as it financially covers them.

McCracken et al. [2020] researches the impacts of Covid-19 on mental and physical health during the corona pandemic in Sweden. With an online national cross-sectional survey ($n = 1212$; mean age at 36.1 years and 73% are females), the results showed that Sweden had significant depression, anxiety and insomnia levels at 30%, 24.2% and 38%, respectively. They compared the impacts of Covid-19 on mental health in Sweden with China and Italy, and it seems to at the same level as these two countries. The pandemic appears to be affecting the mental health of those who are already affected by mental health issues. The results of this may provide more support for these people in vulnerable groups, and it may also help in developing new psychological therapies that are suitable for the ongoing corona pandemic and probably for similar pandemics in the future.

Brink [2021] investigates the mental health of the youth in Denmark. They hypothesized that the lockdown has had a significant effect on the youth's mental well-being, they sent out a questionnaire which was answered by 400 students at Niels Brocks Youth Education, among the students 6% responded that they have suffered mentally to the point that they feel that "life is not worth living", additionally, 28% responded that they are not mentally well. They conject that this generation of youths will have a scarred mental health going into the future, they note that they have effectively been in solitary confinement and they are unable to emotionally manage this crisis due to not being fully developed.

Occhipinti et al. [2021] suggests different political approaches as a response to the exacerbation of public mental health during the Covid-19 pandemic. They note that an all-encompassing and long-term solution is infeasible and too expensive in most contexts, they note that previously reactive and proactive policy responses to public mental health issues has had next to no effects. They use Australia's decades-long struggle with public mental health issues and America's ongoing opioid crisis as examples of failed policy responses.
They criticize the fact that the predominant approach to research on mental health issues has been using retrospective data to investigate independent risk factors such as drug abuse, childhood abuse, etc. They note that these studies fail to account for the interactive effects of the risk factors, so projections on mental health using these models are generally incorrect. Additionally, they comment that contemporary and future studies need to recognize feedback loops, threshold effects, non-independence and non-linearity between relevant risk factors in mental health research.
Also, the Brain and Mind Center at the University of Sydney leveraged years of research to develop models to inform policy and planning for a proper response to the effects of the

Covid-19 pandemic on public mental health. Their models project prevalence of psychological distress, rates of help-seeking, wait times, self-harm hospitalizations and suicide deaths, due to the pandemic. To improve on some of these figures in the short term (2021-2025) their models suggest investments in childcare, employment programs and job creations, active follow-up after suicide attempts and improvement of digitally coordinated specialist mental-health services.

Petersen et al. [2021] described the impact of Covid-19 on the physical and mental health of the Danish population during the spring of 2020, that is the first wave of the pandemic and lockdown. This article compares the Wilcoxon Signed Rank test with self-reported illness worry (Whiteley-6-R), emotional distress (SCL-90), and physical symptom burden (SLC-90) measures based on a sample of the Danish adult population ($n = 2190$). However, the study found that concerns about illness, emotional distress and burden of physical symptoms increased only marginally during Covid-19 pandemic compared to pre-pandemic times. The population of Denmark trust the Danish government and feel that the government managed the pandemic well.
The paper concludes that the first wave of the Covid-19 pandemic did not seriously affect the physical and mental health of the adult population in Denmark. Future research should focus on the impact of a second wave of the pandemic and related restrictions that the Danish government can take.

Josephson et al. [2021] documents the socioeconomic impact of the pandemic on families, adults, and children in low-income countries. Research is based on longitudinal household survey data from Ethiopia, Malawi, Nigeria, and Uganda from face-to-face household interviews prior to Covid-19 and telephone interviews conducted during the pandemic. It shows that around 256 million people, which means 77% of the population live in households that have lost their job during the pandemic. Access to food supplies, medicines and other basic necessities has exacerbated the Covid-19 pandemic. They also found that the student-teacher contact has dropped from 96% before Covid-19 to just 17%. These findings can help governments and global organizations to study and to alleviate the impacts of the Covid-19 pandemic in low-income countries.

Addison et al. [2020] discusses macroeconomic dimensions with a focus on developing countries, starting from China and then expanding to the whole world, summarizing knowledge of the global economic consequences of the Covid-19 pandemic and the difference between the financial crisis of 2007-2009 and the Covid-19 crisis. It then discusses the world's commodity markets, including oil, metals and food trade as well as a study in health care and the role of economic and social support in determining the macroeconomic outcomes of the pandemic. They also investigated how the low-income countries and middle-income countries are handling the crisis, and concluded that it depends on how much fiscal space for maneuvering is available.

Chen et al. [2020] uses cross country panel data to discuss the impact of various non-pharmacological interventions, which were used by the government to inhibit(reduce) the spread of the Covid-19 pandemic. It states that the lockdown leads to a reduced spread rate, and bans on gatherings appear to be more efficient than closing companies and schools down, but both types of lockdowns have caused large declines in the gross domestic product. Moreover, it is shown that stay-at-home orders are inefficient in countries with

larger households and in developing countries. Motivation from the governments played an important role, as it can make their populations more confident. The main objective of the article was to study the relationship between COVID-19 control measures and disease spread, and in addition to this, it also examines the pandemic and economic activity during it.

1.2 Research Summary

It is clear that the pandemic has had severe effects on several aspects of society, Occhipinti et al. [2021] clearly highlights the scope of the mental health issues nations need to address. Notably, it is going to be expensive to recuperate public mental health to a pre-pandemic level. Chen et al. [2020] notes that even though certain stringency policies reduce the spread rate, it also reduces the gross domestic product.

We are primarily inspired by Chen et al. [2020] as they develop models to understand how socioeconomic conditions and policy interventions influence the spread rate of the virus while monitoring the health of the economy. With that we present our questions of interest.

1.2.1 Research Questions

- Which conditions influence the Covid-19 spread rate across Denmark?
  - Which effects do socioeconomic conditions have?
  - Which effects do political responses have?
- Is there an increase in volatility in the Danish economy?
  - If so, is such an increase similar across Danish regions?

Chapter 2 will include a section that presents some of our thoughts on how to model the spread rate across municipalities, additionally, it will include a section on how the financial markets have been affected by the pandemic.

Chapter 3 presents panel data modeling which then serves as the groundwork for analyzing the socioeconomic factors' effect on the spread rate, this methodology was inspired by Li and Kapri [2021].

As for assessing the pandemic's influence on the Danish economy, we will use OMX C25 and regional stock indices as indicators for the Danish economy, we will then analyze them using a regime switching time series framework to model the volatility dynamics. Chapter 4 presents the regime switching modeling framework we will use to investigate the volatilities.

Following chapters 3 and 4, we implement and present our results in chapter 5. Finally, we conclude on these results in chapter 6.

Chapter 2

Preliminary Study

2.1 Municipality Data

This section will present the groundwork for a study of the dynamics of the Covid-19 spread rate, that is commenting on our strategy and the collected data.

2.1.1 Strategy

Our focus will be to determine the effects certain government responses and socioeconomic conditions have on the spread rate of the virus. The modeling framework will be discussed later in subsection 2.1.3.
Studying these effects across seemingly socioeconomically homogeneous municipalities will give insight into how their differences affect the spread of the virus.

The Covid-19 virus is an airborne transmitted disease; having frequent physical contact with or simply being in the vicinity of others increases the chance of contracting the virus. So it is natural to consider the population density as a relevant variable. [Høiby, 2020]
It is common for children to have physical and social interactions through school, kindergarten and free time activities thus an indicator capturing any of these effects might have an impact on the spread of the virus [Øvlisen, Rysgård, Bregendahl and Pedersen, 2021].

Vaccinations were not available until late 2020 and it was mostly only given to elderly and particularly exposed individuals at that time. The vaccines reduce symptoms and lessen the risk of getting infected by the virus. Having a large unvaccinated population will likely increase the spread rate [Kristensen, 2021]. Choosing a suitable indicator that captures the effects of the vaccine will improve modeling of the virus' spread rate.

The government's stringency policies might have effects on the spread rate of the virus, but the policies themselves will not directly affect the spread rate, however, in case the government decides to send children home from institutions[1] then the spread rate will decrease more in municipalities that have a large percentage of children in institutions. So it is important to correctly specify an indicator that captures this interaction [Li and Kapri, 2021].

Another important effect to consider is that some municipalities are neighboring one another, so in some cases, an individual living in one municipality might work in another, thus there are spatial effects to consider. So incorporating this spatial correlation into the modeling scheme can potentially improve the results.

[1] Daycare, kindergarten and primary school.

2.1.2 The Data

The data collection has been done by using several databases; *Johns Hopkins Coronavirus Resource Center*, *Our World in Data*, *European Centre for Disease Prevention and Control*, *OxCGRT*, and *Danmarks Statistik*.

Below is a list of all the collected data that we deem relevant to the study of the research questions.

- New cases
- Cumulative cases
- Stringency Index
- Gini index
- Percentage of vaccinated citizens (Fully vaccinated)
- Amount of jobs
- Percentage of jobs being service oriented
- Percentage of population that are children (age 2 to 15)
- Square meters per citizen in urbanized areas
- Indicator of spatial association between municipalities
- Populations

Some of the variables in the list can be defended due the discussion in the beginning of this section, however, some of the collected data needs some explanation.

The inclusion of percentage of jobs being service oriented is due to service jobs often being associated with human contact and social interactions which are prerequisite for spreading the virus. Additionally, we suspect that there is an interaction between stringency index and the percentage of jobs being service oriented as lockdowns of areas with high percentage of service jobs will likely have a bigger decrease in the prerequisites for virus spread.

Indicators of spatial association was collected for municipalities it was done by noting which municipalities that are neighboring one another and collecting it in a matrix.

The Gini index is included as a control variable due to Oshinubi et al. [2022], they found that the the Gini index captured some of the effects imposed by certain socioeconomic factors. However, it did not show any significance in the first wave, and it was used in a study between high and low income countries, it is included nonetheless.

We choose to model the relative change of Covid-19 in each municipality, i.e. modeling the spread rate as

$$\text{Relative Growth Rate}_{i,t} = \text{Case Per Capita}_{i,t} = \frac{\text{Case}_{i,t} - \text{Case}_{i,t-1}}{\text{Population}_i}, \tag{2.1}$$

where Population_i is the population of the ith municipality, $\text{Case}_{i,t}$ are cumulative cases of registered infections by Covid-19 in the ith municipality at time t. For brevity, the index, i, will now be referred to as the ith *individual*.

The relative growth rate allows us to model the intensity of the spread rate at a given time during the pandemic, the *relativity* is with respect to population, i.e. we do not need to include the population as an explanatory value to account for the size of populations for each individual which is one less parameter to estimate.

Summarizing statistics can be seen in table 2.1 below.

	N	Mean	St.Dev.	Min	Max
Service.concentration.pct	67326	0.765	0.083	0.586	0.955
Stringency.index	67326	51.146	13.698	24.070	72.220
New.cases	67326	20.756	103.730	0.000	4777.000
Cumulative.cases	67326	2228.956	6527.096	0.000	224311.000
Fully.vaccinated	67326	14051.938	33721.336	0.000	493874.000
Gini.index	67326	27.011	3.612	22.680	46.160
Population	67326	59408.112	73631.018	1775.000	633724.000
SqrMeter.per.citizen.urban.areas	67326	684.514	371.056	48.100	2159.300
Children.institutionalized.pct	67326	0.164	0.020	0.108	0.216
Vaccinated.pct	67326	0.242	0.320	0.000	0.876
Relative.growth.rate	67326	0.000	0.001	0.000	0.011
Stringency.index.I.Service.concentration.pct	67326	0.000	1.206	-4.600	4.888
Stringency.index.I.Children.institutionalized.pct	67326	0.000	0.296	-1.442	1.343
Jobs	67326	32451.459	50916.172	854.000	450890.000

Table 2.1. Summarizing statistics for Danish municipality data.

The dates range from the 8th of March 2020 to the 23rd of January 2022, this means that there are 687 days of observations for each of the 98 Danish municipalities.

2.1.3 Panel Data Modeling

Panel data modeling is a natural way to model the data we have presented so far, we will introduce the theory in formal detail in chapter 3, however, it is fitting to discuss the modeling scheme's potential and limitations at this time.

For casual practitioners, it might be tempting to pool all empirically relevant variables and simply run *ordinary least squares* (OLS), however, the omission of other relevant variables will cause biased estimation which, if the bias is large enough, will wrongly infer causalities hence the model is invalidated.
One might be able to rely on the consistency of estimators, i.e. the bias gets smaller the more data is used in the estimation. However, it is in most practical cases impossible to say how much less the bias becomes when increasing the number of observations, so this method is not always reliable.
Instead, a practitioner could include more variables that they might have omitted, however, increasing the number of variables also requires more observation to allow for more degrees of freedom to reduce parameter inflation. In practice, it might be infeasible to include more variables as they might not be observable or can be expensive to collect.

So the pooling modeling scheme might not be the correct way to model these dynamics, so extensions to the pooling scheme can be made to include individual and time effects.
The individual effects try to capture the effects that are constant over time for a specific individual, so any omitted constant at the individual level is included in the individual effects. An example of these effects could be geographical area.
The time effects capture dynamics that are constant over individuals but change over time, examples of these effects could be date effects like Christmas or seasonal effects that are

relatively homogeneous across individuals.

So to summarize, the different models for panel data allow for a flexible modeling scheme, especially the omission of certain types of variables can be defended. There are certain variables that cannot be captured by these time or individual effects and omission of these causes omission bias, however, the inclusion of more variables as already mentioned will cause inflation of parameter variance, this is the infamous bias-variance trade-off.

Multicollinearity

Parameter variance inflation can be caused by removing degrees of freedom by including additional variables but it can also be caused by a high correlation between variables, often referred to as multicollinearity.

As we have a large data set, multicollinearity is not our biggest concern. However, an ex-ante way to check for multicollinearity is to check for high correlation between variables, an ex-post way is to check the variance inflation factor, VIF, after model estimation . In figure 2.1 below are the correlations between the discussed variables.

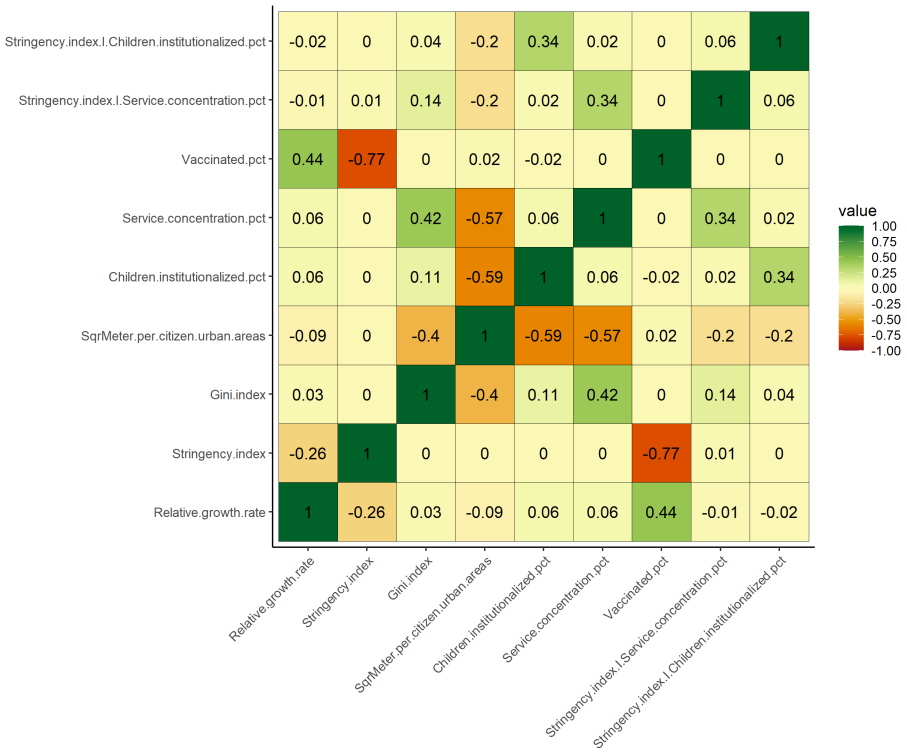

Figure 2.1. Correlation between variables.

The figure shows that the percentage of fully vaccinated and stringency index are highly

negatively correlated, empirically this might be due to the lowering of the stringency policies when people are vaccinated.
Another thing to notice is that the percentage of vaccinated is positively correlated with the relative growth rate, which might be due to the same phenomena, namely that as more people are vaccinated, the vaccination percentage predictor spuriously captures the effect of relieving stringency policies from the higher vaccination percentage which in turn increases the relative growth rate.

As already discussed, the policies themselves will not have a direct impact on the spread of the virus, it is through the interaction with other variables we expect it to affect the spread rate. With that said, the stringency index is composed of a number of different metrics that governments are able to adjust and tweak. Given the number of metrics, a change in the stringency index does not mean a change to all metrics, nevertheless, some overlaps can occur through the stringency index when the government implements changes. For example, included in service jobs are pedagogues and teachers so in case the government decides to close down schools the pedagogues and teachers will isolate, so the two interaction terms will might be correlated conditioned on school closings.

2.2 Assessment of the Danish Economy

Several Danish indices are available, such as the OMX C25, Copenhagen large cap, mid cap and small cap price index, they are all noted on the NASDAQ OMX COPENHAGEN stock exchange.

The OMX C25 index, previously known as the OMX C20 index, consists of the 25, previously 20, most traded Danish shares on the Copenhagen Stock Exchange. The OMX C25 index can be used as an indicator of the financial health of the Danish economy, hence it might provide insightful information about the financial effects the Covid-19 pandemic has had on the Danish economy.
Comincioli [1996] investigates the causal relationship between the economy and the stock market, although, they use the US economy and the S&P500 index in their study. They use a *Granger causality* test, which is an F-test determining whether a time series is useful in forecasting another, their findings suggest that the S&P500 is useful in forecasting the economy but not the other way around.

The OMX C25 index is a capitalization-weighted index created using the daily time series for each stock and their market value for said specific index. This means that the price of the OMX C25 index is calculated by

$$C25_t = \sum_{i=1}^{25} sv_{i,t} \frac{mv_{i,t}}{\sum_{i=1}^{25} mv_{i,t}}. \tag{2.2}$$

Here $sv_{i,t}$ denotes the stock i's value at time t and $mv_{i,t}$ denotes the i'th company's market value at time t, which is given by

$$mv_{i,t} = \text{Number of Stocks} \cdot sv_{i,t}$$

As an addition to the OMX C25 index, we have made regional indices, this is to assess the health of the regional economies.
First, the regional placement of the headquarters of each exchange listed company was located and then a regional index was calculated using the same procedure as shown in equation (2.2).

Table 2.2 below shows the number of companies in each of the regional indices.

Nordjylland	Midtjylland	Syddanmark	Hovedstaden	Sjælland
8	18	15	84	5

Table 2.2. Number of companies for each regional index.

From table 2.2 it is seen that a vast number of the companies are placed in the Hovedstaden region while the remaining regions have significantly fewer companies. Having a low amount of companies in an index can potentially mean that the index is a bad indicator of the economy, however, due to the lack of a better indicator we continue the research.

Summarizing statistics for these indices are seen in table 2.3 below. For notational brevity we now abbreviate Nordjylland, Midtjylland, Syddanmark, Hovedstaden and Sjælland, by NJ, MJ, SD, HS and RS, respectively.

	Obs			Price in DKK			
Symbol	Observations	First.obs	Last.obs	Mean	Std.dev	Min	Max
OMXC25	1323	2016-12-20	2022-04-06	1337.5	303.3	980.8	2020.7
NJ	1573	2016-01-04	2022-04-13	139.0	10.4	108.4	173.2
MJ	1573	2016-01-04	2022-04-13	135.5	49.1	79.9	270.1
SD	1573	2016-01-04	2022-04-13	31.5	11.3	15.2	59.6
HS	1573	2016-01-04	2022-04-13	582.6	139.4	363.5	962.4
RS	1573	2016-01-04	2022-04-13	451.3	77.3	348.0	692.5

Table 2.3. Summarizing statistics for the regional indices.

Table 2.3 shows the summary statistics of each of our regional indices and the OMX C25 index. Given that the OMX C25 index consists of the 25 most traded stocks on the Danish market, it is not surprising that the mean, minimum and maximum values are noticeably larger when compared to the regional indices.

For a complete table of the summarizing statistics for each index and each individual stock see table A.9 in appendix A. The resulting regional indices will act as indicators of how the financial markets are affected by the pandemic regionally.

2.2.1 Conditional Mean Model

The casual inspection of the log returns of OMX C25 seen in figure 1.5, suggested that there is some evidence for an increase in volatility during the pandemic. For a more formal investigation of the indices, modeling the distribution of the log returns is required.

The strategy is to model the conditional distribution of

$$y_t \mid \mathcal{I}_{t-1},$$

where $\mathcal{I}_{t-1}$ is the σ-algebra generated by the process $y_0, \ldots, y_{t-1}$ and y_t is the log returns. It is common to model the conditional mean and conditional variance separately to reduce computation time, we will be using an ARIMA framework for the conditional mean and a regime switching GARCH framework for the conditional variance.

The rest of this chapter will focus on modeling the conditional mean and checking the residuals for signs of heteroscedasticity. We now assume the reader is familiar with Box-Jenkins methodology including estimating ARIMA models, detecting (weak) stationarity and its conditions, detecting seasonality and diagnostic checks for the residuals [NCSS, 2022].

The time series in the ARMA model is required to be stationary, testing for this we use the ADF-test, which tests for non-stationarity through a unit root test, that is the ADF-test fits the auxiliary model

$$\Delta y_t = \alpha + \beta t + \gamma y_{t-1} + \sum_{L=1}^{\rho} \theta_L \Delta y_{t-L} + \varepsilon_t,$$

where y_t are the log returns, and then tests whether γ is different from 1, i.e. there is no unit root hence stationarity. The ρ denotes the number of lags, α denotes a constant drift

component and β denotes a time trend. The test is conducted for the presence of no drift and no trend, drift and no trend and finally for drift and trend. The result for the ADF test on the OMX C25 index is seen in table 2.4 below.

Table 2.4. Augmented Dickey-Füller Test OMX C25.

	No drift & no trend		Drift & no trend		Drift & trend	
lag	value	p-value	value	p-value	value	p-value
0	-36.14297	0.01	-36.18949	0.01	-36.17678	0.01
1	-24.15318	0.01	-24.20153	0.01	-24.19349	0.01
2	-20.90442	0.01	-20.96269	0.01	-20.95616	0.01
3	-18.08967	0.01	-18.15341	0.01	-18.14836	0.01
4	-15.95231	0.01	-16.02040	0.01	-16.01631	0.01
5	-15.29359	0.01	-15.37072	0.01	-15.36738	0.01
6	-13.43026	0.01	-13.50845	0.01	-13.50581	0.01
7	-12.90548	0.01	-12.98514	0.01	-12.98442	0.01
8	-11.84636	0.01	-11.92906	0.01	-11.92859	0.01
9	-10.98900	0.01	-11.07528	0.01	-11.07466	0.01
10	-10.32572	0.01	-10.41021	0.01	-10.41099	0.01
11	-9.95050	0.01	-10.03764	0.01	-10.03912	0.01
12	-9.86402	0.01	-9.96075	0.01	-9.96169	0.01
13	-9.48218	0.01	-9.58364	0.01	-9.58431	0.01
14	-8.78711	0.01	-8.88401	0.01	-8.88598	0.01
15	-9.07921	0.01	-9.18977	0.01	-9.19030	0.01
16	-8.93159	0.01	-9.04145	0.01	-9.04405	0.01
17	-8.66337	0.01	-8.77712	0.01	-8.77975	0.01
18	-8.24805	0.01	-8.36545	0.01	-8.36746	0.01
19	-7.99499	0.01	-8.11587	0.01	-8.11774	0.01
20	-8.12799	0.01	-8.25523	0.01	-8.25756	0.01
21	-8.34578	0.01	-8.48420	0.01	-8.48620	0.01
22	-8.35520	0.01	-8.50501	0.01	-8.50600	0.01
23	-8.44367	0.01	-8.60399	0.01	-8.60497	0.01
24	-8.14122	0.01	-8.29644	0.01	-8.29978	0.01
25	-8.04207	0.01	-8.20153	0.01	-8.20581	0.01
26	-7.53193	0.01	-7.68354	0.01	-7.68915	0.01
27	-7.47807	0.01	-7.63777	0.01	-7.64299	0.01
28	-7.55473	0.01	-7.72277	0.01	-7.72806	0.01
29	-7.34774	0.01	-7.51172	0.01	-7.51926	0.01
30	-7.26497	0.01	-7.43727	0.01	-7.44408	0.01
31	-7.06136	0.01	-7.23393	0.01	-7.24156	0.01

The table shows that the OMX C25 log return series are stationary testing for up to 31 lags. The same ADF tests are conducted for the remaining indices, however, given the size of table 2.4, we summarize the results in table 2.5 below.

Symbol	ndnt	dnt	dt
OMXC25	0	0	0
NJ	0	0	0
MJ	0	0	0
SD	0	0	0
HS	0	0	0
RS	0	0	0

Table 2.5. The three ADF versions are abbreviated by *ndnt*, *dnt* and *dt*, that is they abbreviate no drift and no trend, drift and no trend and drift and trend, respectively. These variables count the number of p-values exceeding the significance level of 0.05, hence counting which indices where the test results fail to reject the null hypothesis of the presence of a unit root.

The next step is fitting a conditional mean model, and since the ADF tests showed that we had no unit roots in any of the indices hence they are not integrated processes, the ARMA model is adequate. An ARMA model is given on the following form

$$Y_t = c + \varepsilon_t + \sum_{i=1}^{p} \varphi_i Y_{t-i} + \sum_{i=1}^{q} \theta_i \varepsilon_{t-i}.$$

Here c denotes a constant while p and q are called the autoregressive and the moving average orders, respectively. Furthermore, φ_i and θ_i denotes parameters where $\varphi_p \neq 0$ and $\theta_q \neq 0$, lastly ε_t is the error term of the ARMA model which we assume is normally distributed hence allowing us to use maximum likelihood estimation [H.Shumway and S.Stoffer, 2017]. The orders of the ARMA models have been chosen using Akaike's information criterion, AIC. Table 2.6 below shows the chosen ARMA order for the different indices.

	Symbol	p	q
5	OMXC25	0	0
6	NJ	3	0
7	MJ	2	2
8	SD	0	0
9	HS	0	0
10	RS	0	3

Table 2.6. Orders of ARMA models for the different indices.

Filtering the time series with the ARMA-filters we expect the errors to be uncorrelated across time, we examine this by observing the ACF/PACF plot. Additionally, the ACF plot can be used to check if there is autocorrelation in the squared residuals, which is a sign of heteroscedasticity hence justifying the modeling of the conditional variance. Figure 2.2 below shows the ACF of the residuals and the squared residuals of the mean filtered log return series of the OMX C25 index.

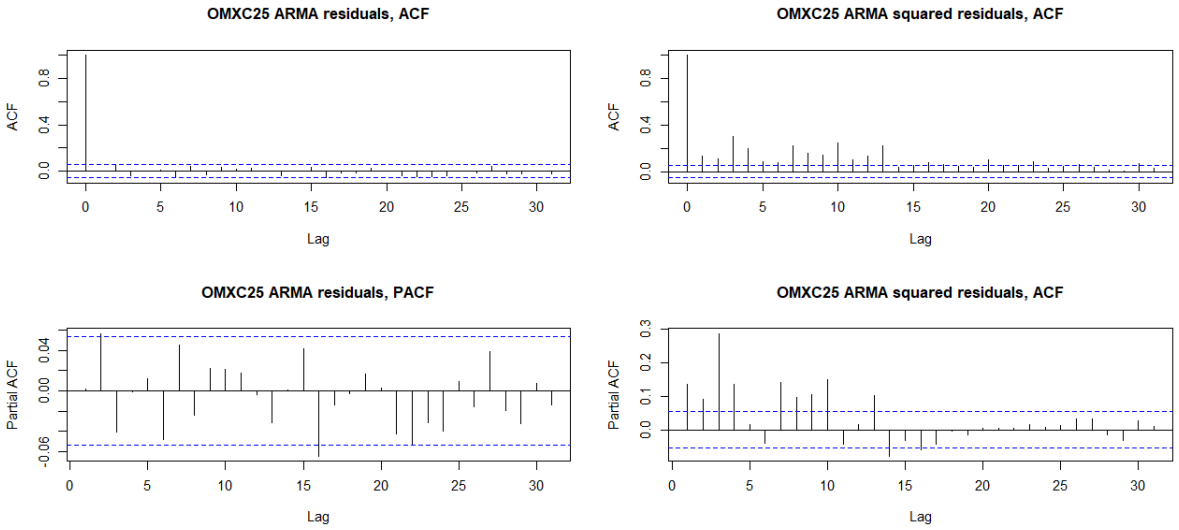

Figure 2.2. ACF and PACF plots of the residuals and squared residuals of the ARMA filtered OMXC25 log returns.

Looking at the ACF and PACF plots in figure 2.2, it is clear that there is no autocorrelation for the residuals. However, looking at the ACF and PACF for the squared residuals, it is clear that there are signs of autocorrelation, which advocates further examination of conditional variance. Chapter 4 presents the theory of regime switching GARCH models, and section 5.2 continues the study of the conditional distributions of the log returns.

Chapter 3

Panel Data Modeling

This chapter includes an introduction to panel data models; the one-way error component regression model the two-way error component regression model and the spatial error component regression model.

3.1 One-Way Error Component Regression Model

Equation (3.1) below illustrates a linear regression model using panel data.

$$y_{i,t} = \alpha + X_{i,t}^{'}\beta + u_{i,t} \quad i = 1, \ldots, N; \quad t = 1, \ldots, T \tag{3.1}$$

here $y_{i,t}$ denotes the dependent variable, the relative growth rate in our case, for indices i denoting individual and t denoting time. α is a constant, β is a $K \times 1$ parameter vector, and $X_{i,t}^{'}$ is the i,t-th observation of K explanatory variables.

Remark 1. For OLS applied on equation (3.1) to be the best linear unbiased estimator, BLUE, we need to make assumptions such that the Gauss-Markov theorem applies [Pollock, 2000]. To be explicit, for it to be BLUE we assume that the regression is linear in parameters, the model is correctly specified, the errors are randomly sampled, we need exogeneity or at least predeterminedness of the errors with respect to the regressors, no multicollinearity between regressors and spherical errors, i.e. homoscedasticity and no autocorrelation.

Assumption 1. In general, we assume that the models we present are correctly specified, the errors are randomly sampled, there is no multicollinearity and the regressions are linear in parameters.

Assumption 1 will always be in effect throughout this chapter, the remaining assumptions to obtain BLUE estimators will be discussed in more detail for each model as some of these models impose specific non-spherical error components.

Remark 2. The regression in (3.1) is often referred to as a pooled regression and the error term $u_{i,t}$ is typically assumed i.i.d. distributed across i and t, for the reasons outlined in the previous remark.

Now by assuming that the error can be written as

$$u_{i,t} = \mu_i + \nu_{i,t} \tag{3.2}$$

where μ_i is an unobserved individual effect and $\nu_{i,t}$ is the idiosyncratic error, the error, $u_{i,t}$, may exhibit heteroscedasticity but it must have a zero conditional mean, i.e. $\mathrm{E}[u_{i,t} \mid X_{i,t}] = 0$ which is also often referred to as a predeterminedness assumption.
Additionally, μ_i and $\nu_{i,t}$ are assumed independent for all values of i and t. Equation (3.2) is referred to as the *one-way error component* and together with (3.1), they are referred to as the *one-way error component regression model*.

Assumption 2. (i) μ_i is independent across i and (ii) orthogonal to $X_{i,t}$ [Davidson and MacKinnon, 2003].

This is an assumption of μ_i being independent $\forall i$ as well as an assumption of predeterminedness between μ_i and the explanatory variables, $X_{i,t}^{'}$, i.e. $\mathrm{E}[\mu_i \mid X_{i,t}] = 0$ in this case.

Assumption 3. (i) $\nu_{i,t}$ is independent across i (ii) and t, (iii) it is identically distributed and is (iv) orthogonal to $X_{i,t}$.

This assumption is a predeterminedness assumption between the disturbance term $\nu_{i,t}$ and $X_{i,t}$ as well as an assumption of homoscedasticity and no autocorrelation across time and cross-sections, note that it implies that $\mathrm{E}[\nu_{i,t}^2 \mid X_{i,t}] = \mathrm{E}[\nu_{i,t}^2] =: \sigma_\nu^2, \quad \forall i, t.$

Equation (3.1) and (3.2) can be written in vector form by

$$y = \alpha\iota_{NT} + X\beta + u = Z\delta + u \tag{3.3}$$

$$u = Z_\mu\mu + \nu \tag{3.4}$$

where y is $NT \times 1$, X is $NT \times K$, $Z = [\iota_{NT}, X]$, $\delta = (\alpha^{'}, \beta^{'})^{'}$ and ι_{NT} is a vector of ones of dimension NT. The error component equation has the term $Z_\mu := I_N \otimes \iota_T$ where I_N is an identity matrix of dimension $N \times N$ and again ι_T is a vector of ones of dimension T and $\mu = (\mu_1, \ldots, \mu_N)^{'}$.

3.1.1 Fixed Effects Model

Assumption 4. Under the assumption $\mathrm{E}[\mu_i \mid X_{i,t}] \neq 0$, model (3.3) is a *individual fixed-effects* model and μ_i can be interpreted as a *within-group mean*, i.e. a deterministic term or *fixed effect* that is inherent to individual i.

Note that the independence and orthogonality part of assumption 2 is implied by assumption 4 since the individual effect is now treated as a constant.

Remark 3. There is also the possibility of a different type of error component, that is $u_{i,t} = \lambda_t + \nu_{i,t}$. Under the assumption of $\mathrm{E}[\lambda_t \mid X_{i,t}] \neq 0$ we have *time fixed effects*, i.e. λ_t can be interpreted as a mean that is the same across all individuals but different across time.
In fact, it is important to realize that even though we are focusing our attention on the individual effects, all the results that are based on the individual effects can be translated to a time effects perspective by carefully swapping the indices and relevant variables.

It is also possible to combine the two to get a two-way error component regression model, we explore this further in section 3.2.

Under assumption 4 it makes sense to rewrite (3.3) and (3.4) such that

$$y = \alpha\iota_{NT} + X\beta + Z_\mu\mu + \nu = Z\delta + Z_\mu\mu + \nu. \tag{3.5}$$

Remark 4. It is possible to impose the restriction of $\sum_{i=1}^{N} \mu_i = 0$ to avoid perfect multicollinearity, also known as the dummy variable trap. In practice, the imposition allows estimation of μ_i and α separately and not simply $(\mu_i + \alpha)$.

To obtain OLS estimates of this regression start by defining the partitioning matrix $Z^* := [Z, Z_\mu]$ and $\gamma := (\delta', \mu')'$, such that the OLS estimate is given by

$$\hat{\gamma}_{OLS} = (Z^{*'} Z^*)^{-1} Z^{*'} y.$$

OLS is perfectly fine in this case, it will yield unbiased and consistent estimates under the orthogonality assumption in assumption 3, however, the inversion of $Z^{*'} Z^*$ with dimension $(N + K + 1) \times (N + K + 1)$ can be practically infeasible.
To circumvent this issue, we need to define projection matrices and present a useful statistical theorem.

Definition 1: Projection Matrix

A projection matrix, P_X, for X is defined as

$$P_X = X(X'X)^{-1}X'$$

It is the orthogonal projection onto the column space of X, $\mathcal{S}(X)$. Additionally, the projection onto the orthogonal complement of $\mathcal{S}(X)$ is given by

$$Q_X = I - P_X$$

Q_X is often called the residual maker.

Some trivial properties of the projection matrix include that they are symmetric, $P_X' = P_X$, and idempotent, $P_X = P_X^2$. Now to an important result [Robinson, 2020].

Theorem 1: Frisch-Waugh-Lowel theorem (FWL)

Let a partitioned linear regression be given by

$$y = X_1\beta_1 + X_2\beta_2 + u,$$

under regulatory assumptions 1 the OLS estimate $\hat{\beta}_1$ and residuals $\hat{u}$ obtained by applying OLS on

$$y = X\beta + u,$$

where $X = [X_1, X_2]$ and $\beta = (\beta_1', \beta_2')'$, is the same as OLS estimates and residuals obtained by applying OLS on

$$Q_{X_2} y = Q_{X_2} X_1 + u,$$

where $Q_{X_2} X_2 = 0$ and $Q_{X_2} u = u$.

For the proof of theorem 1, we refer the reader to Robinson [2020].

By premultiplying (3.5) with Q_{Z_μ}, also known as performing *within transformation*, and using the FWL-theorem we find estimates for the fixed effects by applying OLS to

$$Q_{Z_\mu} y = Q_{Z_\mu} X\beta + \nu \tag{3.6}$$

which yields the fixed effects estimator, also known as the *least square dummy variable* estimator (LSDV),

$$\hat{\beta} = (X' Q_{Z_\mu} X)^{-1} X' Q_{Z_\mu} y \tag{3.7}$$

where the (finite sample) covariance of the estimator, under assumption 3, is given by

$$\begin{aligned}\mathrm{Var}(\hat{\beta}) &= \mathrm{E}[(\hat{\beta} - \mathrm{E}[\beta])(\hat{\beta} - \mathrm{E}[\beta])'] &(3.8)\\ &= \sigma_\nu^2 (X' Q_{Z_\mu} X)^{-1}. &(3.9)\end{aligned}$$

Remark 5. Reducing the amount of explanatory variables by accounting for the fixed effects through the FWL-theorem is effectively removing degrees of freedom.

If we relax the homoscedasticity and no autocorrelation part of assumption 3, we will get a *sandwich* form of the covariance of the estimate, which is an indication of non-efficiency. Relaxing those parts, defining $\mathrm{E}[\nu\nu'] = \Omega$ and assuming that β_0 is the true parameter to (3.6), we get the following sandwich covariance of the OLS estimates (3.8)

$$\begin{aligned}\mathrm{Var}(\hat{\beta}) &= \mathrm{Var}(\hat{\beta} - \beta_0)\\ &= (X' Q_{Z_\mu} X)^{-1} X' Q_{Z_\mu} \mathrm{E}[\nu\nu'] Q_{Z_\mu} X (X' Q_{Z_\mu} X)^{-1}\\ &= (X' Q_{Z_\mu} X)^{-1} X' Q_{Z_\mu} \Omega Q_{Z_\mu} X (X' Q_{Z_\mu} X)^{-1} &(3.10)\end{aligned}$$

where we used that $\tilde{\beta} - \beta_0 = (X' Q_{Z_\mu} X)^{-1} X' Q_{Z_\mu} \nu$.

A way to regain efficiency is to use GLS instead of OLS, the general idea is to correct for the heteroscedasticity and autocorrelation by premultiplying by the square root of the precision matrix of the errors. Square rooting a matrix can be ambiguous, so to be explicit, we define the precision matrix by the decomposition $\Omega^{-1} = \Psi\Psi'$. That is premultiplying by Ψ' yields

$$\Psi' Q_{Z_\mu} y = \Psi' Q_{Z_\mu} X\beta + \Psi'\nu, \tag{3.11}$$

note that $\mathrm{E}[\Psi'\nu\nu'\Psi] = I$, such that the errors, $\Psi'\nu$, are now a white noise.

Remark 6. One might argue that regressions (3.6) and (3.11) are not the same, in fact, they are the same since linear regressions are invariant under non-singular linear transformations. Given that covariance matrices are positive definite it implies that the precision matrix is positive definite thus Ψ is non-singular.

Now applying OLS on (3.11) yields the GLS estimator given by

$$\hat{\beta}_{GLS} = (X' Q_{Z_\mu} \Omega^{-1} Q_{Z_\mu} X)^{-1} X' Q_{Z_\mu} \Omega^{-1} Q_{Z_\mu} y \tag{3.12}$$

with variance

$$\begin{aligned}\mathrm{Var}(\hat{\beta}_{GLS}) &= \mathrm{Var}(\hat{\beta}_{GLS} - \beta_0)\\ &= (X' Q_{Z_\mu} \Omega^{-1} Q_{Z_\mu} X)^{-1} X' Q_{Z_\mu} \Omega^{-1} Q_{Z_\mu} \mathrm{E}[\nu\nu'] Q_{Z_\mu} \Omega^{-1} Q_{Z_\mu} X (X' Q_{Z_\mu} \Omega^{-1} Q_{Z_\mu} X)^{-1}\\ &= (X' Q_{Z_\mu} \Omega^{-1} Q_{Z_\mu} X)^{-1} X' Q_{Z_\mu} \Omega^{-1} \Omega\Omega^{-1} Q_{Z_\mu} X (X' Q_{Z_\mu} \Omega^{-1} Q_{Z_\mu} X)^{-1}\\ &= (X' Q_{Z_\mu} \Omega^{-1} Q_{Z_\mu} X)^{-1}. &(3.13)\end{aligned}$$

Now, the GLS estimator is more efficient than the LSDV estimator, this can be seen by looking

at the difference in their precision matrices, i.e.

$$\begin{aligned}
\text{Var}(\hat{\beta}_{GLS})^{-1} - \text{Var}(\hat{\beta})^{-1} &= X^{'}Q_{Z_\mu}\Omega^{-1}Q_{Z_\mu}X - X^{'}Q_{Z_\mu}X(X^{'}Q_{Z_\mu}\Omega Q_{Z_\mu}X)^{-1}X^{'}Q_{Z_\mu}X \\
&= X^{'}Q_{Z_\mu}(\Omega^{-1} - Q_{Z_\mu}X(X^{'}Q_{Z_\mu}\Omega Q_{Z_\mu}X)^{-1}X^{'}Q_{Z_\mu})Q_{Z_\mu}X \\
&= X^{'}Q_{Z_\mu}(\Psi\Psi^{'} - Q_{Z_\mu}X(X^{'}Q_{Z_\mu}(\Psi\Psi^{'})^{-1}Q_{Z_\mu}X)^{-1}X^{'}Q_{Z_\mu})Q_{Z_\mu}X \\
&= X^{'}Q_{Z_\mu}\Psi(I- \\
&\Psi^{-1}Q_{Z_\mu}X(X^{'}Q_{Z_\mu}(\Psi\Psi^{'})^{-1}Q_{Z_\mu}X)^{-1}X^{'}Q_{Z_\mu}(\Psi^{'})^{-1})\Psi^{'}Q_{Z_\mu}X \\
&= X^{'}Q_{Z_\mu}\Psi(I- \\
&\Psi^{-1}Q_{Z_\mu}X(X^{'}Q_{Z_\mu}(\Psi^{-1})^{'}\Psi^{-1}Q_{Z_\mu}X)^{-1}X^{'}Q_{Z_\mu}(\Psi^{-1})^{'})\Psi^{'}Q_{Z_\mu}X \\
&= X^{'}Q_{Z_\mu}\Psi(I - P_{\Psi^{-1}Q_{Z_\mu}X})\Psi^{'}Q_{Z_\mu}X \\
&= X^{'}Q_{Z_\mu}\Psi Q_{\Psi^{-1}Q_{Z_\mu}X}\Psi^{'}Q_{Z_\mu}X
\end{aligned}$$

where we have used the idempotency property of projection matrices in the second equality. Now since projection matrices are positive semi-definite and are in a quadratic form, the result is positive semi-definite so the GLS estimator is efficient.

FGLS for Fixed Effects

As GLS is practically impossible due to the covariance matrix of the idiosyncratic errors being unknown, we instead obtain *feasible* GLS, FGLS, by estimating the covariance matrix. Wooldridge [2010] suggests relaxing part (*ii*) and (*iii*) of assumption 3, that is, letting the idiosyncratic errors be heteroscedastic and autocorrelated across time but not across sections. Due to the relaxation of this assumption the covariance structure of the idiosyncratic error can now be written as $\Omega = I_N \otimes \Sigma$. So an efficient estimator of Ω can be obtained as follows.

1. Run a fixed effects regression $y = Z\delta + Z_\mu\mu + \nu$ using the LSDV estimator (3.7).
2. Use the residuals, $\hat{\nu}_{i,t}$, from the first step to estimate $\hat{\Sigma} = N^{-1}\sum_{i=1}^{N}\hat{\nu}_i\hat{\nu}_i^{'}$.
3. Now the estimator is given by $\hat{\Omega} = I_N \otimes \hat{\Sigma}$.

Note that $\nu_i = (\nu_{i,1}, \ldots, \nu_{i,t})^{'}$. Now substitute the estimator into (3.12) and (3.13) to get FGLS estimators of the parameters and their covariances.

Robust Covariance Estimation

As an alternative to FGLS we can use robust matrices, that is, finding heteroscedasticity- and autocorrelation-robust covariance matrix (HAC-matrix) estimators that correct the standard errors of the OLS estimates. Consider the following joint representation of the one-way error component regression model

$$y_i = Z_i\delta + \mu_i\iota_T + v_i, \quad \forall i$$

where y_i is the T observations for the ith individual stacked in a $T \times 1$ vector, it then follows that $Z_i = [\iota_T, X_i]$, X_i is $T \times K$, μ_i is a scalar, $\delta = (\alpha, \beta')^{'}$, ι_T is a vector of ones and ν_i is $T \times 1$. Applying the within transformation yields

$$Q_i y_i = Q_i X_i \beta_i + v_i$$

where we have omitted the subscript on Q_i that shows the matrix whose column space we project *off*. Define $S_A := S(A) := \operatorname{plim}\left(N^{-1}A\right)$ [1], now by applying the restriction $\beta = \beta_1 = \cdots = \beta_N$, note that β is the same as in (3.6), we can find the asymptotic variance by

$$\begin{aligned}
\operatorname{Var}\left(\operatorname{plim}\left(N^{1/2}\left(\hat{\beta}-\beta_0\right)\right)\right) &= \mathrm{E}\left[\operatorname{plim}\left(N\left(\hat{\beta}-\beta_0\right)\left(\hat{\beta}-\beta_0\right)'\right)\right] \\
&= \mathrm{E}\left[\operatorname{plim}\left(N\left(X'QX\right)^{-1}X'Q\nu\nu'QX\left(X'QX\right)^{-1}\right)\right] \\
&= \mathrm{E}\left[\operatorname{plim}\left(N\left(N^{-1}X'QX\right)^{-1}N^{-1}X'Q\nu\nu'QXN^{-1}\left(N^{-1}X'QX\right)^{-1}\right)\right] \\
&= \left(S_{X'QX}\right)^{-1}V\left(S_{X'QX}\right)^{-1},
\end{aligned}$$

where $V := S_{X'Q\Omega QX}$. Now the central limit theorem, CLT, yields

$$\lim\left(\sqrt{N}(\hat{\beta}-\beta_0)\right) \sim \mathcal{N}\left(0, \left(S_{X'QX}\right)^{-1}V\left(S_{X'QX}\right)^{-1}\right)$$

An estimator of V is then given by

$$\hat{V} = \sum_{i=1}^{N} N^{-1}X_i'Q\hat{\nu}_i\hat{\nu}_i'QX,$$

where $\hat{\nu}_i = Q_iy_i - Q_iX_i\hat{\beta}$.
Hansen [2007] shows that this estimator is in fact consistent for $N \to \infty$ regardless of the relative size of N and T.

Remark 7. The reason to use this estimator is whenever (*ii*) and (*iii*) of assumption 3 are not met, namely, whenever there is heteroscedasticity and autocorrelation in the idiosyncratic error ν.

In case there is no autocorrelation we can use

$$\hat{V}_{CS} = \sum_{i=1}^{N}\sum_{t=1}^{T}(QX)_{i,t}(X'Q)_{i,t}\hat{u}_{i,t}^2/(NT-N-K).$$

However, Stock and Watson [2008] investigates this estimator through a Monte Carlo study and shows that it is inconsistent for $T > 2$, as an alternative, they suggest the following correction

$$\hat{V}_{FE} = \frac{(T-1)}{(T-2)}\left[V_{CS} - \frac{1}{N(T-1)}\sum_{i=1}^{N}\left(\frac{1}{T}\sum_{t=1}^{T}(QX)_{it}(QX)_{it}'\right)\left(\frac{1}{(T-1)}\sum_{s=1}^{T}\hat{u}_{is}^2\right)\right]. \tag{3.14}$$

This estimator is consistent for $N \to \infty$, regardless of the relative size of N and T [Baltagi, 2021].

There are several other robust covariance estimators, including the Newey-West estimator, the Beck and Katz estimator, etc. Millo [2017], one of the authors behind the comprehensive `plm`-package for panel data modeling in `R`, discusses several of these estimators and how they handle these estimators computationally.

Remark 8. It is common practice to present the parameter estimates with their robust

[1] Note that $\operatorname{plim} = \operatorname{plim}_{N\to\infty}$, we will write it out explicitly in cases where it otherwise would be ambiguous. This also holds for $\lim = \lim_{N\to\infty}$.

standard errors for a comparison. We will make a similar approach without documenting all the robust estimators, we again refer to the work by Millo [2017] for a presentation of each of the robust estimators.

3.1.2 Random Effects

Assumption 5. Under the assumption $\mathrm{E}[\mu_i|X_{i,t}] = 0$, the model given by equation (3.3) is a *random effects* model and μ_i can be interpreted as an error inherent to the ith municipality.

Remark 9. In the special case where $\mathrm{E}[u_{i,t}u_{j,s}] = 0, \forall i, j, t, s, i \neq j, t \neq s$ and $\mathrm{E}[u_{i,t}^2] = \sigma^2, \forall i, t$, (3.3) reduces to a pooled regression and OLS is the best linear unbiased estimator, BLUE.

Additionally, μ_i is assumed independent of $\nu_{i,t}$ as it was with the pooled regression. Define now $\sigma_\mu^2 := \mathrm{Var}(\mu_i)$ and $\sigma_\nu^2 := \mathrm{Var}(\nu_{i,t})$ for all i and t, such that

$$\begin{aligned}\mathrm{Cov}\left(u_{i,t}, u_{j,s}\right) &= E\left[u_{i,t}u_{j,s}\right] \\ &= E\left[\left(\mu_i + \nu_{i,t}\right)\left(\mu_j + \nu_{j,s}\right)\right] \\ &= E\left[\mu_i\mu_j\right] + E\left[\nu_{i,t}\nu_{j,s}\right].\end{aligned}$$

That is,

$$\mathrm{Cov}\left(u_{i,t}, u_{j,s}\right) = \left\{ \begin{array}{cc} \sigma_\mu^2 + \sigma_\nu^2 & (i = j, t = s) \\ \sigma_\mu^2 & (i = j, t \neq s) \\ 0 & (i \neq j) \end{array} \right\}. \tag{3.15}$$

This means that

$$\begin{aligned}E[uu^{'}] &:= \Omega = I_N \otimes \Sigma, \\ \Sigma &= \sigma_\nu^2 I_T + \sigma_\mu^2 J_T\end{aligned} \tag{3.16}$$

where $J_T = \iota_T \iota_T^{'}$. Equation 3.16 can be written more explicitly by:

$$\Omega = \begin{bmatrix} \Sigma & \mathbf{O} & \cdots & \cdots & \mathbf{O} \\ \mathbf{O} & \Sigma & \cdots & \cdots & \mathbf{O} \\ \vdots & \vdots & \ddots & & \vdots \\ \vdots & \vdots & & \ddots & \vdots \\ \mathbf{O} & \cdots & \cdots & \cdots & \Sigma \end{bmatrix}, \Sigma = \begin{bmatrix} \sigma_\mu^2 + \sigma_\nu^2 & \sigma_\mu^2 & \cdots & \cdots & \sigma_\mu^2 \\ \sigma_\mu^2 & \sigma_\mu^2 + \sigma_\nu^2 & \cdots & \cdots & \vdots \\ \vdots & \vdots & \ddots & & \vdots \\ \vdots & \vdots & & \ddots & \vdots \\ \sigma_\mu^2 & \cdots & \cdots & \cdots & \sigma_\mu^2 + \sigma_\nu^2 \end{bmatrix},$$

where $\mathbf{O}$ is a zero matrix of the same dimensions as Σ. β can be calculated by using GLS if σ_μ^2 and σ_ν^2 are known, the GLS formulas are derived similarly as for (3.11)

$$\hat{\beta}_{GLS} = (X^{'}(I_N \otimes \Sigma)^{-1}X)^{-1}X^{'}(I_N \otimes \Sigma)^{-1}y \tag{3.17}$$

$$\mathrm{Var}(\hat{\beta}_{GLS}) = (X^{'}(I_N \otimes \Sigma)^{-1}X)^{-1} \tag{3.18}$$

or by using FGLS, if we have estimators for σ_μ^2 and σ_ν^2.
Alternatively, we can assume that the covariance matrix is determined through some scedastic function dependent on some parameters γ, i.e. $\Omega(\gamma) \approx \Omega$.

FGLS for Random Effects

We can use fixed effect and pooled regression to find estimators for σ_μ^2 and σ_ν^2.

1. Run a fixed effects regression $y = Z\delta + Z_\mu\mu + \nu$ using the LSDV estimator (3.7).
2. Use the residuals, $\hat{\nu}_{i,t}$, from the first step to estimate $\hat{\sigma}_\nu^2 = \sum_{i,t=1}^{N,T} \frac{\hat{\nu}_{i,t}^2}{NT-N-K}$.
3. Run pooled regression $y = Z\delta + u$ using OLS.
4. Use the residuals, $\hat{u}_{i,t}$, to estimate $s_{PR}^2 = \sum_{i,t=1}^{N,T} \frac{\hat{u}_{i,t}^2}{NT-N-K}$
5. Finally, we have $s_{PR}^2 \approx \hat{\sigma}_\mu^2 + \hat{\sigma}_\nu^2$ which leads to $\hat{\sigma}_\mu^2 \approx s_{PR}^2 - \hat{\sigma}_\nu^2$

Now use the estimates $\hat{\sigma}_\nu^2$ and $\hat{\sigma}_\mu^2$ in (3.16) to obtain the FGLS estimator

$$\hat{\beta}_{FGLS} = (X'(I_N \otimes \hat{\Sigma})^{-1}X)^{-1}X'(I_N \otimes \hat{\Sigma})^{-1}y \tag{3.19}$$

$$\text{Var}(\hat{\beta}_{FGLS}) = (X'(I_N \otimes \hat{\Sigma})^{-1}X)^{-1} \tag{3.20}$$

The five steps above are presented by Baltagi [2021] a bit differently, however, the above method is equivalent to their presentation. Baltagi [2021] and several other works of literature calls this method the SWAR method due to it being developed and investigated by Swamy and Arora [1972]. The method also holds for the more general two-way error component case, we will present this method in more detail in section 3.2.

3.1.3 Testing

Testing for fixed effects vs. pooled regression

To test whether the model should include fixed effects or not an F-test is used. It tests the joint significance of the individual effects using the following null hypothesis given by $H_0 : \mu_1 = \mu_2 = \cdots = \mu_{N-1} = 0$. By Baltagi [2021], a Chow test using the restricted residual sum of squares (RRSS) and unrestricted residual sum of squares (URSS) allows for a regression comparison, with (RRSS) using the residuals from the pooled model seen in equation (3.3) and (URSS) using the LSDV residuals seen in equation (3.6). With this, we get the following F-test.

$$F_0 = \frac{(RRSS - URSS)/(N-1)}{URSS/(NT-N-K)} \overset{H_0}{\sim} F_{N-1,N(T-1)-K} \tag{3.21}$$

Testing Random effect vs. pooled regression

Following Baltagi [2021] the Breusch-Pagan test is used to inspect whether or not the model should include random effects. Defining the null hypothesis as $H_0 : \sigma_\mu^2 = 0$, i.e. there is no reason to use random effects. The test statistic is given by

$$\text{LM} = \frac{NT}{2(T-1)}\left[1 - \frac{\hat{u}'(I_N \otimes J_T)\hat{u}}{\hat{u}'\hat{u}}\right]^2 \sim \chi^2(1), \tag{3.22}$$

where $\hat{u}$ are the pooled regression vector of residuals. Additionally, if we were testing a time random effect, $H_0 : \sigma_\lambda^2 = 0$, we would use

$$\text{LM} = \frac{NT}{2(N-1)} \left[1 - \frac{\hat{u}'(J_N \otimes I_T)\hat{u}}{\hat{u}'\hat{u}} \right]^2 \sim \chi^2(1).$$

Testing Random effect vs. Fixed effect

In case both the fixed effects and random effects model are viable options, we use a Hausman test to help find the preferred model. The null hypothesis for the Hausman test is $H_0 : \hat{\beta}_{FE} = \hat{\beta}_{RE}$, the Hausman test statistic is given by the following

$$H = (\hat{\beta}_{FE} - \hat{\beta}_{RE})' (\text{Var}(\hat{\beta}_{FE}) - \text{Var}(\hat{\beta}_{RE}))^{-1} (\hat{\beta}_{FE} - \hat{\beta}_{RE}) \sim \chi^2(\dim(\hat{\beta})), \tag{3.23}$$

where $\dim(\hat{\beta})$ denotes the number of parameters, $\hat{\beta}_{FE}$ and $\hat{\beta}_{RE}$ denotes the estimated parameters under fixed effects and random effects, respectively.
In case we reject the null hypothesis, that is, there is a significant difference between the two estimates, we acknowledge there is individual level omission bias, that is the random effects model is misspecified. In this case, the fixed effects model is the preferred model as it accounts for all the (constant) individual level predictors.

Remark 10. It is important to realize in practice that for dependent variables, that have intricate underlying dynamics, it might be practically infeasible to include enough individual level predictors to make the Hausman test insignificant.

The next section will discuss an augmentation that adds a time effect to the error component, it captures effects that are the same through all cross-sections but are changing over time. An empirical argument for the inclusion of these effects could be that there is a new strain of Covid-19 on the rise in a country that has a different rate of spread. Another argument is that due to Denmark being so interconnected, the spread of the virus is more homogeneous across the country, the time effects will in this case capture this interconnectivity.

3.2 Two-Way Error Component Regression Model

The one-way regression model was given in equations (3.1) and (3.2) in section 3.1, we now expand the error component to allow for individual and time effects, the *two-way error component regression model* is given by:

$$\begin{aligned} y_{i,t} &= \alpha + X_{i,t}^{'}\beta + u_{i,t} \quad i = 1, \dots, N; \quad t = 1, \dots, T \\ u_{i,t} &= \mu_i + \lambda_t + \nu_{i,t} \quad i = 1, \dots, N \quad t = 1, \dots, T. \end{aligned} \tag{3.24}$$

Here $y_{i,t}$ is identical to the previous notation used in (3.1). Additionally, μ_i denotes the unobservable individual effects, whereas λ_t denotes unobservable time effects and $\nu_{i,t}$ denotes the idiosyncratic error. In vector form, the system can be written as

$$\begin{aligned} y &= Z\delta + u \\ u &= Z_\mu \mu + Z_\lambda \lambda + \nu, \end{aligned} \tag{3.25}$$

where $Z_\lambda = \iota_N \otimes I_T$ is a $NT \times T$ matrix of time dummies and $\lambda = (\lambda_1, \dots, \lambda_T)^{'}$, and as before, $Z_\mu = I_N \otimes \iota_T$ is a $NT \times N$ matrix and $\mu = (\mu_1, \dots, \mu_N)^{'}$.

3.2.1 The Two-Way Fixed Effects model

Analogously to assumption 4, let μ_i and λ_t be fixed parameters and $\nu_{i,t} \sim (0, \sigma_\nu^2)$ stochastic, then (3.24) is a two-way fixed effects model. The model now becomes

$$y = Z\delta + Z_\mu \mu + Z_\lambda \lambda + \nu. \tag{3.26}$$

While it is possible to use OLS it is ill-advised to do so, given that, like in section 3.1.1, the inversion of $Z^{*'}Z^*$ where $Z^* := [Z, Z_\mu, Z_\lambda]$ can be practically infeasible. As an alternative, Baltagi [2021] suggests using a within transformation on the basis of the FWL-theorem presented in theorem 1. To get the within transformation matrix consider

$$\begin{aligned} Q_{Z_\mu} &= I_{NT} - Z_\mu (Z_\mu' Z_\mu)^{-1} Z_\mu' \\ Q_{Z_\lambda} &= I_{NT} - Z_\lambda (Z_\lambda' Z_\lambda)^{-1} Z_\lambda', \end{aligned}$$

now, by multiplying these two projection matrices together we get a new projection matrix which projects onto the orthogonal complement of the span of Z_μ and Z_λ, their product yields

$$\begin{aligned} Q_{\mu\lambda} &:= Q_{Z_\mu} Q_{Z_\lambda} \\ &= \left(I_{NT} - Z_\mu (Z_\mu' Z_\mu)^{-1} Z_\mu'\right)\left(I_{NT} - Z_\lambda (Z_\lambda' Z_\lambda)^{-1} Z_\lambda'\right) \\ &= I_{NT} - Z_\mu (Z_\mu' Z_\mu)^{-1} Z_\mu^{'} - Z_\lambda (Z_\lambda' Z_\lambda)^{-1} Z_\lambda' \\ &+ Z_\lambda (Z_\lambda' Z_\lambda)^{-1} Z_\lambda' Z_\mu (Z_\mu' Z_\mu)^{-1} Z_\mu' \\ &= I_N \otimes I_T - I_N \otimes \bar{J}_T - \bar{J}_N \otimes I_T + (\bar{J}_N \otimes I_T)(I_N \otimes \bar{J}_T) \\ &= I_N \otimes I_T - I_N \otimes \bar{J}_T - \bar{J}_N \otimes I_T + \bar{J}_N \otimes \bar{J}_T \\ &= E_N \otimes E_T, \end{aligned} \tag{3.27}$$

where $E_N = I_N - \bar{J}_N$ and $E_T = I_T - \bar{J}_T$ and $\bar{J}_N = J_N/N$ and $\bar{J}_T = J_T/T$. The within transformation $Q_{\mu\lambda}$ removes the time and individual dependent variables from (3.26). The OLS estimation of equation (3.2) using the within transformation (3.27) yields the following

expression

$$\tilde{\beta} = (X^{'} Q_{\mu\lambda} X)^{-1} X^{'} Q_{\mu\lambda} y. \tag{3.28}$$

Remark 11. Just as with the one-way error component model, if we relax the assumption of no heteroscedasticity and/or no autocorrelation of the errors $\nu_{i,t}$ the variance of the parameter estimates has a sandwich form and OLS will be inefficient. To regain efficiency we again need to use GLS or FGLS, and as an alternative, we can use the robust estimators discussed for the one-way fixed effects model.

3.2.2 The Two-Way Random Effects Model

Analogously to assumption 5, if we assume that $\mathrm{E}[\mu_i \mid X_{i,t}] = \mathrm{E}[\lambda_t \mid X_{i,t}] = 0$ and assume that μ_u and λ_t are independent of $\nu_{i,t}$ then (3.25) is a random effects model. As with the one-way random effects model, define now $\mathrm{Var}(\mu_i) = \sigma_\mu^2$, $\mathrm{Var}(\lambda_t) = \sigma_\lambda^2$ and $\mathrm{Var}(\nu_{i,t}) = \sigma_\nu^2$ for all i and t such that

$$\begin{aligned}
\mathrm{Cov}(u_{i,t}, u_{j,s}) &= \mathrm{E}[u_{i,t}, u_{j,s}] \\
&= \mathrm{E}[(\mu_i + \lambda_t + \nu_{i,t})(\mu_j + \lambda_s + \nu_{j,s})] \\
&= \mathrm{E}[\mu_i \mu_j] + \mathrm{E}[\lambda_t \lambda_s] + \mathrm{E}[\nu_{i,t} \nu_{j,s}],
\end{aligned}$$

that is

$$\mathrm{Cov}(u_{i,t}, u_{j,s}) = \left\{ \begin{array}{c} \sigma_\mu^2 + \sigma_\lambda^2 + \sigma_\nu^2 \quad i = j, t = s \\ \sigma_\mu^2 \quad i = j, t \neq s \\ \sigma_\lambda^2 \quad i \neq j, t = s \\ 0 \quad i \neq j, t \neq s \end{array} \right\}$$

Now writing it more compactly using matrix notation yields

$$\begin{aligned}
\Omega &= \mathrm{E}[uu^{'}] \\
&= Z_\mu \, \mathrm{E}[\mu\mu^{'}] Z_\mu^{'} + Z_\lambda \, \mathrm{E}[\lambda\lambda^{'}] Z_\lambda^{'} + \sigma_\nu^2 I_{NT} \\
&= \sigma_\mu^2 (I_N \otimes J_T) + \sigma_\lambda^2 (J_N \otimes I_T) + \sigma_\nu^2 (I_N \otimes I_T) \\
&= I_N \otimes (\sigma_\mu^2 J_T + \sigma_\nu^2 I_T) + (J_N \otimes \sigma_\lambda^2 I_T) \\
&= I_N \otimes (\sigma_\mu^2 J_T + \sigma_\nu^2 I_T + \sigma_\lambda^2 I_T) + (J_N - I_N) \otimes \sigma_\lambda^2 I_T \\
&= I_N \otimes \Sigma + (J_N - I_N) \otimes \Lambda,
\end{aligned}$$

where $\Lambda := \sigma_\lambda^2 I_T$ and $\Sigma := \sigma_\mu^2 J_T + \sigma_\nu^2 I_T + \Lambda$. Writing it out explicitly yields

$$\Omega = \begin{bmatrix} \Sigma & \Lambda & \cdots & \cdots & \Lambda \\ \Lambda & \Sigma & \cdots & \cdots & \vdots \\ \vdots & \vdots & \ddots & & \vdots \\ \vdots & \vdots & & \ddots & \vdots \\ \Lambda & \cdots & \cdots & \cdots & \Sigma \end{bmatrix}, \Sigma = \begin{bmatrix} \sigma_\mu^2 + \sigma_\lambda^2 + \sigma_\nu^2 & \sigma_\mu^2 & \cdots & \cdots & \sigma_\mu^2 \\ \sigma_\mu^2 & \sigma_\mu^2 + \sigma_\lambda^2 + \sigma_\nu^2 & \cdots & \cdots & \vdots \\ \vdots & \vdots & \ddots & & \vdots \\ \vdots & \vdots & & \ddots & \vdots \\ \sigma_\mu^2 & \cdots & \cdots & \cdots & \sigma_\mu^2 + \sigma_\lambda^2 + \sigma_\nu^2 \end{bmatrix},$$

$$\Lambda = \begin{bmatrix} \sigma_\lambda^2 & 0 & \cdots & \cdots & 0 \\ 0 & \sigma_\lambda^2 & \cdots & \cdots & \vdots \\ \vdots & \vdots & \ddots & & \vdots \\ \vdots & \vdots & & \ddots & \vdots \\ 0 & \cdots & \cdots & \cdots & \sigma_\lambda^2 \end{bmatrix}.$$

Here the Σ and Λ are both matrices of dimension $T \times T$ and I_N and J_N are both matrices of dimension $N \times N$, making the covariance matrix, Ω, an $NT \times NT$ matrix.

GLS and FGLS for Two-Way Random Effects

The following computations in this subsection rely heavily on linear algebra results.

As with the one-way case we need to account for the inefficiency of OLS whenever we have random effects, so similar to what we did in (3.11) a GLS estimator of the parameters can be obtained by premultiplying (3.25) with Ψ' where $\Omega^{-1} = \Psi\Psi'$, i.e.

$$\sigma_\nu \Psi' y = \sigma_\nu \Psi' Z\delta + \sigma_\nu \Psi' u. \tag{3.29}$$

Note that in this case $\mathrm{E}[\sigma_\nu \Psi' \nu\nu' \Psi' \sigma_\nu] = \sigma_\nu^2 I$, in the one-way case the error component had unit variance which differs from this case, this is due to the multiplication of the standard deviation, σ_ν. Additionally, remark 6 still holds for this case as it is a non-singular linear transformation.
Then applying OLS to (3.29) yields

$$\begin{aligned} \hat{\delta}_{GLS} &= (Z'\Omega^{-1}Z)^{-1} Z'\Omega^{-1} y \\ \mathrm{Var}(\delta_{GLS}) &= (Z'\Omega^{-1}Z)^{-1} \end{aligned} \tag{3.30}$$

The covariance matrix is almost never known in practice so we need to discuss ways to estimate it. So start by rewriting the covariance matrix

$$\begin{aligned} \Omega &= \sigma_\mu^2 (I_N \otimes J_T) + \sigma_\lambda^2 (J_N \otimes I_T) + \sigma_\nu^2 (I_N \otimes I_T) \\ &= T\sigma_\mu^2 (I_N \otimes \bar{J}_T) + N\sigma_\lambda^2 (\bar{J}_N \otimes I_T) + \sigma_\nu^2 (I_N \otimes I_T) \\ &= T\sigma_\mu^2 \left((E_N + \bar{J}_N) \otimes \bar{J}_T \right) + N\sigma_\lambda^2 \left(\bar{J}_N \otimes (E_T + \bar{J}_T) \right) + \sigma_\nu^2 ((E_N + \bar{J}_N) \otimes (E_T + \bar{J}_T)) \\ &= \sigma_\nu^2 (E_N \otimes E_T) + (T\sigma_\mu^2 + \sigma_\nu^2)(E_N \otimes \bar{J}_T) \\ &+ (N\sigma_\lambda^2 + \sigma_\nu^2)(\bar{J}_N \otimes E_T) + (T\sigma_\mu^2 + N\sigma_\lambda^2 + \sigma_\nu^2)(\bar{J}_N \otimes \bar{J}_T). \end{aligned}$$

These four terms on the RHS are in fact a spectral decomposition of the covariance matrix. The first thing to notice is that each of the Kronecker products are projections, hence we define $Q_1 := E_N \otimes E_T$, $Q_2 := E_N \otimes \bar{J}_T$, $Q_3 := \bar{J}_N \otimes E_T$ and $Q_4 := \bar{J}_N \otimes \bar{J}_T$, to show that they are projections simply verify their idempotency and symmetry.

Projection matrices can only have eigenvalues 1 and 0, to show this consider x to be an eigenvector of a projection P with eigenvalue λ then $Px = \lambda x$, now using the idempotency property of P yields

$$PPx = \lambda Px = \lambda^2 x,$$

now since $x \neq \mathbf{0}$ then $\lambda^2 = \lambda$ which has solutions 1 and 0.
Now, since the projections only has these two eigenvalues the scalars $\lambda_1 := \sigma_\nu^2$, $\lambda_2 := T\sigma_\mu^2 + \sigma_\nu$, $\lambda_3 := N\sigma_\lambda + \sigma_\nu^2$ and $\lambda_4 = T\sigma_\mu^2 + N\sigma_\lambda^2 + \sigma_\nu^2$ must be the eigenvalues of the covariance matrix. To realize this, consider the eigendecomposition of the projections $Q_i = U_i \Lambda_i^* U_i^{-1}$ where the U_i matrix is a square matrix with eigenvectors as columns, and the Λ_i^* is a diagonal matrix with the eigenvalues as diagonal elements, now since the eigenvalues of the projections are either 0 or 1 multiplying by λ_i yields

$$\begin{aligned}\lambda_i Q_i &= U_i \lambda_i \Lambda_i^* U_i^{-1} \\ &= U_i \Lambda_i U_i^{-1},\end{aligned}$$

where $\Lambda_i = \lambda_i \Lambda_i^*$. The spectral decomposition of Ω can now be written as

$$\Omega = \sum_{i=1}^{4} \lambda_i Q_i.$$

The multiplicity of each of the eigenvalues of the covariance matrix is the trace of the corresponding projection matrix, to see this consider

$$\begin{aligned}\operatorname{tr}(Q_i) &= \operatorname{tr}\big(U_i \Lambda_i^* U_i^{-1}\big) \\ &= \operatorname{tr}\big(\Lambda_i^* U_i U_i^{-1}\big) \\ &= \operatorname{tr}(\Lambda_i^*)\end{aligned}$$

where the property $\operatorname{tr}(AB) = \operatorname{tr}(BA)$ for square matrices A and B was used in the second equality.
Finally, the specific values of the multiplicities can now be derived, consider now

$$\begin{aligned}\operatorname{tr}(Q_1) &= \operatorname{tr}(E_N \otimes E_T) \\ &= \operatorname{tr}(E_N)\operatorname{tr}(E_T) \\ &= \operatorname{tr}\big(I_N - \bar{J}_N\big)\operatorname{tr}\big(I_T - \bar{J}_T\big) \\ &= \big[\operatorname{tr}(I_N) - \operatorname{tr}\big(\bar{J}_N\big)\big]\big[\operatorname{tr}(I_T) - \operatorname{tr}\big(\bar{J}_T\big)\big] \\ &= (N-1)(T-1),\end{aligned}$$

where the property $\operatorname{tr}(A \otimes B) = \operatorname{tr}(A)\operatorname{tr}(B)$ for square matrix A and B has been used in the second equality, and $\operatorname{tr}(A + B) = \operatorname{tr}(A) + \operatorname{tr}(B)$ was used in the fourth equality.
Similar results can be obtained for the remaining projection matrices, the results are given by

$$\begin{aligned}\operatorname{tr}(Q_1) &= (N-1)(T-1) \\ \operatorname{tr}(Q_2) &= N-1 \\ \operatorname{tr}(Q_3) &= T-1 \\ \operatorname{tr}(Q_4) &= 1.\end{aligned}$$

The spectral decomposition is useful to us as it follows that

$$\Omega^r = \sum_{i=1}^{4} \lambda_i^r Q_i,$$

where r is an arbitrary scalar.
Notice now that $Q_i u \sim (0, \lambda_i Q_i)$ such that

$$\widehat{\lambda_i} = u' Q_i u / \operatorname{tr}(Q_i), \tag{3.31}$$

are estimators of λ_i for $i = 1, 2, 3$. Given the definitions of λ_i for $i = 1, 2, 3$ and using (3.31) estimators of the parameters, σ_ν^2, σ_μ^2 and σ_λ^2, are given by

$$\begin{aligned}
\tilde{\sigma}_\nu^2 &= u' Q_1 u / [(N-1)(T-1)] \\
\tilde{\sigma}_\mu^2 &= \frac{u' Q_2 u / [N-1] - u' Q_1 u / [(N-1)(T-1)]}{T} \\
\tilde{\sigma}_\lambda^2 &= \frac{u' Q_3 u / [T-1] - u' Q_1 u / [(N-1)(T-1)]}{N}.
\end{aligned} \tag{3.32}$$

As the true disturbances, u, are unknown, replacing them by the residuals, $\hat{u}$, obtained by applying the two-way within transformation given by (3.27) will yield feasible estimators of λ_i for $i = 1, 2, 3$.

$$\begin{aligned}
\hat{\sigma}_\nu^2 &= \hat{u}' Q_1 \hat{u} / [(N-1)(T-1)] \\
\hat{\sigma}_\mu^2 &= \frac{\hat{u}' Q_2 \hat{u} / [N-1] - \hat{u}' Q_1 \hat{u} / [(N-1)(T-1)]}{T} \\
\hat{\sigma}_\lambda^2 &= \frac{\hat{u}' Q_3 \hat{u} / [T-1] - \hat{u}' Q_1 \hat{u} / [(N-1)(T-1)]}{N}
\end{aligned} \tag{3.33}$$

Amemiya [1971] investigates the asymptotic properties of these estimators and notes that they share the same asymptotic distribution, that is, the asymptotic distribution of the estimators in (3.32) are the same as the ones in (3.33). Finally, we have an estimator for the covariance matrix given by

$$\hat{\Omega} = I_N \otimes (\hat{\sigma}_\mu^2 J_T + \hat{\sigma}_\nu^2 I_T + \hat{\sigma}_\lambda^2 I_T) + (J_N - I_N) \otimes \hat{\sigma}_\lambda^2 I_T,$$

which substituted into (3.30) yields the FGLS estimators of the parameters and their variances.

Baltagi [2021] notes that in practice it is always good advice to compare different estimators which motivates the next set of estimators.
Swamy and Arora [1972] develops the next set of estimators for the eigenvalues of the covariance matrix through a 3-step method.
They start by applying the two-way within transformation to (3.25) which yields

$$\begin{aligned}
Q_1 y &= Q_1 X \beta + \nu \\
&= P_{Q_1 X} Q_1 y + Q_{Q_1 X} Q_1 y,
\end{aligned}$$

note that the FWL-theorem was used in the first equation and the identity $I = P_{Q_1 X} + Q_{Q_1 X}$ was used in the second one. The second term on the right hand side, RHS, reduces to ν such that

$$\begin{aligned}
\nu' \nu &= (Q_1 y - P_{Q_1 X} Q_1 y)' (Q_1 y - P_{Q_1 X} Q_1 y) \\
&= y' Q_1 y - y' Q_1 P_{Q_1 X} Q_1 y.
\end{aligned}$$

An estimator of λ_1 is then given by

$$\widehat{\widehat{\lambda}}_1 = \left[y' Q_1 y - y' Q_1 P_{Q_1 X} Q_1 y \right] / \left[(N-1)(T-1) - K \right]. \tag{3.34}$$

They do similar transformations with Q_2 and Q_3 to get estimators of λ_2 and λ_3 which are

given by

$$\widehat{\widehat{\lambda}}_2 = \left[y^{'} Q_2 y - y^{'} Q_2 P_{Q_2 X} Q_2 y \right] / [(N-1) - K]$$

and

$$\widehat{\widehat{\lambda}}_3 = \left[y^{'} Q_3 y - y^{'} Q_3 P_{Q_3 X} Q_3 y \right] / [(T-1) - K].$$

Now they use these estimates to obtain estimators $\hat{\hat{\sigma}}_\nu^2$, $\hat{\hat{\sigma}}_\mu^2$ and $\hat{\hat{\sigma}}_\lambda^2$ similar to how we did for (3.33). Next is to use these estimators to obtain

$$\hat{\hat{\Omega}} = I_N \otimes (\hat{\hat{\sigma}}_\mu^2 J_T + \hat{\hat{\sigma}}_\nu^2 I_T + \hat{\hat{\sigma}}_\lambda^2 I_T) + (J_N - I_N) \otimes \hat{\hat{\sigma}}_\lambda^2 I_T,$$

and finally, use this estimator in (3.30) to get another estimator of the parameters and their variances.

3.3 Spatial Error Component Regression Model

Given the nature of the data used in this project, specifically that the municipalities in our data lie up against one another, it follows that some events or effects specific to one municipality could potentially have some effects on neighboring municipalities, these effects are called spatial or spatial spillover effects. Anselin et al. [2008] proposes a linear regression model formulated by

$$y = \alpha + X\beta + u \tag{3.35}$$

with two-way error components

$$u = (\iota_T \otimes I_N)\,\mu + (I_T \otimes \iota_N)\,\lambda + \varepsilon \tag{3.36}$$

$$\varepsilon = \rho\,(I_T \otimes W_N)\,\varepsilon + \nu, \tag{3.37}$$

where W_N is a $N \times N$ matrix of spatial weights with zero diagonal elements. Assume $\mu \sim i.i.d.(0, \sigma_\mu^2 I_N)$ and $\lambda \sim i.i.d.(0, \sigma_\lambda^2 I_T)$, these vectors denote the individual and time effects respectively, furthermore, ε is a vector of spatially autocorrelated innovations following the process given in (3.37). The vector ν is assumed $i.i.d.(0, \sigma_\nu^2 I_{NT})$ and independent of μ_i and λ_t. The model given by equations (3.35), (3.36) and (3.37) is called the spatial two-way error component regression model or simply the Anselin model, as it was first derived by Luc Anselin in 1988. In fact, there are more general spatial models than the one presented above, however, we find this model to be adequate and we refer to Anselin et al. [2008] for a repository of spatial panel data models.
It is important to notice that the stacking of observations is done by first arranging by time and then individual, i.e. the first N elements of y are the first observations for each individual, the next N observations are the second observation for each individual, etc.

Now, define $B := I_N - \rho W_N$ such that we can rewrite (3.37) as

$$\begin{aligned}
\varepsilon - \rho\,(I_T \otimes W_N)\,\varepsilon &= \nu \\
(I_T \otimes I_N)\varepsilon - (I_T \otimes \rho W_N)\,\varepsilon &= \nu \\
(I_T \otimes (I_N - \rho W_N))\,\varepsilon &= \nu \\
\varepsilon &= (I_T \otimes (I_N - \rho W_N))^{-1}\,\nu \\
\varepsilon &= \left(I_T \otimes B^{-1}\right)\nu.
\end{aligned}$$

We can now write our error component as

$$u = (\iota_T \otimes I_N)\,\mu + (I_T \otimes \iota_N)\,\lambda + \left(I_T \otimes B^{-1}\right)\nu \tag{3.38}$$

with the variance given by

$$\begin{aligned}
\Omega := \mathrm{E}[uu^{'}] &= \sigma_\mu^2(J_T \otimes I_N) + \sigma_\lambda^2(I_T \otimes J_N) + \sigma_\nu^2(I_T \otimes (B'B)^{-1}) \\
&= \sigma_\nu^2 \left[J_T \otimes \left(\frac{\sigma_\mu^2}{\sigma_\nu^2} I_N \right) + I_T \otimes \left(\frac{\sigma_\lambda^2}{\sigma_\nu^2} J_N + (B^{'}B)^{-1} \right) \right] \\
&= \sigma_\nu^2 \Sigma.
\end{aligned}$$

3.3.1 Maximum Likelihood Estimation

Now under the assumption of normality, the log-likelihood function, ignoring the constant, is given by

$$\begin{aligned}\ell &= -\frac{1}{2}\ln|\Omega| - \frac{1}{2}u'\Omega^{-1}u \\ &= -\frac{NT}{2}\ln\sigma_\nu^2 - \frac{1}{2}\ln|\Sigma| - \frac{1}{2\sigma_\nu^2}u'\Sigma^{-1}u. \end{aligned} \tag{3.39}$$

To simplify further we need the following corollary [Magnus, 1982].

Corollary 1

Let Λ be a diagonal $q \times q$ matrix, $q \geq 2$, with positive diagonal elements, A and B square matrices of order p, and s_q a $q \times 1$ vector of ones, then the $pq \times pq$ matrix G is given by,

$$G = \Lambda\iota_q\iota_q'\Lambda \otimes A + \Lambda \otimes B,$$

has determinant

$$|G| = |\Lambda|^p|C||B|^{q-1},$$

where

$$C = B + \alpha A \quad \textit{and} \quad \alpha = \mathrm{tr}(\Lambda),$$

furthermore, if G is non-singular, its inverse is

$$G^{-1} = \frac{1}{\alpha}\iota_q\iota_q' \otimes (C^{-1} - B^{-1}) + \Lambda^{-1} \otimes B^{-1}.$$

Now using corollary 1 yields

$$\begin{aligned}|\Sigma| &= \left| J_T \otimes \left(\frac{\sigma_\mu^2}{\sigma_\nu^2}I_N\right) + I_T \otimes \left(\frac{\sigma_\lambda^2}{\sigma_\nu^2}J_N + (B'B)^{-1}\right)\right| \\ &= |I_T|^N \left|\frac{\sigma_\lambda^2}{\sigma_\nu^2}J_N + (B'B)^{-1} + \frac{T\sigma_\mu^2}{\sigma_\nu^2}I_N\right| \left|\frac{\sigma_\lambda^2}{\sigma_\nu^2}J_N + (B'B)^{-1}\right|^{T-1} \\ &= \left|\frac{\sigma_\lambda^2}{\sigma_\nu^2}J_N + (B'B)^{-1} + \frac{T\sigma_\mu^2}{\sigma_\nu^2}I_N\right| \left|\frac{\sigma_\lambda^2}{\sigma_\nu^2}J_N + (B'B)^{-1}\right|^{T-1}\end{aligned}$$

and

$$\begin{aligned}\Sigma^{-1} = \bar{J}_T \otimes &\left[\left(\frac{\sigma_\lambda^2}{\sigma_\nu^2}J_N + (B'B)^{-1} + \frac{T\sigma_\mu^2}{\sigma_\nu^2}I_N\right)^{-1} - \left(\frac{\sigma_\lambda^2}{\sigma_\nu^2}J_N + (B'B)^{-1}\right)^{-1}\right] \\ &+ I_T \otimes \left(\frac{\sigma_\lambda^2}{\sigma_\nu^2}J_N + (B'B)^{-1}\right)^{-1}.\end{aligned}$$

Substituting these back into the (3.39) and simplifying yields

$$\begin{aligned}\ell &= -\frac{NT}{2}\ln\sigma_\nu^2 - \frac{1}{2}\ln|\Sigma| - \frac{1}{2\sigma_\nu^2}u'\Sigma^{-1}u \\ &= -\frac{NT}{2}\ln\sigma_\nu^2 - \frac{1}{2}\left|\frac{\sigma_\lambda^2}{\sigma_\nu^2}J_N + (B'B)^{-1} + \frac{T\sigma_\mu^2}{\sigma_\nu^2}I_N\right| - \frac{T-1}{2}\left|\frac{\sigma_\lambda^2}{\sigma_\nu^2}J_N + (B'B)^{-1}\right|^{T-1} \\ &- \frac{1}{2\sigma_\nu^2}u'\left\{\bar{J}_T \otimes \left[\left(\frac{\sigma_\lambda^2}{\sigma_\nu^2}J_N + (B'B)^{-1} + \frac{T\sigma_\mu^2}{\sigma_\nu^2}I_N\right)^{-1} - \left(\frac{\sigma_\lambda^2}{\sigma_\nu^2}J_N + (B'B)^{-1}\right)^{-1}\right]\right. \\ &\left. + I_T \otimes \left(\frac{\sigma_\lambda^2}{\sigma_\nu^2}J_N + (B'B)^{-1}\right)^{-1}\right\}u.\end{aligned}$$

It is clear that the computationally difficult terms, determinants and inverses, in the log-likelihood get bigger as N grows.
Now maximizing the log-likelihood function yields the desired parameter estimates.

Special Cases

If we assume that we have no individual effects or no time effects, the likelihood expression simplifies a great deal. Start by assuming that we have no time effects such that (3.38) becomes

$$u = (\iota_T \otimes I_N)\,\mu + \left(I_T \otimes B^{-1}\right)\nu,$$

hence

$$\begin{aligned}\mathrm{E}[uu'] &= \sigma_\mu^2(J_T \otimes I_N) + \sigma_\nu^2(I_T \otimes (B'B)^{-1}) \\ &= \sigma_\nu^2\left[J_T \otimes \left(\frac{\sigma_\mu^2}{\sigma_\nu^2}I_N\right) + I_T \otimes \left(B'B\right)^{-1}\right] \\ &= \sigma_\nu^2\Sigma_\mu.\end{aligned}$$

Using corollary 1 yields

$$|\Sigma_\mu| = \left|(B'B)^{-1} + T\frac{\sigma_\mu^2}{\sigma_\nu^2}I_N\right|\left|(B'B)^{-1}\right|^{T-1},$$

and

$$\Sigma_\mu^{-1} = \bar{J}_T \otimes \left(\left((B'B)^{-1} + T\frac{\sigma_\mu^2}{\sigma_\nu^2}I_N\right)^{-1} - B'B\right) + I_T \otimes B'B.$$

Now analogously we assume there are no individual effects such that

$$u = (I_T \otimes \iota_N)\,\lambda + \left(I_T \otimes B^{-1}\right)\nu$$

hence

$$\begin{aligned}\mathrm{E}[uu'] &= \sigma_\lambda^2(I_T \otimes J_N) + \sigma_\nu^2(I_T \otimes (B'B)^{-1}) \\ &= \sigma_\nu^2\left[I_T \otimes \left(\frac{\sigma_\lambda^2}{\sigma_\nu^2}J_N + (B'B)^{-1}\right)\right] \\ &= \sigma_\nu^2\Sigma_\lambda.\end{aligned}$$

Now the determinant of Σ_λ is given by

$$|\Sigma_\lambda| = \left| I_T \otimes \left(\frac{\sigma_\lambda^2}{\sigma_\nu^2} J_N + (B^{'} B)^{-1} \right) \right|^T$$

with inverse

$$\Sigma_\lambda^{-1} = I_T \otimes \left(\frac{\sigma_\lambda^2}{\sigma_\nu^2} J_N + (B^{'} B)^{-1} \right)^{-1}.$$

To avoid cluttering we avoid writing out the log-likelihood functions with their covariance matrices, however, it is trivial to simply substitute these into (3.39) to get the log-likelihood.

Chapter 4

Regime-Switching Models

Under tranquil market conditions, many types of financial time series show low volatility persistence, and in other periods during financial crises or major international events they shift in their behavior.
A way of modeling this behavior is to augment the GARCH modeling framework by introducing regime switching, i.e. the RS-GARCH model.

4.1 Regime Switching GARCH Model

The standard GARCH(1,1) model is given by

$$y_t = \mu_t + \epsilon_t = \mu_t + \sqrt{h_t}u_t \quad u_t \sim i.i.d.\mathcal{D}(0,1,\xi)$$
$$h_t = \alpha_0 + \alpha_1\epsilon_{t-1}^2 + \beta h_{t-1}^2,$$

where μ_t is the conditional mean, ϵ_t is the the error process, $\mathcal{D}$ is some specified distribution and ξ is a vector representing distribution specific parameters like skewness, etc. To ensure positivity of the conditional variance we assume that $\alpha_0 > 0, \alpha_1 > 0$ and $\beta \geq 0$, and to ensure stationarity we assume that $\alpha_1 + \beta_1 < 1$. Under these conditions the process y_t has an unconditional variance given by $\sigma^2 := \mathrm{E}[(y_t - \mu_t)^2] = \frac{\alpha_0}{1-\alpha_1-\beta}$.

Assumption 6. For simplicity, the conditional mean is assumed to be zero, that is $\mu_t = 0$.

Remark 12. Regime switching is an augmentation that allows for switching structural dynamics of the process y_t, depending on the application the structural changes can be applied to the conditional mean, the conditional variance, the underlying standardized innovation process, or any combination of those. However, for our applications the conditional mean has been filtered away as described in 2.1, hence our primary focus will be on regime switching in the conditional variance.

The RS-GARCH model is an expansion of the standard GARCH model which allows for regime specific structural dynamics of the conditional variance of y_t, hence the specification of h_t is dependent on which regime we are in at time t.
We will need to assume that y_t is not autocorrelated, i.e. $E[y_t, y_{t-1}] = 0$, in fact under assumption 6 this is the case [Bauwens et al., 2006].

The regime switching are introduced through a homogeneous[1] Markov chain state variable $s_t \in \{1, 2, \ldots, n\}$ which is realised by

$$\Pr(s_t = j \mid s_{t-1} = i, s_{t-2} = k, \ldots, \mathcal{I}_{t-1}) = \Pr(s_t = j \mid s_{t-1} = i) =: p_{i,j} \tag{4.1}$$

which denotes the probability of transitioning from state $s_{t-1} = i$ to state $s_t = j$. Now define

[1] A Markov chain being homogeneous means that the transition probabilities are independent from time.

the (probability) transition matrix by

$$P := \begin{bmatrix} p_{1,1} & \cdots & p_{1,n} \\ \vdots & \ddots & \vdots \\ p_{n,1} & \cdots & p_{n,n} \end{bmatrix}.$$

The following constraints hold $0 < p_{i,j} < 1, \forall i,j \in \{1,2,\ldots,n\}$ and $\sum_{j=1}^{n} p_{i,j} = 1, \forall i \in \{1,2,\ldots,n\}$, where the second constraint means that every row from the transition matrix sums to unity.

Now, an RS-GARCH(1,1) model under assumption 6 can be written as

$$\begin{aligned} y_t &= \sqrt{h_{s_t,t}}u_{s_t,t}, \quad u_{s_t,t} \sim i.i.d.\mathcal{D}_{s_t}(0,1) \\ h_{s_t,t} &= \alpha_{0,s_t} + \alpha_{1,s_t}y_{t-1}^2 + \beta_{s_t}h_{s_{t-1},t-1} \\ p_{i,j} &= \Pr\left(s_t = j \mid s_{t-1}\right), \quad j = 1,2,\ldots,n, \end{aligned} \tag{4.2}$$

where the unconditional variance in each regime is given by

$$\sigma_{s_t}^2 = \mathrm{E}[y_t^2|s_t] = \frac{\alpha_{0,s_t}}{1-\alpha_{1,s_t}-\beta_{s_t}}. \tag{4.3}$$

Note that *unconditional* variance is slightly misleading as it is clearly dependent on the state. The conditional variance can be interpreted as

$$h_{s_t,t} \equiv h(h_{s_{t-1},t-1}, y_{t-1}, \theta_{s_t}) \tag{4.4}$$

where $\theta_{s_t} := (\alpha_{0,s_t}, \alpha_{1,s_t}, \beta_{s_t})$ is a vector of model specific parameters, i.e. the conditional variance is a function of past values of y, h and its regime dependent model parameters. It is easily generalized to higher order GARCH models by including the appropriate parameters in the model specific parameter vector and the additional past values of h and y.

Remark 13. Note that the distribution, $\mathcal{D}_{s_t}$, of the standardised innovations can be dependent on the state, s_t, e.g. it can be a skewed normal distribution in one state and a skewed Student's t-distribution in another. We will only consider the case where the distribution is the same, e.g. normal, across states but distribution specific parameters can change, like shape and skewness.

The final element of the formulation of the RS-GARCH model is the specification of the conditional distribution of the standardised innovations, note that $u_{s_t,t} = y_t/h_{s_t,t}$. The conditional distribution of the y_t model can now be written as

$$y_t \mid (s_t, \mathcal{I}_{t-1}) \sim \mathcal{D}(0, h_{s_t,t}, \xi_{s_t}),$$

where $\mathcal{D}(0, h_{s_t,t}, \xi_{s_t})$ denotes the specified conditional distribution with zero mean, conditional variance $h_{s_t,t}$ and a vector ξ_{s_t} containing distribution specific parameters. Note, the standardised innovations have distribution $u_{s_t,t} \sim i.i.d.\mathcal{D}(0,1,\xi_{s_t})$.
We can now write the conditional PDF of y_t compactly as

$$f_{\mathcal{D}}(y_t \mid s_t, \mathcal{I}_{t-1}; \Psi),$$

where $\Psi \equiv (\theta_1, \xi_1, \ldots, \theta_n, \xi_n, P)$.

For estimation through maximum likelihood, it is required to choose which type of conditional distribution the standardized innovations have, common choices for financial time series are normal, student-t and generalized error distribution (GED).

The PDF of the standard normal distribution is given by

$$f_N(u_{s_t,t}) = \frac{1}{\sqrt{2\pi}} e^{-\frac{1}{2}u_{s_t,t}^2}.$$

It follows that $u_{s_t,t} \sim i.i.d.N(0,1)$ thus $y_t \mid (s_t, \mathcal{I}_{t-1}) \sim N(0, h_{s_t,t})$. The normal distribution does not account for the fat tails often seen in financial data, to overcome this, the standardized Student-t distribution is often used, that is

$$f_S(u_{s_t,t} \mid \nu_{s_t}) = \frac{\Gamma(\frac{\nu_{s_t}+1}{2})}{\sqrt{(\nu_{s_t}-2)\pi}\Gamma(\frac{\nu_{s_t}}{2})} \left(1 + \frac{u_{s_t,t}^2}{(\nu_{s_t}-2)}\right)^{-\frac{\nu_{s_t}+1}{2}}, \qquad u_{s_t,t} \in \mathbb{R},$$

where $\Gamma(\cdot)$ is the gamma function and ν_{s_t} is the number of degrees of freedom. With this it then follows that $u_{s_t,t} \sim i.i.d.t(0,1,\nu_{s_t})$ and $y_t \mid (s_t, \mathcal{I}_{t-1}) \sim t(0, h_{s_t,t}, \nu_{s_t})$ [Petersen, 2015].

Another distribution of interest is the standardized generalized error distribution, abbreviated as GED. The GED is given by

$$f_{GED}(u_{s_t,t} \mid \tau_{s_t}) = \frac{\tau e^{-\frac{1}{2}\left|\frac{u_{s_t,t}}{\lambda}\right|^{\tau_{s_t}}}}{\lambda 2^{(1+\frac{1}{\tau_{s_t}})}\Gamma(\frac{1}{\tau_{s_t}})}, \qquad \lambda = \left(\frac{\Gamma(\frac{1}{\tau_{s_t}})}{4^{\frac{1}{\tau_{s_t}}}\Gamma(\frac{3}{\tau_{s_t}})}\right)^{\frac{1}{2}}, \qquad u_{s_t,t} \in \mathbb{R},$$

where $\tau_{s_t} > 0$ is the shape parameter. Special cases of the distribution are obtained for different values of τ_{s_t}, for $\tau_{s_t} = 1$ the GED reduces to the standard Laplace distribution, $\tau_{s_t} = 2$ gives the standard normal distribution and $\tau_{s_t} \to \infty$ gives a uniform distribution on the interval $[-1,1]$. For the GED it follows that $u_{s_t,t} \sim i.i.d.GED(0,1,\tau_{s_t})$ and $y_t \mid (s_t, \mathcal{I}_{t-1}) \sim GED(0, h_{s_t,t}, \tau_{s_t})$.

As an extension to the distributions shown above, Trottier and Ardia [2016] developed a simple way of introducing skewness to any unimodal[2] standardized distribution by introducing an additional parameter $\zeta > 0$, which denotes the asymmetry. Let a symmetric unimodal standardized PDF be given by $f_1(z)$, and let the skewed unimodal PDF be given by $f_\zeta(z)$, with mean and variance given by

$$\mu_\zeta = M_1(\zeta - \zeta^{-1})$$
$$\sigma_\zeta^2 = (1 - M_1^2)(\zeta^2 + \zeta^{-2}) + 2M_1^2 - 1,$$

where $M_1 = 2\int_0^\infty u f_1(u)du$. Then PDF of the skewed distribution is given by

$$f_\zeta(z) \equiv \frac{2\sigma_\zeta}{\zeta + \zeta^{-1}} f_1(z_\zeta), \qquad z_\zeta \equiv \begin{cases} \zeta^{-1}(\sigma_\zeta z + \mu_\zeta) & \text{if} \quad z \geq -\mu_\zeta/\sigma_\zeta \\ \zeta(\sigma_\zeta z + \mu_\zeta) & \text{if} \quad z < -\mu_\zeta/\sigma_\zeta \end{cases} \tag{4.5}$$

The equation above shows how skewness can be introduced to a PDF already defined previously using only the PDF and a parameter ζ describing the asymmetry. Note that if $\zeta = 1$ then $f_\zeta(z) = f_1(z)$.

[2] A unimodal distribution is a distribution with one clear peak

We get the CDF by integrating the PDF such that

$$F_\zeta(x) \equiv \int_{-\infty}^{x} f_\zeta(z)\,\mathrm{d}\,z$$
$$= \begin{cases} \frac{2\sigma_\zeta}{\zeta+\zeta^{-1}} \int_{-\mu_\zeta/\sigma_\zeta}^{x} f_1\left(\zeta^{-1}[\sigma_\zeta z+\mu_\zeta]\right)\mathrm{d}\,z + \frac{2\sigma_\zeta}{\zeta+\zeta^{-1}} \int_{-\infty}^{-\mu_\zeta/\sigma_\zeta} f_1(\zeta[\sigma_\zeta z+\mu_\zeta])\,\mathrm{d}\,z, \\ \text{for } x \geq -\frac{\mu_\zeta}{\sigma_\zeta} \\ \\ \frac{2\sigma_\zeta}{\zeta+\zeta^{-1}} \int_{-\infty}^{x} f_1(\zeta[\sigma_\zeta z+\mu_\zeta])\,\mathrm{d}\,z, \\ \text{for } x < -\frac{\mu_\zeta}{\sigma_\zeta} \end{cases}$$

Now using integration by substitution for the first expression yields

$$F_\zeta(x) = \frac{2}{\zeta+\zeta^{-1}}\zeta \int_0^{\zeta^{-1}[\sigma_\zeta x+\mu_\zeta]} f_1(u)\,\mathrm{d}\,u + \frac{2}{\zeta+\zeta^{-1}}\zeta^{-1} \int_{-\infty}^{0} f_1(u)\,\mathrm{d}\,u, \quad x \geq -\frac{\mu_\zeta}{\sigma_\zeta}$$
$$= \frac{2}{\zeta+\zeta^{-1}}\left[\zeta\cdot\left(F_1\left(\zeta^{-1}[\sigma x+\mu]\right)-F_1(0)\right)+\zeta^{-1}F_1(0)\right], \quad x \geq -\frac{\mu_\zeta}{\sigma_\zeta}$$

where F_1 is the standard normal CDF, doing similarly to the second expression yields

$$F_\zeta(x) = \frac{2}{\zeta+\zeta^{-1}}\zeta^{-1} \int_{-\infty}^{\zeta[\sigma_\zeta x+\mu_\zeta]} f_1(u)\,\mathrm{d}\,u, \quad x < -\frac{\mu_\zeta}{\sigma_\zeta}$$
$$= \frac{2}{\zeta+\zeta^{-1}}\zeta^{-1}F_1(\zeta[\sigma_\zeta x+\mu_\zeta]), \quad x < -\frac{\mu_\zeta}{\sigma_\zeta}.$$

Example 1

This example acts as an illustration of how skewness is introduced to a standardized unimodal PDF. Now assume that $u \sim N(0,1)$, then the PDF of u is given by

$$f_N(u) = \frac{1}{\sqrt{2\pi}}e^{-\frac{1}{2}u^2}.$$

Now applying (4.5) yields

$$f_\zeta(u) = \frac{2\sigma_\zeta}{\zeta+\zeta^{-1}}\frac{1}{\sqrt{2\pi}}e^{-\frac{1}{2}u_\zeta^2}, \qquad u_\zeta \equiv \begin{cases} \zeta^{-1}(\sigma_\zeta u+\mu_\zeta) & \text{if} \quad u \geq -\mu_\zeta/\sigma_\zeta \\ \zeta(\sigma_\zeta u+\mu_\zeta) & \text{if} \quad u < -\mu_\zeta/\sigma_\zeta \end{cases}$$

Figure 4.1 below shows these PDFs plotted over the interval $[-5,5]$.

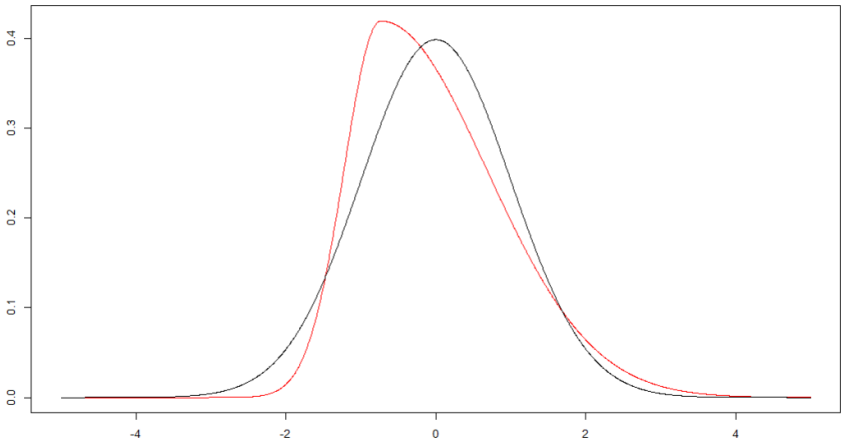

Figure 4.1. Skewness transform of a standard normal distribution with asymmetry parameter $\zeta = 1.7$.

We now present some extensions to the basic GARCH model, each of these extensions redefines the conditional variance specification of $h_{s_t,t}$ [Ardia et al., 2019]. To avoid notational cluttering in the following specifications, we omit the index that represents the specific state, s_t.

The first extension is the Exponential GARCH model, eGARCH, this extension tries to model the *leverage effect*[3], the specification is given by

$$\ln(h_t) \equiv \alpha_0 + \alpha_1(|u_{t-1}| - \mathrm{E}\left[|u_{t-1}|\right]) + \alpha_2 u_{t-1} + \beta \ln(h_{t-1}). \tag{4.6}$$

The leverage effect predicts that $\alpha_2 < 0$ in the eGARCH specification. For the eGARCH model the vector of model specific parameters are given by $\theta = (\alpha_0, \alpha_{1,}, \alpha_2, \beta)'$. Positivity of h_t through the model specification and stationarity requires $\beta < 1$. Under these conditions the unconditional variance is given by

$$\sigma^2 = \mathrm{E}[|\ Z_t\ |^2] e^{\alpha_0(1-\beta)^{-1}} \prod_{i=1}^{\infty} \mathrm{E}[e^{\beta^{i-1} g(Z_t)}] \tag{4.7}$$

where $g(z_t) = \alpha_1(|u_{t-1}| - \mathrm{E}\left[|u_{t-1}|\right]) + \alpha_2 u_{t-1}$ as shown by He et al. [2002]. The second extension is the gjrGARCH model, which also tries to capture the leverage effect, here the conditional variance is given by

$$h_t \equiv \alpha_0 + (\alpha_1 + \alpha_2 \mathbb{I}\left\{y_{t-1} < 0\right\}) y_{t-1}^2 + \beta h_{t-1}. \tag{4.8}$$

Here $\mathbb{I}$ is an indicator function which takes the value 1 if the condition $y_{t-1} < 0$ is met and 0 otherwise, here the leverage effect predicts that $\alpha_2 > 0$. Like with the eGARCH the vector of additional variables are given by $\theta = (\alpha_0, \alpha_1, \alpha_2, \beta)'$. Positivity requires $\alpha_0 > 0, \alpha_1 > 0, \alpha_2 \geq 0, \beta \geq 0$ and stationarity requires $\alpha_1 + \alpha_2 \mathrm{E}[u_t^2 \mathbb{I}\left\{u_t < 0\right\}] + \beta < 1$. Under these conditions the unconditional variance is given by

$$\sigma^2 = \frac{\alpha_0}{1 - \alpha_1 - \alpha_2 \mathrm{E}[u_t^2 \mathbb{I}\left\{u_t < 0\right\}] - \beta}. \tag{4.9}$$

[3]The leverage effect is that negative stock returns increase the volatility more than positive returns.

4.1.1 Model estimation & the Hamilton filter

Following Ardia et al. [2019], the estimation of the RS-GARCH model can be done using a maximum likelihood approach if the problem of *path-dependency* is accounted for. The path-dependency problem occurs when for a sample of size T and with n regimes the evaluation of n^T volatility paths becomes incomprehensible due to large sample sizes, note that even with small sample sizes the evaluation of each path is incomprehensible. But the problem can be avoided by following the procedure suggested by Ardia et al. [2018]. They suggested assuming that the conditional variance $h_{s_t,t}$ follows n *separate* GARCH-type processes which evolve in parallel.

The estimation scheme is then done iteratively by applying the Hamilton filter presented by Hamilton [2010] which we reiterate below.
Now since the transition probabilities follow an unobserved Markov chain seen in (4.1) we need to instead make inference on the states given the observations on y_t, that is the inference will be on the form

$$\begin{aligned} z_{t|t} &:= (z_{1,t|t}, \dots, z_{n,t|t})' \\ z_{j,t|t} &:= \Pr(s_t = j \mid \mathcal{I}_t; \Psi) = \Pr(s_t = j \mid Y_t = y_t, \mathcal{I}_{t-1}; \Psi), \quad s_t \in \{1, \dots, n\} \end{aligned}$$

Notice that by applying the law of total probability on $z_{i,t|t-1}$ yields

$$\begin{aligned} z_{i,t|t-1} &= \Pr(s_t = i \mid \mathcal{I}_{t-1}; \Psi) \\ &= \sum_{k=1}^{n} \Pr(s_t = i \mid s_{t-1} = k, \mathcal{I}_{t-1}; \Psi) \Pr(s_{t-1} = k \mid \mathcal{I}_{t-1}; \Psi) \\ &= \sum_{k=1}^{n} p_{k,i} \cdot z_{k,t-1|t-1}. \end{aligned}$$

Now using Bayes formula on $z_{j,t|t}$ yields

$$\begin{aligned} z_{j,t|t} &= \Pr(s_t = j \mid Y_t = y_t, \mathcal{I}_{t-1}; \Psi) \\ &= \frac{\Pr(Y_t = y_t \mid s_t = j, \mathcal{I}_{t-1}; \Psi) \Pr(s_t = j \mid \mathcal{I}_{t-1}; \Psi)}{\Pr(Y_t = y_t \mid \mathcal{I}_{t-1}; \Psi)}, \\ &= \frac{f_{\mathcal{D}}(y_t \mid j, \mathcal{I}_{t-1}; \Psi) \cdot z_{j,t|t-1}}{\Pr(Y_t = y_t \mid \mathcal{I}_{t-1}; \Psi)}, \end{aligned}$$

now using the law of total probability, we can rewrite the denominator as follows

$$\Pr(Y_t = y_t \mid \mathcal{I}_{t-1}; \Psi) = \sum_{i=1}^{n} \Pr(Y_t = y_t \mid s_t = i, \mathcal{I}_{t-1}; \Psi) \Pr(s_t = i \mid \mathcal{I}_{t-1}; \Psi) \tag{4.10}$$

$$= \sum_{i=1}^{n} f_{\mathcal{D}}(y_t \mid i, \mathcal{I}_{t-1}; \Psi) \cdot z_{i,t|t-1}, \tag{4.11}$$

which finally yields

$$\begin{aligned} z_{j,t|t} &= \frac{f_{\mathcal{D}}(y_t \mid j, \mathcal{I}_{t-1}; \Psi) \cdot z_{j,t|t-1}}{\sum_{i=1}^{n} f_{\mathcal{D}}(y_t \mid i, \mathcal{I}_{t-1}; \Psi) \cdot z_{i,t|t-1}} \\ z_{j,t|t-1} &= \sum_{k=1}^{n} p_{k,i} \cdot z_{k,t-1|t-1}. \end{aligned} \tag{4.12}$$

The iterative calculation of $z_{j,t|t-1}$ and $z_{j,t|t}$ is called the *Hamilton filter*. We will refer to $z_{j,t|t-1}$ as the *predicted probability*, since it is the predicted probability of being in state j

given information up to $t-1$, and we will refer to $z_{j,t|t}$ as the *filtered probability*, it can be considered as an updated belief about the current state from $z_{j,t|t-1}$.
Now the Hamilton filter can be more compactly written using matrix-vector notation, first define

$$\eta_t := (\eta_{1,t}, \dots, \eta_{n,t})',$$
$$\eta_{i,t} := f_{\mathcal{D}}(y_t \mid i, \mathcal{I}_{t-1}; \Psi),$$

the Hamilton filter can then be written compactly as

$$\begin{aligned} z_{t|t} &= \frac{1}{z'_{t|t-1}\eta_t} z_{t|t-1} \odot \eta_t \\ z_{t|t-1} &= P' z_{t|t} \end{aligned} \tag{4.13}$$

where $\odot$ denotes the Hadamard product, i.e. element-wise product of the entries.

Remark 14. Note that the Hamilton filter needs initial values $z_{1|0}$ to start the filtering, Hamilton [1994] suggests $z_{1|0} = n^{-1}\mathbf{1}$ or optimizing them through the MLE method described below. Note that $\mathbf{1}$ is a vector of ones with dimension n.

As a final note on the Hamilton filter, we can also obtain smoothed probabilities due to an algorithm developed by Kim [1994], the smoothed probabilities are given on vector form by

$$z_{t|T} = z_{t|t} \odot \left[P \left[z_{t+1|T} \oslash z_{t+1|t} \right] \right] \tag{4.14}$$

where $\oslash$ denotes the Hadamard division, which is the element-wise division of the entries.

The next step is maximizing the likelihood, the likelihood function is given by

$$\mathcal{L}(\Psi|\mathcal{I}_T) \equiv \prod_{t=1}^{T} f_{\mathcal{D}}(y_t|\Psi, \mathcal{I}_{t-1}), \tag{4.15}$$

The conditional density of y_t can be written more explicitly by using (4.10) and the expression for $z_{t|t-1}$ in (4.12), that is

$$f_{\mathcal{D}}(y_t|\Psi, \mathcal{I}_{t-1}) \equiv \sum_{i=1}^{K} \sum_{j=1}^{K} p_{i,j} z_{i,t-1|t-1} f_{\mathcal{D}}(y_t|s_t = j, \Psi, \mathcal{I}_{t-1}).$$

Then by applying a numerical optimization algorithm, like the Broyden–Fletcher–Goldfarb–Shanno, BFGS, algorithm with appropriate restrictions and initial values of Ψ, we minimize the negative log-likelihood $-\ln \mathcal{L}(\Psi|\mathcal{I}_T)$ to get the MLE estimates $\hat{\Psi}$.

The speed of the maximization procedure of the log-likelihood function can be improved upon by choosing strategic initial values, see Ardia et al. [2019] for a procedure to choose initial parameter values.

4.1.2 Summarizing the estimation procedure

The estimation procedure is done by applying the following steps.

1. Choose distribution of the innovation process and choose initial model parameters, Ψ, either arbitrarily or using an algorithmic approach like the one presented in Ardia et al.

[2019].[4] Additionally, choose the initial $z_{1|0}$ either arbitrarily between 0 and 1 or use remark 14.
2. Apply the Hamilton filter by iterating (4.13) for all t.
3. Minimize the negative log-likelihood in (4.15) using the BFGS-algorithm, or some other optimization algorithm, under the constraints imposed by the chosen GARCH model.
4. Repeat step 2. an 3. until convergence.

The estimation procedure summarised in the steps above is sometimes referred to as an *expectation-maximisation* algorithm, EM-algorithm.

Application of the results in this chapter will be presented in section 5.2.

[4]Note that the initial parameters need to conform to specific model constraints.

Chapter 5

Implementation & Results

This chapter will present the results of our study, the first part of this chapter is dedicated to our panel study of the Covid-19 spread rate and the second part is for the study of regional stock indices.

5.1 Panel Data Modeling

This section can be considered an extension of the preliminary study in section 2.1.
First off, we have included an additional variable to the regression which is a double lagged dependent variable. An issue with this is that including lagged variables transforms the modeling procedure into a dynamic panel data modeling scheme. Many of the statistical properties of the estimators discussed in the theory section break down by including lagged variables, specifically, including lagged variables introduces correlation between regressors and the error component. That is, the error component is no longer orthogonal to the regressors and the statistical properties of the estimators are dependent on this assumption, in fact, the estimators are biased in this scenario, so to see why this problem arises consider the model

$$y_{i,t} = y_{i,t-1}\delta + X_{i,t}\beta + u_{i,t}, \quad i = 1, \dots, N; \quad t = 1, \dots, T$$

where $u_{i,t} = \mu_i + \nu_{i,t}$ is the usual one-way error component. Now

$$\Delta y_{i,t} = \Delta y_{i,t-1}\delta + \Delta X_{i,t}\beta + \Delta u_{i,t}, \tag{5.1}$$

where Δ is the first difference operator with respect to time, now consider

$$\begin{aligned}
\mathrm{E}[\Delta y_{i,t-1}\Delta u_{i,t}] &= \mathrm{E}[y_{i,t-1}\Delta u_{i,t}] - \mathrm{E}[y_{i,t-2}\Delta u_{i,t}] \\
&= \mathrm{E}[y_{i,t-1}\Delta u_{i,t}] \\
&= \mathrm{E}[y_{i,t-1}u_{i,t}] - \mathrm{E}[y_{i,t-1}u_{i,t-1}] \\
&= -\sigma_\nu^2.
\end{aligned}$$

This shows that the regressor $\Delta y_{i,t-1}$ is not orthogonal to the error $\Delta u_{i,t}$. There are ways to circumvent this problem, one way is to develop new estimators through the generalized method of moments or use an instrumental variable that is not dependent on the error [Baltagi, 2021]. A possible instrument is the second-order autoregressive dependent variable, it is not dependent on the error which is seen by

$$\begin{aligned}
\mathrm{E}[\Delta y_{i,t-2}\Delta u_{i,t}] &= \mathrm{E}[y_{i,t-2}\Delta u_{i,t}] - \mathrm{E}[y_{i,t-3}\Delta u_{i,t}] \\
&= \mathrm{E}[y_{i,t-2}\Delta u_{i,t}] \\
&= \mathrm{E}[y_{i,t-2}u_{i,t}] - \mathrm{E}[y_{i,t-2}u_{i,t-1}] \\
&= 0.
\end{aligned}$$

This shows that $\Delta y_{i,t-2}$ can be used as an instrument, and it also shows that $y_{i,t-2}$ is in fact a candidate as an instrument, we opt to use $\Delta y_{i,t-2}$.

Now, the following table contains an overview of the panel data models, presented in chapter 3, planned for estimation.

Pooled regression				
One-way	Individual FE	Time FE	Individual RE	Time RE
Two-way	FE		RE	

Table 5.1. Model overview, showing different one- and two-way error component regression models.

By table 5.1, there are a total of seven panel models, one being pooled regression, four of them being one-way models and the remaining two being two-way models.

As a starting point, the pooled regression model, as seen in equation (3.1), is estimated using the data described in table 2.1. For the estimation of the pooled regression model we use OLS, the resulting parameter estimates, standard error, t-statistic and p-value are seen in the following table.

Dependent variable: log.Relative.growth.rate	Estimate	Std.Error	t.value	p.value
(Intercept)	− 0.25857	0.00888	− 29.11866	0
SqrMeter.per.citizen.urban.areas	− 0.000002	0.000001	− 3.45931	0.00054
lag.lag.log.Relative.growth.rate	0.94550	0.00181	523.49200	0
Vaccinated.pct	0.01498	0.00057	26.04824	0
Service.concentration.pct	0.00124	0.00192	0.64747	0.51733
Children.institutionalized.pct	0.01862	0.00760	2.44923	0.01432
Gini.index	− 0.00001	0.00003	− 0.37434	0.70816
Stringency.index	0.00009	0.00001	6.85295	0
Stringency.index.I.Service.concentration.pct	− 0.00027	0.00010	− 2.73637	0.00621
Stringency.index.I.Children.institutionalized.pct	− 0.00159	0.00040	− 4.02879	0.00006
Observations:	67,326			
R^2:	0.848			
Adjusted R^2:	0.848			

Table 5.2. Pooled regression, the columns show the name of the variables, the parameter estimates, their (non-robust) standard errors, the t-statistic and the last column shows the p-value.
The number of observations and the R^2 value are shown at the bottom of the table. Note that 0 means less than machine epsilon $\varepsilon_M = 2.220 \cdot 10^{-16}$.

While the R^2 value indicates that the pooled regression model is performing well, the model is not likely to be correctly specified from a socioeconomic standpoint. This is due to the omission of multiple interactions and variables that actually drive the spread of the pandemic. For example in the pooled regression, the percentage of vaccinated regressor has a positive sign coefficient which is at least not the interaction we expected it to have. We suspect that it spuriously captured the effect of some omitted variable. So to circumvent this, as we have already discussed in section 2.1, we use available data and special model specifications, namely the one- and two-way error component regression models.
Using these modeling schemes might bring us closer to a non-spurious regression, however, it is unlikely that we can completely eliminate omission bias.

Recall the assumptions outlined in assumption 1 and remark 2 for the pooled regression to be BLUE. Naturally, all of these assumptions are difficult to defend, which is why we try to generalize with more general models.

Each of the models in table 5.1 have been fitted to the data, and tables similar to table 5.2 can be found in appendix A for each of the models.
Specifically, table A.1 to A.6 shows the estimations for the four one-way models and table A.7 and A.8 shows the estimations for the two two-way models. In the following section, we will discuss the error component regressions.

5.1.1 Error Component Regressions

First off, the tables of the fixed effects regression models are done with OLS with robust error correction and FGLS, this is due to the presence of autocorrelation in the residuals of the OLS estimations.
To support this statement, we present the autocorrelation and partial autocorrelation functions evaluated at increasing lags for our residuals of individual and time fixed effects models in figure 5.1 below.

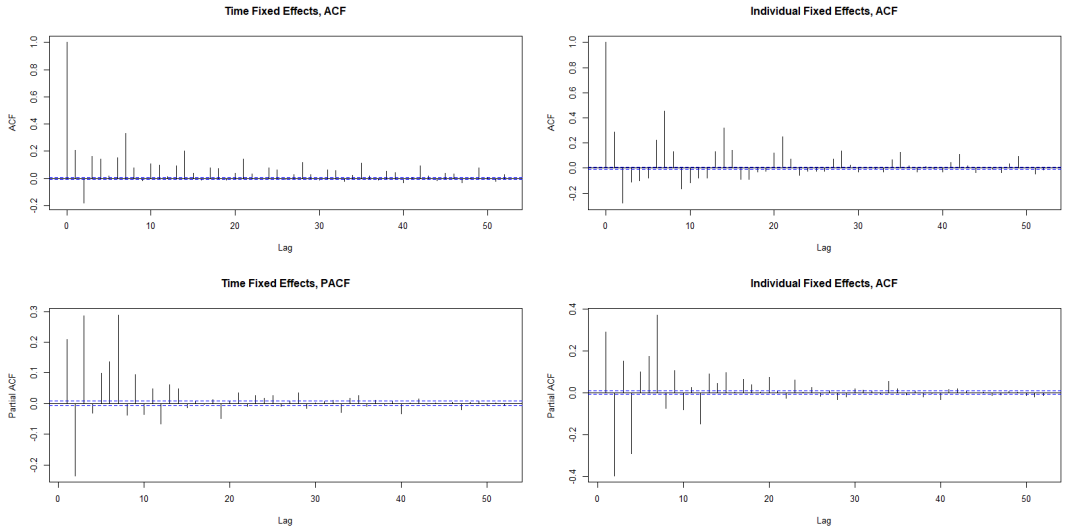

Figure 5.1. The ACF and PACF of the residuals of the individual and time fixed effects models.

The autocorrelations have been found by normalizing the residuals across the municipalities, i.e. the residuals have been demeaned and re-scaled to have a variance of 1 within each municipality, after re-scaling the correlation between the residual vector and its lagged values the autocorrelations are calculated and they are seen in the plots above.
For calculations of the partial autocorrelations, we solved the Yule-Walker equations as described by Borchers [2001].
It is clear that there is autocorrelation present in the residuals of both models, similar results are found for the random effects models and the ACF and PACF can be seen in figure A.1 in appendix A and they show similar patterns.
These patterns are the reason why we account for the inefficiency, imposed by the autocorrelation, through robust standard errors in our OLS regressions and why we have used FGLS.
It is important to keep in mind that the FGLS method for the individual effects is inefficient due to the time dimension being larger than the individual dimension because FGLS estimates $T(T+1)/2$ unique covariance parameters, i.e. we do not have enough degrees of freedom.

Using FGLS, the residuals are rid of autocorrelation in the time effects case as can be seen in figure A.2 in appendix A, the individual case does not respond well to this, which might be due to the lack of efficiency as T is much larger than N.

Following the estimation of the models we need to choose the appropriate model by using the testing methods described in section 3.1.3 to evaluate if we should use pooling vs. random effects vs. fixed effects.
Table 5.3 below shows the test results of pooling vs. random effects for both time and individual effects.

Random effects VS. pooled regression

Individually	Time
"Failed to reject the null hypothesis"	"Failed to reject the null hypothesis"

Table 5.3. Results from random effects VS. pooled regression.

Table 5.3 shows that the test fails to reject the null hypothesis, $H_0 : \sigma_\mu = 0$ and $H_0 : \sigma_\lambda = 0$, in both cases, i.e. a pooled regression model is preferred over a random effects model.

Next in line is the test of fixed effects vs. pooled regression the results are shown in table 5.4 below

Fixed effects VS. pooled regression

Individually	Time
"Fails to reject the null hypothesis"	"Rejects the Null Hypothesis"

Table 5.4. Result from fixed effects VS. pooled regression.

Table 5.4 shows that the null hypothesis, $H_0 : \mu_1 = \mu_2 = \cdots = \mu_{N-1} = 0$ and $H_0 : \lambda_1 = \lambda_2 = \cdots = \lambda_{T-1} = 0$, is rejected only for time fixed effects models. Hence the test suggests a fixed effect model over a pooled regression model for time effects.
The tests so far suggest that fixed effects models are preferred over the random models, but for completion's sake we also apply the Hausman test for fixed vs. random effects, the results are shown in table 5.5 below

Random effects VS. fixed effects

Individually	Time
"Failed to Reject the Null Hypothesis"	"Rejects the Null Hypothesis"

Table 5.5. Result from random effects VS. fixed effects.

Table 5.5 shows that for the individual effects the test fails to reject the null hypothesis and suggests a random effects model, and for the time effects model, the fixed version is preferred.

Considering these three tests, there is a bit of ambiguity for the Hausman test, so let us consider what the LM test in 3.22 and the Hausman test in 3.23 actually test for.
If the LM-test fails to reject the null hypothesis we can assume that the variance of the individual effects is zero or very close, which in this case means that $\text{Var}(\hat{\beta}_{RE}) \approx \text{Var}(\hat{\beta}_{PR})$ which actually leads the Hausman test to test fixed effects vs. pooling.

Considering this, the Hausman test agrees with the F-test for FE vs. pooled as seen by comparing the results in table 5.4 and 5.5.

As a supplant to the tests above, we can compare the different estimates from the regression to help us decide on a proper model. E.g. consider that we apply a pooled regression, a random effects regression and a fixed effects regression, if the estimates in the fixed effects model are vastly different from the pooled regression and the random effects regression it is a sign of omission bias in the random effects and pooled regression. In this case, the fixed effects model is the proper model, however, if there is not much difference in the estimates we will have to rely on the LM-test to sort out whether it should be a RE or pooled model.

Comparing the estimates from pooled regression in table 5.2 and the fixed effects estimates in table A.2, we see that the estimates are in fact very close to each other suggesting that we should not use individual fixed effects, as the tests also suggest.
Doing these comparisons with the rest of the tables in appendix A and using the results from the tests above, suggest that we should use time fixed effects. Especially note that the sign changes on some of the estimates when using time fixed effects.
So there is no evidence for individual effects at all which is why a two-way error component model might be over-parameterized, however, for completion's sake, we have also tested random vs. fixed effects, using the Hausman test, for the two-way case which is seen in table 5.6 below.

Fixed effects VS. pooled regression
"Rejects the null hypothesis"

Table 5.6. Two-way random effects VS fixed effects.

The test suggests that we should use fixed effects in the two-way random case, however, comparing the two-way fixed effects estimates with the one-way time fixed effects model seen in table A.7 and A.4, respectively, we see that the two-way case does not change the estimates considerably. This suggests that the one-way time fixed effects model is adequate and we present the FGLS estimates again in table 5.7. For the robust OLS estimates see table A.3 in appendix A.

Dependent variable: log.Relative.growth.rate	Estimate	Std.Error	t.value	p.value
SqrMeter.per.citizen.urban.areas	− 0.000003	0.0000003	− 12.03464	0
lag.lag.log.Relative.growth.rate	0.49475	0.00346	143.02200	0
Vaccinated.pct	− 0.03366	0.00199	− 16.93296	0
Service.concentration.pct	0.00895	0.00075	11.91704	0
Children.institutionalized.pct	0.02300	0.00303	7.58774	0
Gini.index	0.00002	0.00001	1.29680	0.19470
Stringency.index.I.Service.concentration.pct	− 0.00038	0.00005	− 7.62481	0
Stringency.index.I.Children.institutionalized.pct	− 0.00113	0.00021	− 5.40497	0.0000001
Observations:	67,326			
R^2:	0.935			
Adjusted R^2:	0.935			

Table 5.7. FGLS estimation of time fixed effects.

Recall that we mentioned the VIF in section 2.1 to check for multicollinearity, considering that the standard errors and p-values are so low as they are; we do not consider the VIF.

5.1.2 Spatial Error Component Regression Model

A final extension to our error component regression models is spatial autocorrelation. As explained in section 3.3, the introduction of a spatial error component regression model is to account for spillover effects between municipalities.
Unfortunately, the software we use does not support a spatial weight matrix W_N that has zero columns, which is whenever we have municipalities that do not border other municipalities, e.g. island municipalities.

Given our previous findings, we limit our examination to the one-way time fixed effects model. Now let the model be given as seen in equation (3.35) and with error components as in equations (3.36) and (3.37).

The estimation of our model uses the maximum likelihood estimation described in section 3.3 with the parameters from table 5.7 as initial values. Following this, the result is seen in the table below.

Dependent variable: log.Relative.growth.rate	Estimate	Std.Error	t.value	p.value
rho	− 0.00899	0.00110	− 8.18607	0
lag.lag.log.Relative.growth.rate	0.60236	0.00338	178.26090	0
SqrMeter.per.citizen.urban.areas	− 0.00001	0.0000004	− 13.58425	0
Vaccinated.pct	− 0.06291	0.00355	− 17.72975	0
Service.concentration.pct	0.01371	0.00135	10.12963	0
Gini.index	0.00002	0.00002	0.91546	0.35995
Children.institutionalized.pct	0.03617	0.00505	7.15466	0
Stringency.index.I.Service.concentration.pct	− 0.00088	0.00007	− 13.35159	0
Stringency.index.I.Children.institutionalized.pct	− 0.00285	0.00027	− 10.40108	0
Observations:	67,326			
R^2:	0.938			
Adjusted R^2:	0.938			

Table 5.8. Spatial one-way time fixed effects model estimations.

Table 5.8 shows the spatial time fixed effects model and the main difference going from the one-way time fixed effects is that we have a spatial correlation parameter, ρ. ρ's estimate is a bit small but it is significant.

5.2 Regime Switching Results

Note that from this point forward all the time series will be restricted to an in-sample time period 2018-01-02 to 2021-11-16, this is to ensure that the time series are the same length, and the total amount of data points are then 966. Secondly, we wish to balance the amount of observations from before and during the Covid-19 pandemic starting at the beginning of 2020. Thirdly, we wish to apply an out-of-sample test to determine the best model later in this section.
The out-of-sample data is a bit unorthodox, we have chosen to make the out-of-sample data as a combination of a *volatile* period and a *tranquil* period in order to test our models under a transition back to tranquil market conditions.
So to elaborate further, the first half of the out-of-sample data ranges from 2021-11-17 to 2022-04-07, which is the 99 days following from where the in-sample period ends. The second half ranges from 2017-08-09 to 2017-12-29, which is the 101 days *before* the in-sample period begins. So with this out-of-sample period, we try to capture the ongoing increase in volatility imposed by the pandemic in the first half and simulate a return to tranquil market conditions as before the pandemic in the second half.

The goal now is to use the regime switching GARCH framework presented in chapter 4, to further examine the conditional distribution of

$$y_t \mid \mathcal{I}_{t-1}.$$

Recall that for the estimation of the GARCH models we need the processes in question to exhibit no autocorrelation and that this was the case under assumption 6, this is the case for the log returns that have been filtered through the conditional mean models we presented in section 2.2.
For notational brevity we now denote these filtered log returns with the index abbreviations, that is, we now wish to model

$$y_t \mid (s_t, \mathcal{I}_{t-1}) \sim \mathcal{D}(0, h_{s_t,t}, \xi_{s_t}), \quad \forall t$$

where y_t is either OMXC25_t, NJ_t, MJ_t, SD_t, RS_t or HS_t.

Now using the model specifications and distributions presented in section 4.1, we estimate the possible combinations of GARCH specifications and distributions.
In other words, let the set of different distributions, including the normal, Student's t and GED distributions, and their skewed variations, be denoted by D and let the set of different GARCH specifications, including the standard GARCH (sGARCH), eGARCH and gjrGARCH, be denoted by S. Then we fit a model for each element in the Cartesian product of these two sets, that is

$$D \times S \equiv \{(d, s) \mid d \in D \text{ and } s \in S\},$$

for each of the indices.
Summarising, table 5.9 below shows the different combinations and how they are abbreviated.

Model Specification	Distribution	Abbreviation
sGARCH	Normal	s.no
sGARCH	Student's t	s.st
sGARCH	GED	s.ge
sGARCH	Skewed Normal	s.sn
sGARCH	Skewed Student's t	s.ss
sGARCH	Skewed GED	s.sg
eGARCH	Normal	e.no
eGARCH	Student's t	e.st
eGARCH	GED	e.ge
eGARCH	Skewed Normal	e.sn
eGARCH	Skewed Student's t	e.ss
eGARCH	Skewed GED	e.sg
gjrGARCH	Normal	g.no
gjrGARCH	Student's t	g.st
gjrGARCH	GED	g.ge
gjrGARCH	Skewed Normal	g.sn
gjrGARCH	Skewed Student's t	g.ss
gjrGARCH	Skewed GED	g.sg

Table 5.9. Combinations of model specification, distribution, and the combination's abbreviation.

Initially, we only considered 2 regimes for the modeling procedure, however, as the following results will show, there is evidence for using 3 regimes.
Note, the model selection procedure is discussed in the next section, the rest of the current section presents an example of predicted conditional volatility and discusses the number of regimes. Figure 5.2 below shows the OMXC25_t process with smoothed probabilities calculated using (4.14) in the first plot, and the second plot shows the estimated conditional volatility.

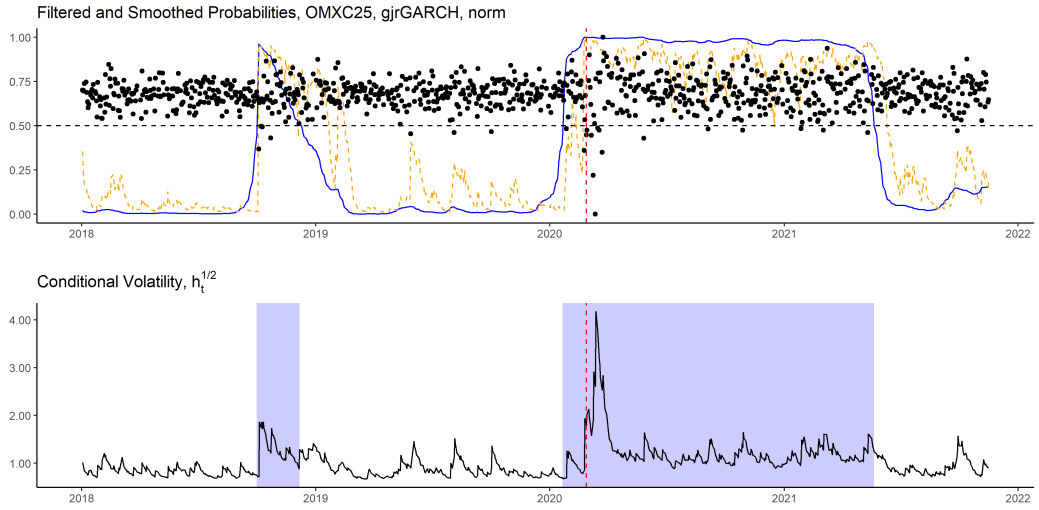

Figure 5.2. Regime Switching gjrGARCH model with normal distributed innovations.
The blue curve is the smoothed probabilities and the orange dashed curve is the filtered probabilities. The black dots are residuals of the fitted ARMA model scaled into an interval from zero to one. The blue dashed lines indicates the first Covid-19 incident in Denmark. In the second plot, the black curve denotes the conditional volatility predicted with the coloured sections representing a state with higher unconditional volatility according to the smoothed probabilities.

Note that the model specification and distribution have been chosen for illustrative purposes in figure 5.2.
By casual inspection of figure 5.2, it seems like just before 2019 we have an increase in volatility that is similar to the conditional volatility during the pandemic, additionally, there is a major spike in volatility right around the first incidence of Covid-19 in Denmark, this indicates that there might be a third regime during the beginning of the pandemic.

This motivates allowing modeling for both 2 and 3 regimes. Figure 5.3 below shows the 3 regime predictions of the conditional volatilities. Again, the model distribution and specification haven been chosen for illustrative purposes.

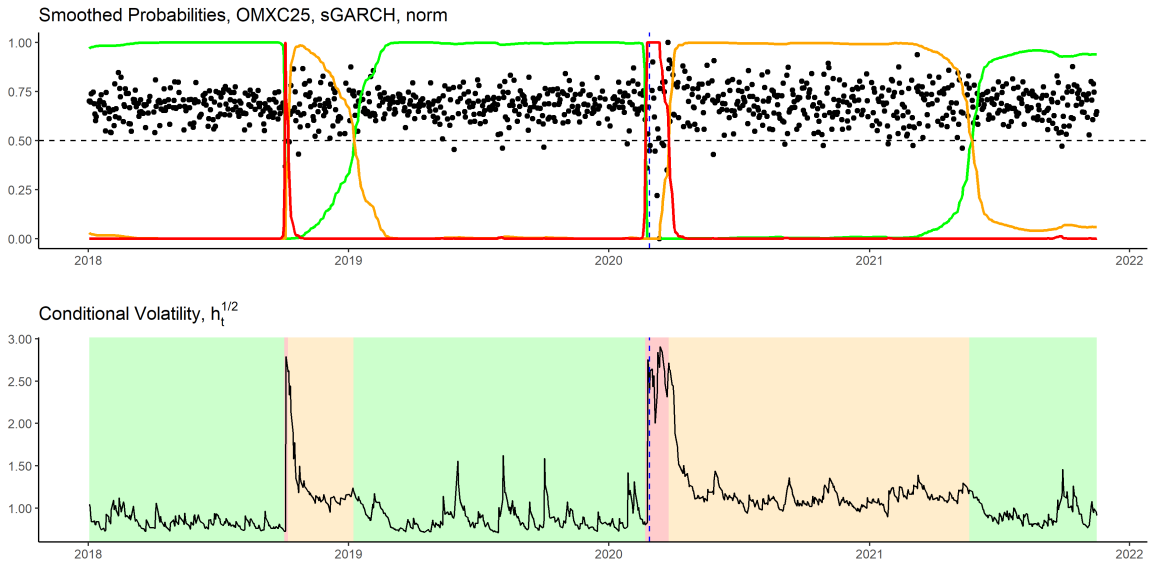

Figure 5.3. Regime Switching standard sGARCH model with normal distributed innovations. The green, orange and red curves are the smoothed probabilities being in either of the 3 regimes. The colors are chosen to represent the unconditional volatility imposed by the estimated models in each regime, where the green regime has least unconditional volatility, red has the most and orange is in between. The black dots are residuals of the fitted ARMA model scaled into an interval from zero to one. The blue dashed lines indicate the first Covid-19 incident in Denmark. In the second plot, the black curve denotes conditional volatility.

For the case of 3 regimes as seen in figure 5.3 an increase in the number of regimes seemingly improves the outcome as it captures the initial shock of the crisis, however, the casual inspections of these plots are not a formal way to select a model, the next section presents a way to select a proper model.

5.2.1 Conditional Coverage Test

In order to find the most suitable combination of model and distribution, a deeper evaluation is required. For such an evaluation we will use a test that evaluates the models' accuracy in predicting out of sample value at risk (VaR), that is, which model is the most accurate in terms of correctly predicting the $\alpha-$quantile loss. The expected $\alpha-$quantile loss refers to the expected proportion α of exceedance, that is the number of expected exceedance points for the confidence level $1-\alpha$ [Ardia et al., 2019].

VaR is a financial metric that estimates the risk of an investment. More specifically VaR is an index that quantifies the risk of potential losses for a company or an investment over a specified period of time.

Let Y be a random variable that represents the outcome of an investment and $0 < \alpha < 1$ the unspecified level of risk. The value at risk of Y is then given by

$$\text{VaR}_{1-\alpha}(Y) := \inf\{y \in \mathbb{R} : \mathbb{P}(Y < -y) \leq \alpha\},$$

where $\text{VaR}_{1-\alpha}(Y)$ represents the extra amount of capital it needs to reduce the probability of bankruptcy to α.
The notion of VaR usually only considers the lower quantile risk, however, it is not uncommon to take short positions in an asset, in that case, the VaR operates on the upper quantile, so to incorporate both ends we redefine VaR for our purposes to

$$\text{VaR}^{l}_{1-\alpha}(Y) := \inf\{y \in \mathbb{R} : \mathbb{P}(Y \leq -y) \leq \frac{\alpha}{2}\}$$
$$\text{VaR}^{u}_{1-\alpha}(Y) := \inf\{y \in \mathbb{R} : \mathbb{P}(-Y \leq -y) \leq \frac{\alpha}{2}\}$$

and now

$$VaR_{1-\alpha}(Y) := \{VaR^{l}_{1-\alpha}(Y), VaR^{u}_{1-\alpha}(Y)\}. \tag{5.2}$$

Figure 5.4 below shows an example of an out of sample VaR forecast for an arbitrary combination of model specification and distribution for OMXC25.

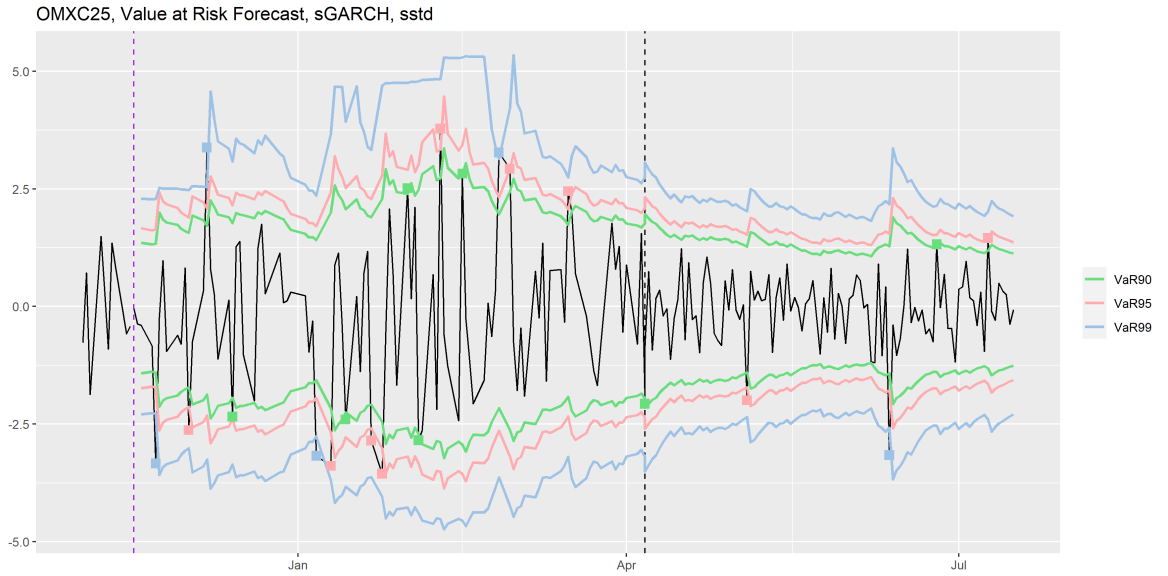

Figure 5.4. Out of sample VaR prediction, the green line is the VaR_{90}, the red line is VaR_{95} and the blue line is VaR_{99}. Exceedance points are represented with squared dots with colours representing the level of exceedance. The data after the purple dashed line is the out-of-sample and the black dashed line at 2022-04-06 represents the tranquil market period.

Figure 5.4 above is made by using a one-step ahead forecast of the VaR using (5.2), that is

$$\text{VaR}_{1-\alpha}(Y_{t+1}|(s_{t+1}, \mathcal{I}_t)),$$

for all t in the out-of-sample period and for each $\alpha \in \{0.01, 0.5, 0.1\}$, additionally, $Y_{t+1}|(s_{t+1}, \mathcal{I}_t)$ is the conditional CDF of OMXC25_t. The states are chosen using the predicted

probabilities from the Hamilton filter as described in chapter 4.

As a measure of model performance, we introduce a backtesting hypothesis test, the conditional coverage, cc, test. This test is designed to determine if the proportion of exceedance is accurate in relation to the VaR confidence level $1-\alpha$. The cc test aims to simultaneously test, for a given confidence level $1-\alpha$, that for our estimated model we have the correct failure rate and independence of the exceedance points. The correct failure rate refers to; the number of exceedance points must be consistent with the VaR confidence level. While the independence of exceedance points refers to that any exceedance points must be independent of previous exceedance points.

The cc test is a likelihood ratio test following a two-part setup, given that the test itself simultaneously tests for correct failure rate and independency. The null hypothesis and the likelihood ratio test equations are shown and briefly explained below, however, for further details and derivation of the test see Dumitrescu et al. [2012] and Roccioletti [2015].

The first part of the cc test tests the null hypothesis

$$H_0 : p = \hat{p} \equiv \frac{x}{T}.$$

Here p denotes the theoretical failure rate, $\hat{p}$ the observed failure rate, x the number of exceedance points and T the total number of observations. Continuing from this, the likelihood ratio test is then given by

$$LR_{uc} = -2ln\left(\frac{(1-p)^{T-x}p^x}{\left[1-\left(\frac{x}{T}\right)\right]^{T-x}\left(\frac{x}{T}\right)^x}\right).$$

The subscript uc denotes the unconditional coverage test. The likelihood ratio test is derived by considering the violation process, the process that makes a point exceed a level of confidence, and is binomial distributed. Under the null hypothesis, the likelihood ratio test asymptotically follows a chi-square distribution with one degree of freedom χ_1^2.

The independency part of the cc test has null hypothesis

$$H_0 : \hat{\pi}_{01} = \hat{\pi}_{11}.$$

Here $\hat{\pi}_{01}$ denotes the estimated probability of having violations tomorrow given today had no violations and $\hat{\pi}_{11}$ denotes the estimated probability of having violations tomorrow given violations today. Let the T_{00} denote the amount of observations where we have no violation today and no violation tomorrow, T_{01} the amount of observations with no violation today and violations tomorrow, T_{10} the amount of observations with violation today and no violation tomorrow and lastly T_{11} the amount of observations with violation today and tomorrow.
Now the estimates of the probabilities are given by

$$\hat{\pi}_{01} = \frac{T_{01}}{T_{00}+T_{01}}, \qquad \hat{\pi}_{11} = \frac{T_{11}}{T_{10}+T_{11}}.$$

The likelihood ratio test is now given by

$$LR_{ind} = -2ln\left(\frac{(1-\pi)^{T_{00}+T_{10}}\pi^{T_{01}+T_{11}}}{(1-\pi_{01})^{T_{00}}\pi_{01}^{T_{01}}(1-\pi_{11})^{T_{10}}\pi_{11}^{T_{11}}}\right),$$

where $\pi = \frac{T_{01}+T_{11}}{T_{00}+T_{01}+T_{10}+T_{11}}$. From this, the likelihood ratio test asymptotically follows a chi-squared distribution with one degree of freedom χ_1^2.

Now combining these likelihood ratio tests, we present the cc test which is given on the following form

$$LR_{cc} = LR_{uc} + LR_{ind}. \tag{5.3}$$

As the test is a combination of two other likelihood ratio tests that each follows a chi-squared distribution with one degree of freedom we then have that LR_{cc} follows a chi-squared distribution with two degrees of freedom χ^2_2.

The test is conducted for both lower and upper VaR and for 90%, 95% and 99% confidence levels, not one but six likelihood ratio tests are calculated for each combination of model and distribution. As an example consider the test for the OMX C25 index using a 2-regime eGARCH model with GED-distributed innovations, the cc test results for this combination are shown in table 5.10 below.

	Exceedance		Test		
VaR	expected.exceed	actual.exceed	LRstat	p-value	Decision
VaR90l	10	14	4.881	0.087	Fail to Reject H0
VaR90u	10	6	3.881	0.144	Fail to Reject H0
VaR95l	5	9	11.277	0.004	Reject H0
VaR95u	5	4	0.366	0.833	Fail to Reject H0
VaR99l	1	5	10.977	0.004	Reject H0
VaR99u	1	1	0.01	0.995	Fail to Reject H0

Table 5.10. Conditional coverage test OMXC25, sGARCH, sstd.

Table 5.10 shows the results for the cc test on the eGARCH GED model for three confidence levels divided into upper and lower levels, so a total of six tests have been conducted for a single model.

The desired result is that we fail to reject the null hypothesis in most cases, so the results like the ones shown in the rightmost column can be used as a model selection criteria. Then limiting the selection to models and distribution combinations in which the test result fails to reject the null hypothesis for as many VaR confidence levels as possible, would narrow down the choices.
However, simply counting the amount of failed rejections sometimes leave us with multiple models, so to choose between the remaining models, we need to find a different measure to select between them. In order to do so, we use the cc test framework to develop another test, we know from the tests above that the cc test follows a chi-squared distribution with two degrees of freedom which means that a sum of the six LR-statistics from testing the upper and lower VaR at the 3 confidence levels must follow a chi-squared distribution with 12 degrees of freedom under all the respective null hypotheses. So to summarize, we get the following test statistic.

$$LR_{scc} = LR_{90l} + LR_{90u} + LR_{95l} + LR_{95u} + LR_{99l} + LR_{99u}. \tag{5.4}$$

So (5.4) is a likelihood ratio test which follows a chi-squared distribution with 12 degrees of freedom, χ^2_{12}, under the combined null hypotheses of each of the test statistics. Here *scc* stands for summarized conditional coverage test. This test allows us to compare the remaining models by then choosing the model producing the highest p-value.

The scc test results for the 2 regime models are shown in the table 5.11 below.

	Exceedance		Test		
mod	expected.exceed	actual.exceed	LRstat	pvalue	Accepted.null.hypotheses
e.no	32	37	34.393	0.0005847	4
e.ss	32	35	25.101	0.0143515	4
g.sn	32	35	27.362	0.0068510	4
s.ge	32	39	31.392	0.0017162	4
s.no	32	40	31.363	0.0017338	4
s.sg	32	36	23.420	0.0243647	4
s.sn	32	37	29.381	0.0034576	4
s.ss	32	38	22.922	0.0283955	4
s.st	32	39	31.392	0.0017162	4

Table 5.11. Summarized conditional coverage test OMXC25, 2 Regimes.

From table 5.11 we see the first column containing an overview of the models conforming with the abbreviations presented in table 5.9.
The test results for the 3 regime models are seen in table 5.12 below.

	Exceedance		Test		
mod	expected.exceed	actual.exceed	LRstat	pvalue	Accepted.null.hypotheses
g.sn	32	36	23.163	0.0263736	5

Table 5.12. Summarized conditional coverage test OMXC25, 3 regimes.

The results shown in tables 5.11 and 5.12 imply, by the number of accepted null hypotheses, that the most suitable model and distribution combination for the OMX C25 index is a 3 regime gjrGARCH model with a skewed normal distribution.

Figure 5.5 below shows the smoothed probabilities for this model.

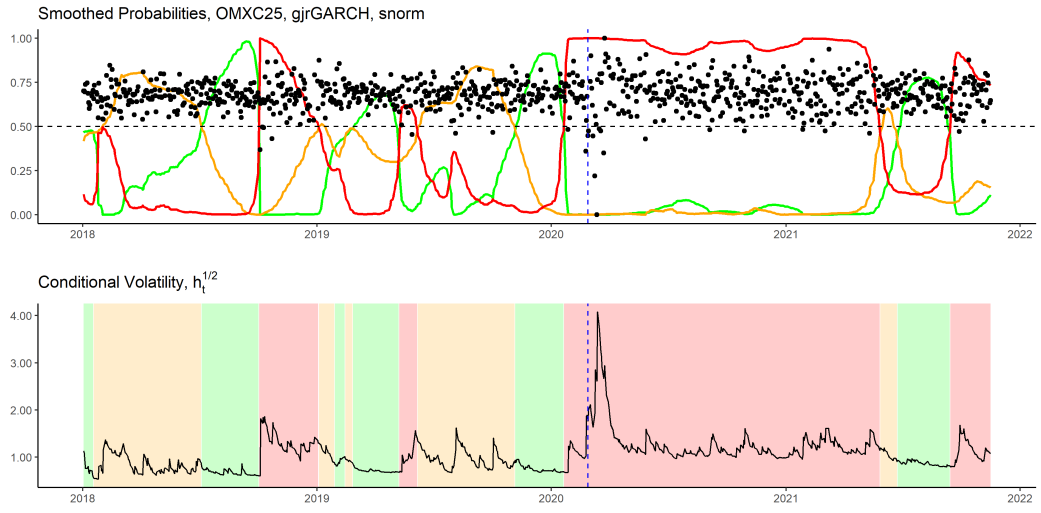

Figure 5.5. Regime Switching gjrGARCH Model with skewed normal distribution for OMXC25.

It is seen here that there are clear signs of regime switching just prior to 2019 and at the start of the Covid-19 pandemic.

Regional Results

Doing the same procedures for the regional indices as for the OMXC25 index yields the models presented in table 5.13 below.

Index	Models	LRstat	pvalue	# Accepted $\mathcal{H}_0$	Regimes
OMXC25	g.sn	23.163	0.03	5	3
NJ	e.sn	5.790	0.93	6	2
MJ	s.no	9.000	0.70	6	3
SD	g.no	8.570	0.74	6	3
HS	s.sn	7.430	0.68	5	3
RS	s.sn	9.749	0.64	6	3

Table 5.13. The best model for each region.

Tables A.10 to A.19 in appendix A show the test results for each regional index.

The smoothed probabilities and conditional volatilities of the best models for the regional indices can be seen in figures 5.6 to 5.9 below.

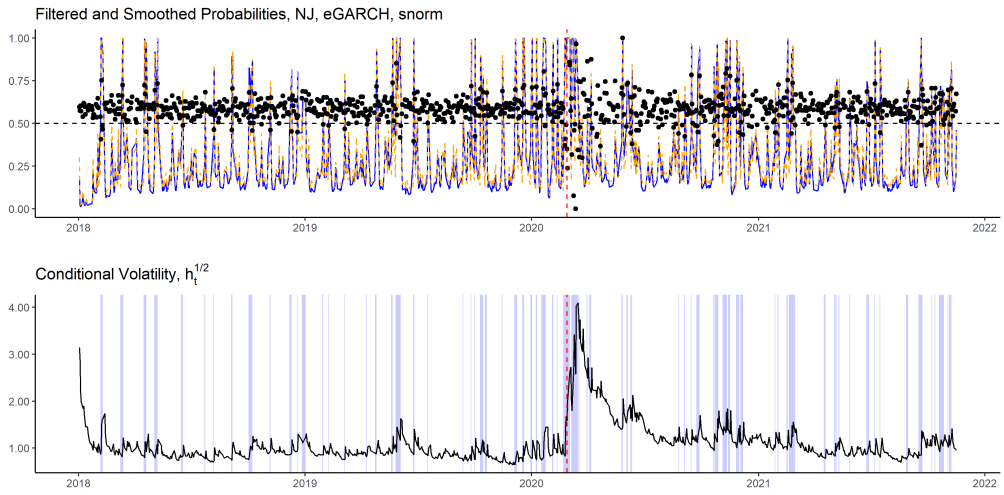

Figure 5.6. Regime switching eGARCH model with skewed normal distribution for NJ.

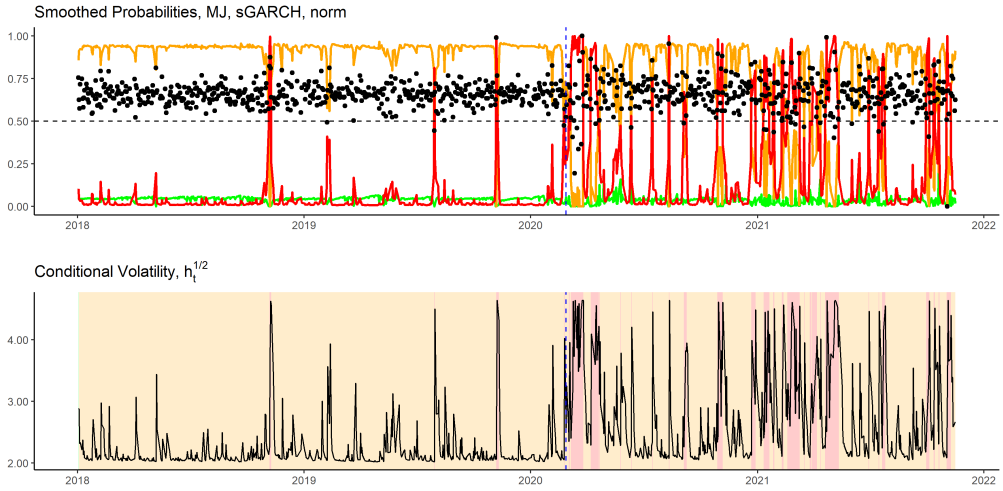

Figure 5.7. Regime switching sGARCH model with normal distribution for MJ.

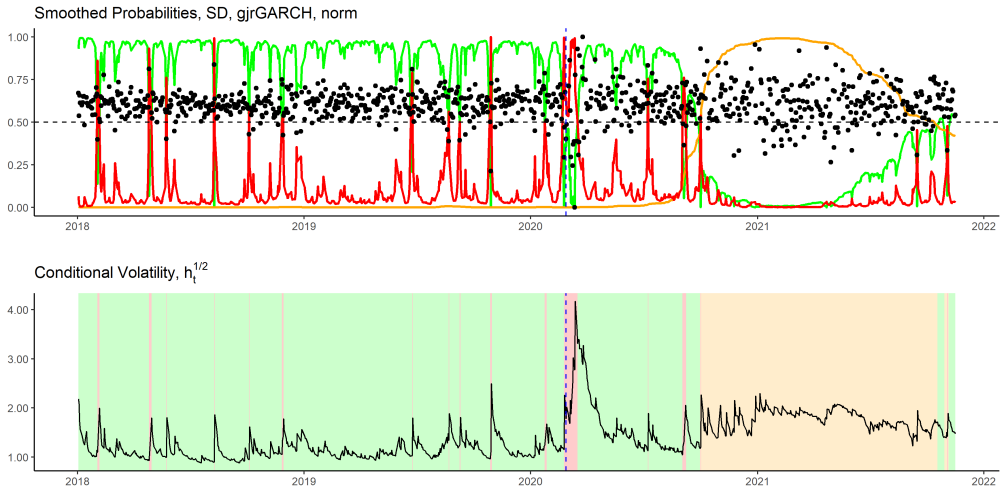

Figure 5.8. Regime switching gjrGARCH model with normal distribution for SD.

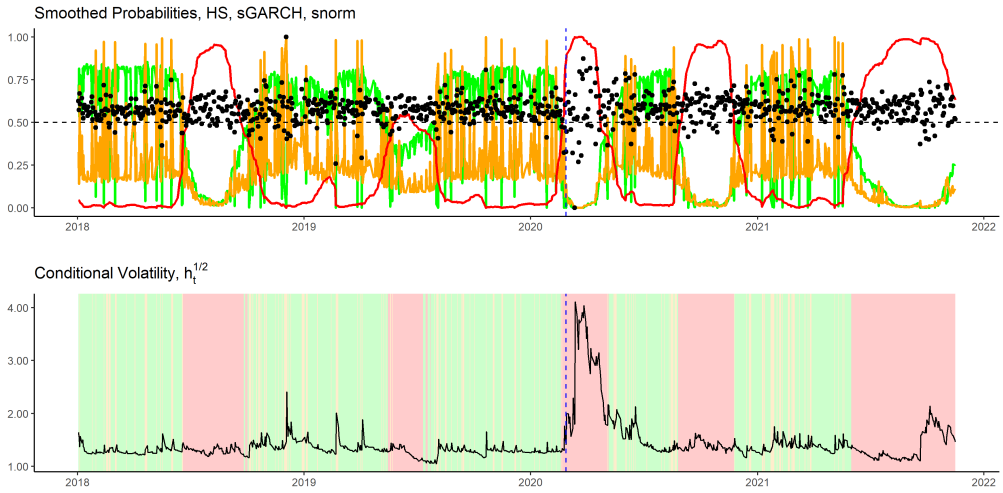

Figure 5.9. Regime switching sGARCH model with skewed normal distribution for HS.

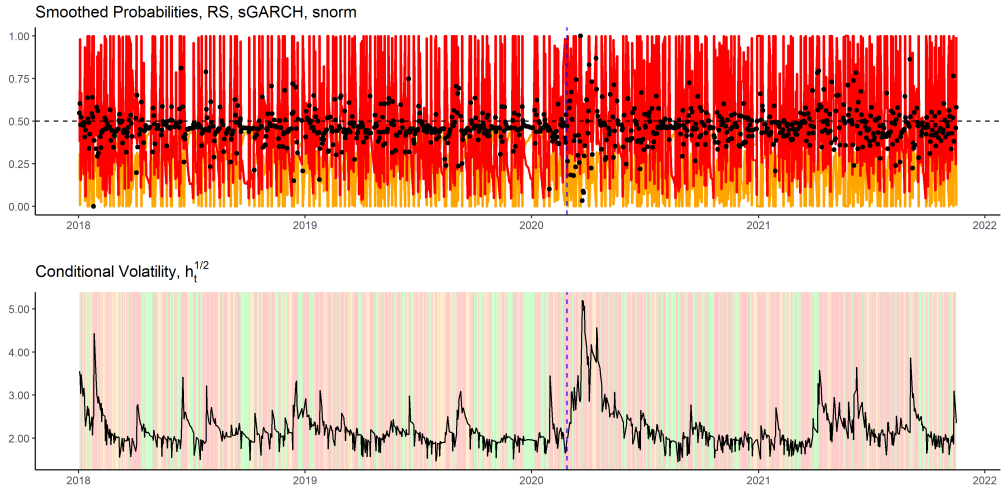

Figure 5.10. Regime switching sGARCH model with skewed normal distribution for RS.

5.2.2 Estimates and Interpretation

By causal inspection of the plots seen in figure 5.6 to 5.10 it is seen that there is an increase in conditional volatility, in each index, after the first case of Covid-19 in Denmark, however, some of the plots are a bit difficult to interpret due to the rather frantic movement of the filtered and smoothed probabilities.
So to get a better interpretation we present the estimates of each model. The model estimates for the OMXC25 process are seen in table 5.14 below

Table 5.14. 3-regime gjrGARCH model estimates with skewed normal distributed innovations, OMXC25.

	Estimate	Std. Error	t value	Pr(>|t|)
$\alpha_{0,1}$	0.00131	0.00047	2.784940e+00	0.00268
$\alpha_{1,1}$	0.00316	0.00109	2.891670e+00	0.00192
$\alpha_{2,1}$	0.00061	0.00014	4.476200e+00	0.00000
β_1	0.99163	0.00160	6.210291e+02	0.00000
ζ_1	1.00252	0.14964	6.699740e+00	0.00000
$\alpha_{0,2}$	0.07019	0.00930	7.547540e+00	0.00000
$\alpha_{1,2}$	0.00009	0.00002	5.050590e+00	0.00000
$\alpha_{2,2}$	0.15105	0.02447	6.172750e+00	0.00000
β_2	0.82357	0.01300	6.335847e+01	0.00000
ζ_2	0.86140	0.08508	1.012519e+01	0.00000
$\alpha_{0,3}$	0.16053	0.02033	7.895810e+00	0.00000
$\alpha_{1,3}$	0.00004	0.00001	5.386870e+00	0.00000
$\alpha_{2,3}$	0.15267	0.02135	7.150380e+00	0.00000
β_3	0.83058	0.01067	7.781798e+01	0.00000
ζ_3	0.74209	0.05291	1.402492e+01	0.00000
$p_{1,1}$	0.99244	0.00921	1.077873e+02	0.00000
$p_{1,2}$	0.00000	0.00000	2.347650e+00	0.00945

Table 5.14. 3-regime gjrGARCH model estimates with skewed normal distributed innovations, OMXC25. *(continued)*

	Estimate	Std. Error	t value	Pr(>|t|)
$p_{2,1}$	0.04397	0.00000	1.172220e+06	0.00000
$p_{2,2}$	0.95603	0.00066	1.451625e+03	0.00000
$p_{3,1}$	0.00000	0.00158	2.400000e-04	0.49990
$p_{3,2}$	0.00426	0.00000	6.031533e+08	0.00000

Each of the parameter estimates in the table conforms with the notation presented in (4.8) for the gjrGARCH model, where the second subscript represents the regime.

To check the stationarity condition, $\alpha_1+\alpha_2\,\mathrm{E}[u_t^2\mathbb{I}\{u_t<0\}]+\beta<1$, for the gjrGARCH model we need to address the expectation $\mathrm{E}[u_t^2\mathbb{I}\{u_t<0\}]$. By Trottier and Ardia [2016] it is given as

$$\mathrm{E}[u_t^2\mathbb{I}\{u_t<0\}]=\frac{2}{(\zeta+\zeta^{-1})\sigma_\zeta^2}\left(\frac{1+M_1^2(\zeta^4-1)}{2\zeta^3}+\mathcal{I}_\zeta\right)$$

where f_1 is a standard normal PDF in our case, additionally, $\mathcal{I}_\zeta$ is given by

$$\mathcal{I}_\zeta\equiv\begin{cases}\zeta^3\int_0^{\mu_\zeta\zeta^{-1}}(u-\mu_\zeta\zeta^{-1})^2f_1(u)du & \text{if} \quad \zeta\geq 1\\ \frac{-1}{\zeta^3}\int_{\mu_\zeta\zeta}^{0}(u-\mu_\zeta\zeta)^2f_1(u)du & \text{if} \quad \zeta<1\end{cases}$$

By applying these formulas we get the values 0.9950931, 0.9026705 and 0.9156124 for each regime, respectively. This indicates that the process is stationary under all regimes, however, the model under the first regime does come close to non-stationarity.
These values are also often referred to as persistence parameters, the higher the value the higher the volatility persistence is. For this model, all the values of persistence are high.

Recall that the leverage effect predicts $\alpha_2>0$ in the gjrGARCH model, it is clear that the model under the first regime does not exhibit a considerably large leverage effect, however, under the second and third regimes, it is larger and significant.
Now consider the ambient volatility, $\alpha_{0,k}$, for each state, it is clearly higher in regimes 2 and 3 than in 1.

The points below summarise the results for the OMXC25 regimes

- Regime 1 has 1) low ambient volatility, 2) high volatility persistence and 3) no leverage effect.
- Regime 2 has 1) medium ambient volatility, 2) high volatility persistence and 3) significant leverage effect.
- Regime 3 has 1) high ambient volatility, 2) high volatility persistence and 3) significant leverage effect.

Next up is the results for the NJ index, the estimates are shown in table 5.15 below.

Table 5.15. 2-regime eGARCH with skewed distributed innovations for NJ.

	Estimate	Std. Error	t value	Pr(>|t|)
$\alpha_{0,1}$	-0.01639	0.00724	-2.26354	0.01180
$\alpha_{1,1}$	0.03762	0.01574	2.38949	0.00844
$\alpha_{2,1}$	-0.04521	0.01600	-2.82477	0.00237
β_1	0.99077	0.00394	251.57417	0.00000
ζ_1	0.89618	0.07586	11.81392	0.00000
$\alpha_{0,2}$	0.08584	0.02972	2.88878	0.00193
$\alpha_{1,2}$	0.21868	0.06911	3.16443	0.00078
$\alpha_{2,2}$	-0.03194	0.04994	-0.63960	0.26122
β_2	0.97532	0.01210	80.57744	0.00000
ζ_2	1.01201	0.10473	9.66305	0.00000
$p_{1,1}$	0.81771	0.13412	6.09702	0.00000
$p_{2,1}$	0.42266	0.08149	5.18659	0.00000

Applying similar arguments as for the OMXC25 3-regimes gjrGARCH estimates we summarize the regime characteristics below. First, for this model, we get the following persistence parameter for the first and second regimes 0.9907677 and 0.9753219. Following these results and the results in table 5.15 we get the following characteristics.

- Regime 1 has 1) low ambient volatility, 2) high volatility persistence and 3) low leverage effect
- Regime 2 has 1) low ambient volatility, 2) high volatility persistence and 3) low leverage effect

Next up is the results for the MJ index, the estimates are shown in table 5.16 below.

Table 5.16. 3-regime sGARCH with normal distributed innovations for MJ.

	Estimate	Std. Error	t value	Pr(>|t|)
$\alpha_{0,1}$	0.00891	0	3.607293e+21	0
$\alpha_{1,1}$	0.07180	0	6.835630e+20	0
β_1	0.92209	0	2.791559e+23	0
$\alpha_{0,2}$	0.30298	0	2.433824e+19	0
$\alpha_{1,2}$	0.00011	0	3.472469e+19	0
β_2	0.83770	0	1.779429e+20	0
$\alpha_{0,3}$	17.49965	0	7.544683e+18	0
$\alpha_{1,3}$	0.00000	0	5.000504e+07	0
β_3	0.34742	0	3.328176e+19	0
$p_{1,1}$	0.03349	0	2.563249e+19	0
$p_{1,2}$	0.96651	0	4.996321e+22	0
$p_{2,1}$	0.04121	0	6.683045e+19	0
$p_{2,2}$	0.88225	0	5.957779e+19	0
$p_{3,1}$	0.00103	0	6.808969e+29	0
$p_{3,2}$	0.21004	0	8.776683e+19	0

For MJ we get the following persistence parameter for the first, second and third regime 0.9938951, 0.8378054 and 0.3474239, respectively. And as before, a summary of the regime characteristics, using table 5.16 and the persistence parameters, is seen in the following points.

- Regime 1 has 1) low ambient volatility, 2) high volatility persistence and 3) no leverage effect
- Regime 2 has 1) low ambient volatility, 2) high volatility persistence and 3) low leverage effect
- Regime 3 has 1) high ambient volatility, 2) medium high volatility persistence and 3) no leverage effect

Now for the results for the SD index, the estimates are shown in table 5.17 below.

Table 5.17. 3-regimes gjrGARCH with normal distributed innovations for SD.

	Estimate	Std. Error	t value	Pr(>|t|)
$\alpha_{0,1}$	0.04999	0	2.390489e+19	0
$\alpha_{1,1}$	0.04709	0	4.996165e+11	0
$\alpha_{2,1}$	0.00010	0	5.000267e+07	0
β_1	0.89303	0	4.132981e+20	0
$\alpha_{0,2}$	0.11185	0	7.094146e+19	0
$\alpha_{1,2}$	0.02367	0	8.889523e+19	0
$\alpha_{2,2}$	0.00014	0	1.627314e+20	0
β_2	0.94483	0	2.448118e+21	0
$\alpha_{0,3}$	0.40559	0	5.170880e+20	0
$\alpha_{1,3}$	0.10258	0	5.481881e+20	0
$\alpha_{2,3}$	0.02618	0	7.752122e+20	0
β_3	0.87122	0	6.589810e+22	0
$p_{1,1}$	0.94509	0	2.262618e+23	0
$p_{1,2}$	0.00000	0	5.572861e+10	0
$p_{2,1}$	0.00339	0	9.991112e+27	0
$p_{2,2}$	0.99661	0	6.466951e+22	0
$p_{3,1}$	0.33036	0	3.395878e+22	0
$p_{3,2}$	0.00609	0	9.899587e+28	0

For SD we get the following persistence parameter for the first, second and third regimes 0.9401759, 0.9026705 and 0.9156124. Using these and table 5.17 a summary of the regime characteristics is seen in the following points.

- Regime 1 has 1) low ambient volatility, 2) high volatility persistence and 3) low leverage effect
- Regime 2 has 1) low ambient volatility, 2) high volatility persistence and 3) low leverage effect
- Regime 3 has 1) medium ambient volatility 2) high volatility persistence and 3) low leverage effect

The estimates for the HS index are shown in table 5.18 below.

Table 5.18. 3-regimes sGARCH with skewed normal distribution for HS.

	Estimate	Std. Error	t value	Pr(>|t|)
$\alpha_{0,1}$	0.02019	0.01904	1.060150e+00	0.14454
$\alpha_{1,1}$	0.01103	0.01838	6.004200e-01	0.27411
β_1	0.94379	0.03571	2.642837e+01	0.00000
ζ_1	1.11650	0.15874	7.033600e+00	0.00000
$\alpha_{0,2}$	3.57593	2.07085	1.726790e+00	0.04210
$\alpha_{1,2}$	0.16889	0.40181	4.203300e-01	0.33712
β_2	0.01083	0.46678	2.320000e-02	0.49075
ζ_2	0.98650	0.12563	7.852480e+00	0.00000
$\alpha_{0,3}$	0.03753	0.03227	1.163110e+00	0.12239
$\alpha_{1,3}$	0.10516	0.25455	4.131200e-01	0.33976
β_3	0.88654	0.02188	4.052506e+01	0.00000
ζ_3	0.60184	0.09504	6.332790e+00	0.00000
$p_{1,1}$	0.65669	0.17327	3.790010e+00	0.00008
$p_{1,2}$	0.34331	0.00000	1.694163e+07	0.00000
$p_{2,1}$	0.65323	28.16485	2.319000e-02	0.49075
$p_{2,2}$	0.31884	0.01862	1.712633e+01	0.00000
$p_{3,1}$	0.00000	0.00014	0.000000e+00	0.50000
$p_{3,2}$	0.01942	0.01163	1.670270e+00	0.04743

For HS we get the following persistence parameter for the first, second and third regimes 0.9548287, 0.1797218 and 0.9917053. With these and table 5.18 a summary of the regime characteristics is seen in the following points.

- Regime 1 has 1) low ambient volatility, 2) high volatility persistence and 3) no leverage effect
- Regime 2 has 1) high ambient volatility, 2)low volatility persistence and 3) no leverage effect
- Regime 3 has 1) low ambient volatility, 2) high volatility persistence and 3) no leverage effect

Finally, the estimates for the RS index are shown in table 5.19 below.

Table 5.19. 3-regimes sGARCH with skewed normal distributed innovations for RS.

	Estimate	Std. Error	t value	Pr(>|t|)
$\alpha_{0,1}$	0.01154	0	2.487513e+19	0
$\alpha_{1,1}$	0.23782	0	9.033776e+19	0
β_1	0.18988	0	3.504945e+19	0
ζ_1	1.00251	0	4.340145e+19	0
$\alpha_{0,2}$	0.01155	0	9.999999e+07	0
$\alpha_{1,2}$	0.23796	0	5.262798e+08	0
β_2	0.18999	0	1.332191e+08	0
ζ_2	1.00527	0	5.101011e+07	0

Table 5.19. 3-regimes sGARCH with skewed normal distributed innovations for RS. *(continued)*

	Estimate	Std. Error	t value	Pr(>|t|)
$\alpha_{0,3}$	0.66558	0	6.746594e+18	0
$\alpha_{1,3}$	0.10014	0	8.000525e+18	0
β_3	0.87248	0	6.925838e+20	0
ζ_3	1.30108	0	6.496285e+18	0
$p_{1,1}$	0.21740	0	1.178309e+20	0
$p_{1,2}$	0.09966	0	1.207471e+19	0
$p_{2,1}$	0.09960	0	8.654950e+20	0
$p_{2,2}$	0.21722	0	2.647527e+19	0
$p_{3,1}$	0.31443	0	8.400883e+19	0
$p_{3,2}$	0.31420	0	1.266224e+20	0

For RS we get the following persistence parameter for the first, second and third regime 0.4276935, 0.4279578 and 0.9726199. Using these parameters and table 5.19 a summary of the regime characteristics is seen in the following points.

- Regime 1 has 1) low ambient volatility, 2) medium high volatility persistence and 3) no leverage effect
- Regime 2 has 1) low ambient volatility, 2) medium high volatility persistence and 3) no leverage effect
- Regime 3 has 1) high ambient volatility, 2) high volatility persistence and 3) no leverage effect

5.2.3 Evaluation of Market Conditions before and During the Pandemic

An evaluation of the market conditions before and during the pandemic is done by considering the volatility imposed by the estimated models.

The unconditional volatility can be used as a tool for evaluation by comparing the unconditional volatility before and during the pandemic.
Using the formulas for unconditional variance, presented in (4.3), (4.7) and (4.9) for the sGARCH, eGARCH and gjrGARCH, respectively, we find the unconditional volatility under each regime by finding the square root of the unconditional variances. That is, we find

$$\sigma^2 \mid k = \mathrm{E}[y_t^2 \mid k],$$

hence

$$\sigma \mid k = \sqrt{\mathrm{E}[y_t^2 \mid k]},$$

where k represents the specific regime. The unconditional variances are shown in table 5.20 below.

	Unconditional Volatility		
Index	$\sigma \mid k = 1$	$\sigma \mid k = 2$	$\sigma \mid k = 3$
OMXC25	0.5166	0.8344	1.3135
NJ	0.6535	2.5043	NA
MJ	1.2082	1.3667	5.1784
SD	0.9141	1.8865	5.5622
HS	0.6686	2.0879	2.1271
RS	0.1420	0.1421	4.9304

Table 5.20. Unconditional volatility under each regime for each index.

Now since the regimes are changing before and during the pandemic, the (partly)[1] unconditional volatilities during these periods are difficult to calculate, what we wish to evaluate is

$$\sigma \mid s_1, \ldots, s_T = \sqrt{\mathrm{E}[y_t^2 \mid s_1, \ldots, s_T]} \tag{5.5}$$

where the states are given by the smoothed probabilities. The expression can be estimated by applying a Monte Carlo method, however, we opt to do something different.

Start by applying the law of total variation to the expectation of $\sigma^2 \mid s_1, \ldots, s_T$ such that

$$\begin{aligned}\mathrm{E}[\sigma^2 \mid s_1, \ldots, s_T] &= \mathrm{E}[y_t^2] - \mathrm{Var}(\mathrm{E}[y_t \mid s_0, \ldots, s_T]) \\ &= \mathrm{E}[y_t^2],\end{aligned}$$

now apply a special case of the law of total expectation such that

$$\begin{aligned}\mathrm{E}[\sigma^2 \mid s_1, \ldots, s_T] &= \mathrm{E}[y_t^2] \\ &= \sum_{i=1}^{n} \mathrm{E}[y_t^2 \mid s_t = i] P(s_t = i).\end{aligned}$$

We know the values of $\mathrm{E}[y_t^2 \mid s_t = i]$ as they are the unconditional variances under each regime, however, the actual value of $P(s_t = i)$ would require that we know the true values of $P(s_0 = i)$ for all $i \in \{1, \ldots, n\}$ which are unknown. Instead we estimate the values of $P(s_t = i)$ by

$$\mathrm{E}[P(s_t = i)] = \frac{1}{T} \sum_{j=1}^{T} \mathbb{I}\{s_j = i\}$$

where the values of s_j are the smoothed probabilities calculated with the Hamilton filter. This means that we have an estimator of the unconditional variance given by

$$\hat{\sigma}^2 \mid s_1, \ldots, s_T = \sum_{i=1}^{n} \mathrm{E}[y_t^2 \mid s_t = i] \, \mathrm{E}[P(s_t = i)]. \tag{5.6}$$

Now an estimator of the unconditional volatility is given by finding the square root of (5.6). The results from applying this estimator before and during the pandemic are seen in table 5.21. Additionally, the table includes the mean conditional volatilities during the same periods.

[1] It is not entirely unconditional as the states are given.

	$\hat{\sigma} \mid s_1, \ldots, s_T$			Mean Conditional Volatility		
Index	Before	During	% Increase	Before	During	% Increase
OMXC25	0.7812	1.0259	31.3268	0.9124	1.2113	32.7542
NJ	0.9012	0.9893	9.7730	0.9694	1.2970	33.7952
MJ	1.4164	2.2709	60.3266	2.2144	2.8003	26.4612
SD	1.0786	1.7296	60.3547	1.1602	1.7087	47.2706
HS	1.1739	1.5907	35.4984	1.3203	1.5533	17.6459
RS	2.5585	3.0373	18.7143	2.1400	2.2786	6.4745

Table 5.21. Unconditional and mean conditional variance before and during the pandemic.

This concludes this chapter, the following chapter will discuss and conclude on the findings presented in the project.

Chapter 6

Conclusion

6.1 Discussion

6.1.1 Municipality Study

Starting with the panel study, one of the major concerns with the results in general is the possibility of measurement errors, errors in the independent variables cause bias in the estimates. However, to defend the results, we have estimated a spatial time fixed effects model using weekly data, the results are shown in table A.20 in appendix A. Naturally, the estimates show different results, however, the important takeaway is that the sign of the estimates remains the same except for the insignificant variable, the Gini index.

Another concern is that the modeling scheme might have been better to do in a dynamic setting, e.g. including additional lagged values of the dependent variable. If the data generating process includes additional lagged variables, we either need to find suitable instruments for these variables or use a method that can model these dynamic terms directly without causing bias.

Results and Interpretation

The square meter per citizen estimate, although small, has unsurprisingly a negative sign which indicates that more space between citizens has a negative impact on the spread rate.

The vaccinated percentage estimate also shows a negative sign, which again is unsurprising as vaccination reduces the chance of contracting the virus hence reducing the spread rate.

The positive sign of service concentration percentage indicates that municipalities with a high percentage of service jobs lead to an increase in the spread rate.
Even more so in the case of children institutionalized percentage, it seems like having a high concentration of children in a municipality increases conditions for spreading the virus.

As expected, the Gini index does not seem to provide any meaningful information about the conditions for spreading the virus, this is possibly due to the other variables capturing the primary heterogeneity across municipalities.

As for the final two independent variables, the interaction terms, they indicate that policy interventions in municipalities with a high concentration of children and/or service jobs are more effective in reducing the spread rate.

Comparison of the Danish Regions

Based on the panel study, we know how certain socioeconomic conditions and political interventions affect the spread rate. Table 6.1 below shows some regional statistics about

the socioeconomic conditions in each region.

Region	Mean Relative Growth Rate	Children %	Service %	Square Meter Per Citizen
NJ	0.000246	15.3977	74.6865	787.30
MJ	0.000263	17.0098	77.1579	633.40
SD	0.000251	15.9708	75.5132	674.50
HS	0.000450	16.1926	87.9467	245.30
RS	0.000326	15.8622	78.9110	677.10
Mean	0.000307	16.0866	78.8431	603.52

Table 6.1. Regional Statistics, the first column is the region, second is the mean relative growth rate, third is percentage of the population that are children, fourth is percentage of jobs being service oriented and the fifth is square meter per citizen in urbanised areas.

Now evaluating the statistics seen in table 6.1 with the estimates seen in 5.8, we see that the NJ region has the lowest mean relative growth rate which is unsurprising due to having the lowest percentage of children, lowest percentage of service jobs and the largest square meters per citizen.
In the other extreme case we see the highest mean relative growth rate being in the HS region which again is not surprising as they have the highest percent of service jobs and lowest square meters per citizen and above average percentage of children.

6.1.2 Index Study

A major concern of the study of the indices is that the model selection procedure has been relatively restrictive. E.g. we restricted the conditional variance specifications to have only one kind of distribution across all regimes, although, their shape and skewness parameters could differ across regimes.

Another concern is that even though the OMX C25 index can be used as an indicator for the Danish economy, the regional indices are not necessarily good indicators for regional economies. A reason for this is that some of the indices are rather small, and some of the firms in their respective indices can be very small as well, hence the indicators will explain the regional economy weakly.
Another reason could be that some region's economy are primarily dependent on public jobs which might not be dependent on the private firms the indices are build from.

Results and Interpretation

Simply by casual inspection of the conditional volatility plots for each region, indicates that the pandemic has caused increases in volatility across all indices, this statement is further solidified by the values seen in table 5.21.
It is not surprising to see an increase in volatility during the pandemic in each region as the regional economies are crippled by worsened job security and supply chains.

Some regions are more affected than others according to table 5.21, consider the increase in mean conditional volatilities we see that the NJ and SD indices have a bigger increase in volatility than the general indicator OMXC25, this suggests that these regions are less economically resilient to the pandemic. The rest of the regional indices have a smaller percentage increase in volatility than the OMXC25.
Although, considering the estimates for the unconditional probabilities, it seems as if the results contradict the results for the conditional volatility increase. For example, the NJ index has the smallest increase in unconditional volatility, and looking at figure 5.6 it is not surprising. Looking at the conditional volatility plot we see that the predicted regimes do not conform with the high conditional volatilities. The change of regimes seemingly captures spikes and not a general increase in volatility. This could indicate that a 3 regimes model would be better, however, according to the summarized conditional coverage tests, that we conducted, the 2 regimes model was better.
Besides the NJ index, the unconditional volatilities for the MJ and HS index also disagree with the mean conditional volatilities.

6.2 Conclusion

We present the research questions again below.

- Which conditions influence the Covid-19 spread rate across Denmark?
  - Which effects do socioeconomic conditions have?
  - Which effects do political responses have?

It seems there are several socioeconomic conditions that influence the spread rate across Denmark including the percentage of children, percentage of service jobs and square meters per citizen. Additionally, the stringency policy interventions seams to have better effect in reducing the spread rate in areas with higher percentage of service jobs and children.

- Is there an increase in volatility in the Danish economy?
  - If so, is such an increase similar across Danish regions?

There is an increase in volatility in the Danish economy which is emphasized by the results for OMXC25 in table 5.21. Additionally, the volatility increase is not homogeneous as we see the volatility increase is different across regional indices seen in the same table.

6.3 Future Research

As for future research there are several points to improve and build upon.
The modeling setup for the panel study could be applied to more macroeconomic level, possibly looking at the socioeconomic conditions across countries in Europe. This would be a more nuanced study as there will be more variability across countries and their specific socioeconomic conditions.
As mentioned, the panel study might have been improved by using more dynamic oriented panel models.

The Danish economy has also drastically changed since the start of conducting this study due to the recent war in south eastern Europe, so the increase in volatility due to these events could also be interesting to model with the same framework.
As for the GARCH modeling scheme, it would be interesting to include exogenous variables like the stringency index to see if the volatility is dependent on the stringency policies imposed by the government. Another possibility is modeling the prices directly through an ARIMA framework and maybe using exogenous variables to explain changes in the conditional mean dynamics.

Another topic of interest was investigating the general mental health in Denmark before and after the pandemic, however, at the time of writing there were not data available to investigate this topic.

Bibliography

Addison, T., Sen, K. and Tarp, F. [2020], 'Covid-19: macroeconomic dimensions in the developing world'.
URL: https://www.wider.unu.edu/sites/default/files/Publications/Working-paper/PDF/wp2020-74.pdf

Amemiya, T. [1971], 'The estimation of the variances in a variance-components model', *International Economic Review* 12(1), 1–13.
URL: http://www.jstor.org/stable/2525492

Anselin, L., Gallo, J. L. and Jayet, H. [2008], *Spatial Panel Econometrics*, Springer Berlin Heidelberg, Berlin, Heidelberg.
URL: https://doi.org/10.1007/978-3-540-75892-1_19

Ardia, D., Bluteau, K., Boudt, K. and Catania, L. [2018], 'Forecasting risk with markov-switching garch models: A large-scale performance study'.
URL: https://pure.au.dk/ws/files/137371173/Forecasting_risk_with_markov_switching_garch_models_VOR18.pdf

Ardia, D., Bluteau, K., Boudt, K., Catania, L. and Trottier, D.-A. [2019], 'Markov-switching garch models in r: The msgarch package'.
URL: https://www.jstatsoft.org/article/view/v091i04

Baltagi, B. H. [2021], *Econometric Analysis of Panel Data*, 6 edn, Springer.

Bauwens, L., Preminger, A. and Rombouts, J. V. [2006], 'Regime switching garch models'.
URL: https://www.researchgate.net/publication/5107819_Regime_switching_GARCH_models

Bennedsen, M., Larsen, B., Schmutte, I. and Scur, D. [2020], 'Preserving job matches during the covid-19 pandemic: firm-level evidence on the role of government aid'.
URL: https://www.economics.ku.dk/research/corona/covid19_projekt_5_.pdf

Borchers, B. [2001], 'The partial autocorrelation function'.
URL: http://www.ees.nmt.edu/outside/courses/GEOP505/Docs/pac.pdf

Brink, A. [2021], 'Seks procent af de unge mener ikke, livet er værd at leve under corona'.
URL: https://ugeavisen.dk/kobenhavn/artikel/seks-procent-af-de-unge-mener-ikke-livet-er-v%C3%A6rd-at-leve-under-corona

Chen, L., Raitzer, D., Hasan, R., Lavado, R. and Velarde, O. [2020], 'What works to control covid-19:econometric analysis of a cross country panel'.
URL: https://www.adb.org/sites/default/files/publication/659521/ewp-625-covid-19-econometric-analysis-cross-country-panel.pdf

Comincioli, B. [1996], 'The stock market as a leading indicator: An application of granger causality', *The Park Place Economist* 1, 13.

Davidson, R. and MacKinnon, J. G. [2003], *Econometric Theory and Methods*, 1 edn, Oxford University Press.

Dumitrescu, E.-I., Hurlin, C. and Pham, V. [2012], 'Backtesting value-at-risk: From dynamic quantile to dynamic binary tests', *Dans Finance* 33(1), 79–112.
URL: https://www.cairn.info/revue-finance-2012-1-page-79.htm

Hamilton, J. D. [1994], *Time Series Analysis*, 1 edn, Princeton University Press.
URL: http://www.amazon.com/exec/obidos/redirect?tag=citeulike07-20&path=ASIN/0691042896

Hamilton, J. D. [2010], *Regime switching models*, Palgrave Macmillan UK, London.
URL: https://doi.org/10.1057/9780230280830_23

Hansen, C. [2007], 'Asymptotic properties of a robust variance matrix estimator for panel data when t is large', *Journal of Econometrics* 141, 597–620.

He, C., Teräsvirta, T. and Malmsten, H. [2002], 'Moment structure of a family of first-order exponential garch models', *cambridge University Press* 18, 19.

H.Shumway, R. and S.Stoffer, D. [2017], *Time Series Analysis and Its Applications*, 4 edn, Springer.

Høiby, N. [2020], 'Hvad er coronavirus'.
URL: https://netdoktor.dk/nyheder/hvad-er-coronavirus.htm

Josephson, A., Kilic, T. and Michler, J. D. [2021], 'Socioeconomic impacts of covid-19 in low-income countries'.
URL: https://www.nature.com/articles/s41562-021-01096-7

Kim, C.-J. [1994], 'Dynamic linear models with markov-switching', *Journal of Econometrics* 60(1), 1–22.
URL: https://www.sciencedirect.com/science/article/pii/0304407694900361

KPMG [2020], 'Government and institution measures in response to covid-19.'.
URL: https://home.kpmg/xx/en/home/insights/2020/04/denmark-government-and-institution-measures-in-response-to-covid.html

Kristensen, P. K. [2021], 'Smitten spreder sig: Det er især blandt børn og uvaccinerede unge, at tallene stiger'.
URL: https://www.dr.dk/nyheder/viden/kroppen/smitten-spreder-sig-det-er-isaer-blandt-boern-og-uvaccinerede-unge-tallene

Li, Y. and Kapri, K. P. [2021], 'Impact of economic factors and policy interventions on the covid-19 pandemic', *Sustainability* 13, 18.
URL: https://www.mdpi.com/2071-1050/13/22/12874/htm

Magnus, J. R. [1982], 'Multivariate error components analysis of linear and nonlinear regression models by maximum likelihood'.
URL: https://www.janmagnus.nl/papers/JRM009.pdf

McCracken, L. M., Badinlou, F., Buhrman, M. and Brocki, K. C. [2020], 'Psychological impact of covid-19 in the swedish population: Depression, anxiety, and insomnia and their associations to risk and vulnerability factors'.
URL: https://www.ncbi.nlm.nih.gov/pmc/articles/PMC7503043/

Millo, G. [2017], 'Robust standard error estimators for panel models: A unifying approach', *Journal of Statistical Software* 82(3), 1–27.
URL: https://www.jstatsoft.org/index.php/jss/article/view/v082i03

NCSS [2022], 'The box-jenkins method'.
URL: https://ncss-wpengine.netdna-ssl.com/wp-content/themes/ncss/pdf/Procedures/NCSS/The_Box-Jenkins_Method.pdf

Occhipinti, J.-A., Skinner, A., Doraiswamy, P. M., Fox, C., Herrman, H., Saxena, S., London, E., Song, Y. J. C. and Hickie, I. B. [2021], 'Mental health: build predictive models to steer policy'.
URL: https://www.nature.com/articles/d41586-021-02581-9

Oshinubi, K., Rachdi, M. and Demongeot, J. [2022], 'Modeling of covid-19 pandemic vis-à-vis some socio-economic factors', *Article 786983* 7, 25.
URL: https://www.frontiersin.org/articles/10.3389/fams.2021.786983/full#h1

Oxford, U. O. [2022], 'Covid-19 government response tracker'.
URL: https://www.bsg.ox.ac.uk/research/research-projects/covid-19-government-response-tracker

Petersen, E. F. [2015], 'Modeling tail distributions with regime switching garch models'.
URL: https://research-api.cbs.dk/ws/portalfiles/portal/58423457/ebbe_filt_petersen.pdf

Petersen, M. W., Dantoft, T. M., Jensen, J. S., Pedersen, H. F., Frostholm, L., Benros, M. E., Carstensen, T. B. W., Ørnbøl, E. and Fink, P. [2021], 'The impact of the covid-19 pandemic on mental and physical health in denmark – a longitudinal population-based study before and during the first wave'.
URL: https://bmcpublichealth.biomedcentral.com/track/pdf/10.1186/s12889-021-11472-7.pdf

Pollock, D. [2000], 'Topics in econometrics'.
URL: https://www.le.ac.uk/users/dsgp1/COURSES/TOPICS/gausmkov.pdf

Robinson, T. S. [2020], 'Fundamental theorems for econometrics'.
URL: https://bookdown.org/ts_robinson1994/10_fundamental_theorems_for_econometrics/frisch.html

Roccioletti, S. [2015], *Backtesting Value at Risk and Expected Shortfall*, 1 edn, Springer.

Stock, J. H. and Watson, M. W. [2008], 'Heteroskedasticity-robust standard errors for fixed effects panel data regression', *Econometrica* 76(1), 155–174.
URL: https://onlinelibrary.wiley.com/doi/abs/10.1111/j.0012-9682.2008.00821.x

Swamy, P. and Arora, S. [1972], 'The exact finite sample properties of the estimators of coefficients in the error components regression models', *Econometrica* 40(2), 261–75.
URL: https://EconPapers.repec.org/RePEc:ecm:emetrp:v:40:y:1972:i:2:p:261-75

Trottier, D.-A. and Ardia, D. [2016], 'Moments of standardized fernandez-steel skewed distribution:applications to the estimation of garch-type mpdels'.
URL: https://www.sciencedirect.com/science/article/pii/S1544612316300836

Wooldridge, J. M. [2010], *Econometric Analysis of Cross Section and Panel Data*, Vol. 1 of *MIT Press Books*, The MIT Press.
URL: https://ideas.repec.org/b/mtp/titles/0262232588.html
vlisen et al.

Øvlisen, T. B., Rysgård, K. K., Bregendahl, U. and Pedersen, J. B. [2021], 'Smitte sender børn hjem på stribe:det går som en steppebrand'.
URL: https://www.dr.dk/nyheder/indland/smittesenderb\T1\ornhjempåstribedet gårsomensteppebrand

Appendix A

Extra Figures and Tables

A.1 Panel Figures and Tables

DV: log.gr.rt	gr.rt	Vac.pct	Stringency	St.I.Se	St.I.Ch
Coefficient	0.94499	0.01509***	0.00009***	− 0.00027***	− 0.00160***
s.e. OLS	0.00181***	0.00058***	0.00001***	0.00010***	0.00040***
s.e. Vw	0.00591***	0.00059***	0.00001***	0.00010***	0.00042***
s.e. Vcx	0.00811***	0.00082***	0.00001***	0.00004***	0.00027***
s.e. Vct	0.03423***	0.00334***	0.00003***	0.00011***	0.00057***
s.e. VBKx	0.00606***	0.00072***	0.00001***	0.00004***	0.00018***
s.e. VBKt	0.01271***	0.00404***	0.00009***	0.00012***	0.00053***
s.e. Vcxt	0.03467***	0.00339***	0.00003***	0.00006***	0.00047***
s.e. Vct.L	0.04347***	0.00611***	0.00006***	0.00013***	0.00060***
s.e. Vnw.L	0.00647***	0.00074***	0.00001***	0.00008***	0.00034***
s.e. Vscc.L	0.04259***	0.00523***	0.00005***	0.00012***	0.00059***
s.e. Vcxt.L	0.04372***	0.00611***	0.00006***	0.00013***	0.00064***
Observations:	67,326				
R^2:	0.846				
Adjusted R^2:	0.845				
Note:	*p<0.1; **p<0.05; ***p<0.01				

Table A.1. Individual fixed effects, OLS and Robust.

Dependent variable: log.Relative.growth.rate	Estimate	Std.Error	t.value	p.value
lag.lag.log.Relative.growth.rate	0.94493	0.00014	6,950.98300	0
Vaccinated.pct	0.01486	0.00015	99.05120	0
Stringency.index	0.00008	0.000002	49.03038	0
Stringency.index.I.Service.concentration.pct	− 0.00027	0.000003	− 77.27983	0
Stringency.index.I.Children.institutionalized.pct	− 0.00161	0.00001	− 113.27490	0
Observations:	67,326			
R^2:	0.848			
Adjusted R^2:	0.848			

Table A.2. FGLS estimation of individual fixed effects.

DV: log.gr.rt	SqMe	gr.rt	Vac.pct	Service	Children	Gini	St.I.Se	St.I.Ch
Coefficient	− 0.000005	0.61984	− 0.04412	0.01317	0.04258	− 0.000002**	− 0.00088	− 0.00354
s.e. OLS	0***	0.00324	0.00324	0.00125	0.00493	0.00002	0.00006	0.00026
s.e. Vw	0***	0.01362	0.00437	0.00179	0.00551	0.00002	0.00006	0.00029
s.e. Vcx	0.000001***	0.02964	0.01469	0.00304	0.01296	0.00004	0.00011	0.00065
s.e. Vct	0.000001***	0.02498	0.00746	0.00187	0.00771	0.00002	0.00012	0.00062
s.e. VBKx	0.000001***	0.01774	0.00796	0.00326	0.01278	0.00005	0.00011	0.00046
s.e. VBKt	0.000001***	0.01005	0.00646	0.00161	0.00631	0.00002	0.00013	0.00067
s.e. Vcxt	0.000001***	0.03630	0.01588	0.00309	0.01404	0.00004	0.00015	0.00086
s.e. Vct.L	0.000001***	0.04640	0.01649	0.00273	0.01740	0.00003	0.00028	0.00154
s.e. Vnw.L	0.000001***	0.01778	0.00605	0.00226	0.00682	0.00003	0.00008	0.00036
s.e. Vscc.L	0.000001***	0.03922	0.01285	0.00238	0.01370	0.00003	0.00022	0.00118
s.e. Vcxt.L	0.000001***	0.05092	0.02080	0.00308	0.02025	0.00004	0.00029	0.00162
Observations:	67,326							
R^2:	0.444							
Adjusted R^2:	0.443							
Note:	*p<0.1; **p<0.05; ***p<0.01							

Table A.3. Time fixed effects, OLS and Robust.

Dependent variable: log.Relative.growth.rate	Estimate	Std.Error	t.value	p.value
SqrMeter.per.citizen.urban.areas	− 0.000003	0.0000003	− 12.03464	0
lag.lag.log.Relative.growth.rate	0.49475	0.00346	143.02200	0
Vaccinated.pct	− 0.03366	0.00199	− 16.93296	0
Service.concentration.pct	0.00895	0.00075	11.91704	0
Children.institutionalized.pct	0.02300	0.00303	7.58774	0
Gini.index	0.00002	0.00001	1.29680	0.19470
Stringency.index.I.Service.concentration.pct	− 0.00038	0.00005	− 7.62481	0
Stringency.index.I.Children.institutionalized.pct	− 0.00113	0.00021	− 5.40497	0.0000001
Observations:	67,326			
R^2:	0.935			
Adjusted R^2:	0.935			

Table A.4. FGLS estimation of time fixed effects

Dependent variable: log.Relative.growth.rate	Estimate	Std.Error	t.value	p.value
(Intercept)	− 0.25857	0.00888	− 29.11866	0
SqrMeter.per.citizen.urban.areas	− 0.000002	0.000001	− 3.45931	0.00054
lag.lag.log.Relative.growth.rate	0.94550	0.00181	523.49200	0
Vaccinated.pct	0.01498	0.00057	26.04824	0
Service.concentration.pct	0.00124	0.00192	0.64747	0.51733
Children.institutionalized.pct	0.01862	0.00760	2.44923	0.01432
Gini.index	− 0.00001	0.00003	− 0.37434	0.70815
Stringency.index	0.00009	0.00001	6.85295	0
Stringency.index.I.Service.concentration.pct	− 0.00027	0.00010	− 2.73637	0.00621
Stringency.index.I.Children.institutionalized.pct	− 0.00159	0.00040	− 4.02879	0.00006
Observations:	67,326			
R^2:	0.848			
Adjusted R^2:	0.848			

Table A.5. Individual random effects.

Dependent variable: log.Relative.growth.rate	Estimate	Std.Error	t.value	p.value
(Intercept)	− 1.57717	0.01480	− 106.55910	0
SqrMeter.per.citizen.urban.areas	− 0.00001	0.0000003	− 17.39257	0
lag.lag.log.Relative.growth.rate	0.65155	0.00313	208.24440	0
Vaccinated.pct	0.00176	0.00241	0.73068	0.46497
Service.concentration.pct	0.01021	0.00125	8.14068	0
Children.institutionalized.pct	0.04671	0.00497	9.40196	0
Gini.index	− 0.00003	0.00002	− 1.15382	0.24857
Stringency.index	− 0.00054	0.00007	− 7.80767	0
Stringency.index.I.Service.concentration.pct	− 0.00088	0.00006	− 13.78489	0
Stringency.index.I.Children.institutionalized.pct	− 0.00395	0.00026	− 15.14999	0
Observations:	67,326			
R^2:	0.463			
Adjusted R^2:	0.463			

Table A.6. Time random effects.

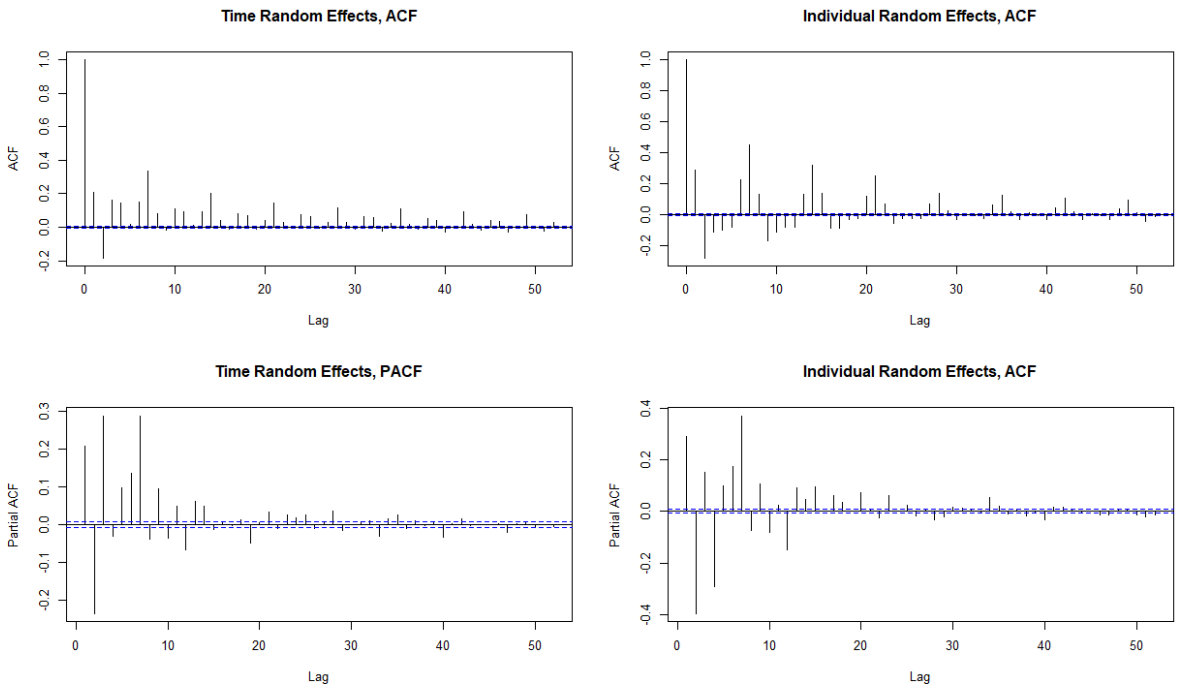

Figure A.1. One-way random effects ACF and PACF.

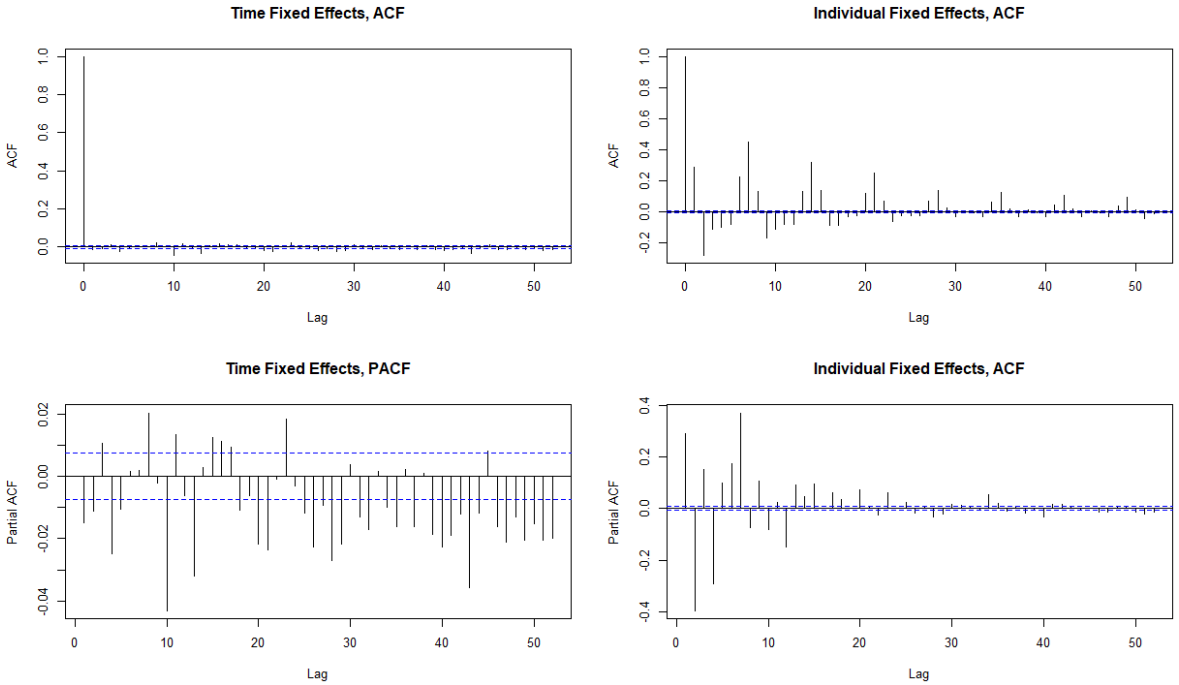

Figure A.2. One-way fixed effects ACF and PACF.

Dependent variable: log.gr.rt	growth.rate	Vaccinated	St.I.Se	St.I.Ch
Coefficient	0.60377	− 0.03936***	− 0.00092***	− 0.00375***
s.e. OLS	0.00329***	0.00355***	0.00006***	0.00026***
s.e. Vw	0.01412***	0.00431***	0.00006***	0.00029***
s.e. Vcx	0.03119***	0.01506***	0.00012***	0.00068***
s.e. Vct	0.02531***	0.00730***	0.00012***	0.00063***
s.e. VBKx	0.01886***	0.00814***	0.00012***	0.00049***
s.e. VBKt	0.01040***	0.00745***	0.00013***	0.00068***
s.e. Vcxt	0.03760***	0.01616***	0.00016***	0.00088***
s.e. Vct.L	0.04904***	0.01454***	0.00029***	0.00158***
s.e. Vnw.L	0.01877***	0.00613***	0.00008***	0.00037***
s.e. Vscc.L	0.04093***	0.01153***	0.00023***	0.00121***
s.e. Vcxt.L	0.05368***	0.01951***	0.00030***	0.00167***
Observations:	67,326			
R^2:	0.36			
Adjusted R^2:	0.359			
Note:	*p<0.1;			
	**p<0.05;			
	***p<0.01			

Table A.7. Two-way fixed effects OLS and Robust.

Dependent variable: log.Relative.growth.rate	Estimate	Std.Error	t.value	p.value
(Intercept)	− 1.57708	0.01480	− 106.55670	0
SqrMeter.per.citizen.urban.areas	− 0.00001	0.0000003	− 17.39323	0
lag.lag.log.Relative.growth.rate	0.65158	0.00313	208.25740	0
Vaccinated.pct	0.00178	0.00240	0.74073	0.45886
Service.concentration.pct	0.01021	0.00125	8.13917	0
Children.institutionalized.pct	0.04671	0.00497	9.40210	0
Gini.index	− 0.00003	0.00002	− 1.15432	0.24837
Stringency.index	− 0.00054	0.00007	− 7.80419	0
Stringency.index.I.Service.concentration.pct	− 0.00088	0.00006	− 13.78445	0
Stringency.index.I.Children.institutionalized.pct	− 0.00396	0.00026	− 15.15038	0
Observations:	67,326			
R^2:	0.464			
Adjusted R^2:	0.463			

Table A.8. Two-way random effects.

A.2 Regime Figures and Tables

Table A.9. Summarizing Statistics.

				Price in DKK			
Symbol	Observations	First.obs	Last.obs	Mean	Std.dev	Min	Max
OMXsmall	1571	2016-01-05	2022-04-13	290.1	103.0	175.8	550.7
OMXmid	1567	2016-01-05	2022-04-07	548.8	138.0	369.9	912.1
OMXlarge	1567	2016-01-05	2022-04-07	287.1	68.8	198.7	455.1
OMXC20	6377	1996-10-10	2022-04-06	554.7	372.3	125.3	1771.0
OMXC25	1323	2016-12-20	2022-04-06	1337.5	303.3	980.8	2020.7
NJ	1573	2016-01-04	2022-04-13	139.0	10.4	108.4	173.2
MJ	1573	2016-01-04	2022-04-13	135.5	49.1	79.9	270.1
SD	1573	2016-01-04	2022-04-13	31.5	11.3	15.2	59.6
HS	1573	2016-01-04	2022-04-13	582.6	139.4	363.5	962.4
RS	1573	2016-01-04	2022-04-13	451.3	77.3	348.0	692.5
AAB	1573	2016-01-04	2022-04-13	98.1	52.3	38.4	197.7
AGAT	1573	2016-01-04	2022-04-13	5.3	3.0	1.8	12.4
AGF_B	1573	2016-01-04	2022-04-13	0.4	0.2	0.2	0.8
ALK_B	1569	2016-01-04	2022-04-07	1550.3	738.7	681.0	3440.0
ALMB	1569	2016-01-04	2022-04-07	14.2	2.2	10.8	20.1
AMBU_B	1569	2016-01-04	2022-04-07	142.5	69.6	37.7	349.5
AOJ_B	1569	2016-01-04	2022-04-07	482.0	285.9	168.0	1345.0
AQP	202	2021-06-28	2022-04-07	128.4	20.2	100.2	172.8
ATLA_DKK	1573	2016-01-04	2022-04-13	7.6	2.4	3.7	15.0
BAVA	1569	2016-01-04	2022-04-07	197.7	59.8	105.9	366.8
BIF	1573	2016-01-04	2022-04-13	0.6	0.2	0.3	1.3

Table A.9. Summarizing Statistics. *(continued)*

				Price in DKK			
Symbol	Observations	First.obs	Last.obs	Mean	Std.dev	Min	Max
BIOPOR	1573	2016-01-04	2022-04-13	2.8	0.8	1.4	5.7
BLVIS_A	1573	2016-01-04	2022-04-13	0.9	0.8	0.2	3.6
BNORDIK_CSE	1569	2016-01-04	2022-04-07	123.9	20.0	93.8	177.5
BO	1569	2016-01-04	2022-04-07	36.6	18.2	9.1	84.0
BOOZT_DKK	344	2020-11-25	2022-04-07	126.7	12.0	102.3	162.1
CARL_A	1569	2016-01-04	2022-04-07	854.3	223.0	533.0	1495.0
CARL_B	1569	2016-01-04	2022-04-07	825.7	164.0	575.0	1183.5
CBRAIN	1569	2016-01-04	2022-04-07	94.8	91.6	19.8	386.5
CEMAT	1573	2016-01-04	2022-04-13	0.4	0.2	0.2	1.1
CHEMM	1569	2016-01-04	2022-04-07	258.9	294.0	25.8	1128.0
CHR	1569	2016-01-04	2022-04-07	555.5	85.3	405.6	754.4
COLO_B	1569	2016-01-04	2022-04-07	740.2	221.4	434.3	1182.5
COLUM	1569	2016-01-04	2022-04-07	11.6	2.7	7.2	18.5
CPHCAP_PREF	1198	2017-07-03	2022-04-13	1.8	0.1	1.7	2.2
CPHCAP_ST	1573	2016-01-04	2022-04-13	3.1	1.5	1.3	7.8
DAB	1569	2016-01-04	2022-04-07	6.4	2.5	2.5	11.9
DANSKE	1569	2016-01-04	2022-04-07	155.5	57.5	69.7	257.5
DANT	1573	2016-01-04	2022-04-13	253.6	78.1	126.0	535.0
DEMANT	1569	2016-01-04	2022-04-07	208.4	64.7	111.5	389.8
DFDS	1569	2016-01-04	2022-04-07	315.1	48.7	219.8	424.0
DJUR	1573	2016-01-04	2022-04-13	262.3	44.6	198.5	382.0
DNORD	1569	2016-01-04	2022-04-07	115.0	26.1	70.7	199.5
DRLCO	752	2019-04-04	2022-04-07	277.7	110.4	120.0	555.0
DSV	1569	2016-01-04	2022-04-07	707.2	391.1	230.7	1679.0
EAC	1573	2016-01-04	2022-04-13	26824.3	23691.6	1190.0	71000.0
ESG	1573	2016-01-04	2022-04-13	38.1	29.7	7.0	80.0
FED	1573	2016-01-04	2022-04-13	105.2	18.6	74.0	148.0
FFARMS	1573	2016-01-04	2022-04-13	57.6	9.1	42.7	86.4
FLS	1569	2016-01-04	2022-04-07	290.1	72.4	173.2	441.8
FLUG_B	1569	2016-01-04	2022-04-07	411.5	152.0	250.0	790.0
FYNBK	1573	2016-01-04	2022-04-13	85.4	16.9	60.0	132.0
GABR	1569	2016-01-04	2022-04-07	626.3	97.4	400.0	988.0
GERHSP	1573	2016-01-04	2022-04-13	129.0	10.6	103.0	150.0
GJ	1573	2016-01-04	2022-04-13	57.7	11.8	39.6	90.0
GMAB	1569	2016-01-04	2022-04-07	1586.0	606.0	674.0	3100.0
GN	1569	2016-01-04	2022-04-07	296.7	125.2	109.5	586.2
GREENH	209	2021-06-17	2022-04-07	35.8	5.5	27.6	47.8
GREENM	1208	2017-06-16	2022-04-13	121.9	31.4	67.5	220.0
GRLA	1573	2016-01-04	2022-04-13	600.4	30.9	534.0	660.0
GYLD_A	1569	2016-01-04	2022-04-07	1862.2	1404.4	633.0	5500.0
GYLD_B	1569	2016-01-04	2022-04-07	474.2	42.9	402.0	585.0
HARB_B	1573	2016-01-04	2022-04-13	93.5	26.1	52.8	149.5

Table A.9. Summarizing Statistics. *(continued)*

				Price in DKK			
Symbol	Observations	First.obs	Last.obs	Mean	Std.dev	Min	Max
HART	1569	2016-01-04	2022-04-07	356.1	81.8	247.0	608.0
HH	1569	2016-01-04	2022-04-07	115.8	46.8	54.4	257.5
HUSCO	349	2020-11-18	2022-04-07	122.0	6.0	112.0	138.6
HVID	1573	2016-01-04	2022-04-13	65.5	20.4	35.0	119.0
IMAIL	1573	2016-01-04	2022-04-13	13.5	5.5	6.2	29.0
ISS	1569	2016-01-04	2022-04-07	196.4	56.1	100.2	286.3
JDAN	1569	2016-01-04	2022-04-07	199.7	48.9	132.0	298.0
JYSK	1569	2016-01-04	2022-04-07	301.8	53.0	200.2	416.9
KBHL	1569	2016-01-04	2022-04-07	5693.2	654.9	4250.0	7600.0
KLEE_B	1573	2016-01-04	2022-04-13	2729.5	316.4	2240.0	4080.0
KRE	1573	2016-01-04	2022-04-13	2907.6	636.9	2131.0	4380.0
LASP	1569	2016-01-04	2022-04-07	488.0	62.1	383.1	665.0
LOLB	1573	2016-01-04	2022-04-13	374.8	90.2	206.0	620.0
LUN	1569	2016-01-04	2022-04-07	271.2	70.5	160.6	475.9
LUXOR_B	1573	2016-01-04	2022-04-13	433.2	78.9	312.0	700.0
MAERSK_A	1569	2016-01-04	2022-04-07	10670.7	3800.3	4988.0	22240.0
MAERSK_B	1569	2016-01-04	2022-04-07	11220.7	3950.5	5394.0	23450.0
MATAS	1569	2016-01-04	2022-04-07	87.5	25.0	47.8	134.5
MNBA	1573	2016-01-04	2022-04-13	147.9	38.6	100.2	260.0
MTHH	1573	2016-01-04	2022-04-13	175.9	85.2	48.6	405.0
NDA_DK	1569	2016-01-04	2022-04-07	65.5	11.7	45.2	88.7
NETC	962	2018-06-07	2022-04-07	427.7	192.5	194.5	855.5
NEWCAP	1573	2016-01-04	2022-04-13	1.2	0.7	0.4	2.5
NKT	1569	2016-01-04	2022-04-07	244.8	121.5	65.9	494.8
NLFSK	1121	2017-10-12	2022-04-07	218.5	71.8	91.1	363.0
NNIT	1569	2016-01-04	2022-04-07	157.0	41.2	87.8	284.0
NORDIC	1573	2016-01-04	2022-04-13	0.6	0.2	0.2	1.2
NORTHM	1569	2016-01-04	2022-04-07	48.7	33.0	12.2	136.4
NOVO_B	1569	2016-01-04	2022-04-07	385.3	123.0	220.7	762.1
NRDF	1573	2016-01-04	2022-04-13	170.5	51.7	96.0	302.0
NTG	1569	2016-01-04	2022-04-07	147.9	137.8	45.2	563.0
NTR_B	1573	2016-01-04	2022-04-13	39.0	6.3	29.5	58.0
NZYM_B	1569	2016-01-04	2022-04-07	345.7	64.2	244.8	537.2
ORPHA	1096	2017-11-16	2022-04-07	66.1	20.8	24.7	135.0
ORSTED	1463	2016-06-09	2022-04-07	584.9	271.5	230.5	1355.0
OSSR	1569	2016-01-04	2022-04-07	36.2	9.0	22.5	56.4
PAAL_B	1569	2016-01-04	2022-04-07	221.3	44.3	151.0	322.0
PARKEN	1573	2016-01-04	2022-04-13	82.7	12.8	61.0	120.0
PARKST_A	1573	2016-01-04	2022-04-13	7.4	3.6	1.6	17.9
PENNEO	473	2020-06-02	2022-04-13	39.4	15.0	14.9	82.8
PNDORA	1569	2016-01-04	2022-04-07	610.3	213.8	253.4	999.5
PRIMOF	1573	2016-01-04	2022-04-13	171.9	59.6	79.0	326.0

Table A.9. Summarizing Statistics. *(continued)*

				Price in DKK			
Symbol	Observations	First.obs	Last.obs	Mean	Std.dev	Min	Max
RBLN_B	1573	2016-01-04	2022-04-13	226.1	64.6	136.0	414.0
RBREW	1569	2016-01-04	2022-04-07	499.2	170.4	248.1	852.2
RIAS_B	1573	2016-01-04	2022-04-13	463.1	78.8	360.0	710.0
RILBA	1569	2016-01-04	2022-04-07	442.6	168.6	249.4	950.0
ROCK_A	1569	2016-01-04	2022-04-07	1713.5	519.8	932.0	3000.0
ROCK_B	1569	2016-01-04	2022-04-07	1881.9	635.0	925.0	3429.0
ROV	1573	2016-01-04	2022-04-13	107.5	49.1	33.0	267.0
RTX	1569	2016-01-04	2022-04-07	173.8	29.7	111.0	279.0
SANI	1573	2016-01-04	2022-04-13	73.0	11.1	54.5	103.0
SAS_DKK	1569	2016-01-04	2022-04-07	10.5	5.9	0.9	24.4
SBS	1573	2016-01-04	2022-04-13	21.4	5.5	12.0	38.0
SCHO	1569	2016-01-04	2022-04-07	571.1	74.8	416.0	750.0
SIF	1573	2016-01-04	2022-04-13	13.9	1.6	8.5	18.3
SIG	1573	2016-01-04	2022-04-13	1.7	0.5	0.7	3.3
SIM	1569	2016-01-04	2022-04-07	558.9	177.8	290.0	932.0
SKAKO	1573	2016-01-04	2022-04-13	63.0	18.5	35.3	116.0
SKJE	1573	2016-01-04	2022-04-13	70.1	16.6	36.5	124.5
SOLAR_B	1569	2016-01-04	2022-04-07	396.8	131.4	197.4	793.0
SPG	1569	2016-01-04	2022-04-07	242.0	78.2	99.3	441.0
SPKSJF	1569	2016-01-04	2022-04-07	104.7	21.7	74.8	190.0
SPNO	1569	2016-01-04	2022-04-07	67.0	11.3	48.5	101.4
STG	1542	2016-02-10	2022-04-07	108.0	16.8	77.9	152.8
STRINV	1573	2016-01-04	2022-04-13	1.1	0.1	0.8	1.4
SYDB	1569	2016-01-04	2022-04-07	190.2	44.2	111.0	264.9
TCM	1090	2017-11-24	2022-04-07	123.3	22.3	89.5	173.5
TIV	1569	2016-01-04	2022-04-07	674.6	102.7	455.0	924.0
TOP	1569	2016-01-04	2022-04-07	286.3	56.0	177.2	415.2
TOTA	1573	2016-01-04	2022-04-13	78.8	26.5	39.1	140.0
TRIFOR	224	2021-05-27	2022-04-07	220.4	35.7	175.0	303.5
TRMD_A	1496	2016-04-19	2022-04-07	54.8	8.4	41.0	82.0
TRYG	1569	2016-01-04	2022-04-07	136.4	22.5	100.1	181.4
UIE	1569	2016-01-04	2022-04-07	1400.1	185.6	1075.0	2020.0
VJBA	1569	2016-01-04	2022-04-07	2.9	0.6	1.9	4.8
VWS	1569	2016-01-04	2022-04-07	137.7	59.2	72.2	312.0
ZEAL	1569	2016-01-04	2022-04-07	148.1	53.3	78.5	294.0

	Exceedance		Test		
mod	expected.exceed	actual.exceed	LRstat	pvalue	Accepted.null.hypotheses
e.ge	32	50	20.379	0.0602477	6
e.no	32	40	5.947	0.9187301	6
e.sg	32	40	7.850	0.7967398	6
e.sn	32	38	5.786	0.9264829	6
e.st	32	50	18.050	0.1141808	6
g.ge	32	51	21.141	0.0483535	6
g.no	32	46	15.746	0.2031487	6
g.sg	32	48	15.122	0.2348323	6
g.sn	32	52	22.092	0.0365016	6
g.ss	32	50	17.663	0.1263127	6
g.st	32	50	17.663	0.1263127	6
s.ge	32	48	17.440	0.1337820	6
s.no	32	46	15.975	0.1923838	6
s.sg	32	49	16.943	0.1517541	6
s.sn	32	45	15.024	0.2401266	6
s.ss	32	52	19.233	0.0830585	6
s.st	32	53	20.501	0.0581827	6

Table A.10. Summarized conditional coverage test NJ, 2 regimes.

	Exceedance		Test		
mod	expected.exceed	actual.exceed	LRstat	pvalue	Accepted.null.hypotheses
e.ge	32	39	8.195	0.7697121	6
e.no	32	46	11.799	0.4619544	6
e.sg	32	43	8.655	0.7320812	6
e.sn	32	49	19.134	0.0853455	6
e.ss	32	52	18.277	0.1075351	6
e.st	32	51	20.190	0.0635761	6
g.ge	32	34	5.957	0.9182341	6
g.no	32	46	16.303	0.1777489	6
g.sg	32	38	7.334	0.8347754	6
g.sn	32	45	13.579	0.3283960	6
g.ss	32	37	7.225	0.8423934	6
g.st	32	42	8.481	0.7465035	6
s.ge	32	41	9.232	0.6829972	6
s.no	32	45	15.024	0.2401266	6
s.sg	32	41	9.232	0.6829972	6
s.sn	32	44	13.316	0.3464970	6
s.ss	32	47	16.294	0.1781383	6
s.st	32	48	17.573	0.1292842	6

Table A.11. Summarized conditional coverage test NJ, 3 regimes.

	Exceedance		Test		
mod	expected.exceed	actual.exceed	LRstat	pvalue	Accepted.null.hypotheses
s.st	32	45	14.791	0.2530656	6

Table A.12. Summarized conditional coverage test MJ, 2 regimes.

	Exceedance		Test		
mod	expected.exceed	actual.exceed	LRstat	pvalue	Accepted.null.hypotheses
s.ge	32	47	17.109	0.1455429	6
s.no	32	39	9.008	0.7022470	6
s.sg	32	48	16.375	0.1746577	6
s.st	32	50	21.077	0.0492642	6

Table A.13. Summarized conditional coverage test MJ, 3 regimes.

	Exceedance		Test		
mod	expected.exceed	actual.exceed	LRstat	pvalue	Accepted.null.hypotheses
e.ge	32	42	13.981	0.3019232	6
e.no	32	49	15.987	0.1918322	6
e.sg	32	40	13.104	0.3615271	6
e.sn	32	48	13.360	0.3434263	6
e.ss	32	43	17.841	0.1206043	6
e.st	32	43	17.307	0.1384094	6
g.ge	32	34	9.066	0.6972831	6
g.no	32	44	14.939	0.2447893	6
g.sg	32	35	11.673	0.4722858	6
g.sn	32	46	13.272	0.3495845	6
g.ss	32	42	9.878	0.6266628	6
g.st	32	36	12.492	0.4070180	6
s.ge	32	36	11.467	0.4893763	6
s.no	32	45	13.612	0.3261681	6
s.sg	32	40	9.382	0.6700025	6
s.sn	32	46	15.984	0.1919700	6
s.ss	32	40	10.957	0.5326074	6
s.st	32	35	11.583	0.4797231	6

Table A.14. Summarized conditional coverage test SD, 2 regimes.

	Exceedance		Test		
mod	expected.exceed	actual.exceed	LRstat	pvalue	Accepted.null.hypotheses
e.ge	32	46	16.483	0.1701014	6
e.no	32	44	17.051	0.1476889	6
e.sn	32	46	16.286	0.1784851	6
e.st	32	49	20.707	0.0548392	6
g.ge	32	48	17.977	0.1163907	6
g.no	32	40	8.566	0.7394844	6
g.sn	32	51	20.146	0.0643740	6
g.ss	32	47	14.237	0.2858307	6
g.st	32	44	13.052	0.3652725	6
s.ge	32	45	13.612	0.3261681	6
s.no	32	46	15.984	0.1919700	6
s.sg	32	40	11.114	0.5191750	6
s.ss	32	46	12.213	0.4287286	6
s.st	32	44	13.052	0.3652725	6

Table A.15. Summarized conditional coverage test SD, 3 regimes.

	Exceedance		Test		
mod	expected.exceed	actual.exceed	LRstat	pvalue	Accepted.null.hypotheses
e.no	31	36	12.718	0.2398689	5
e.sg	31	32	10.654	0.3851020	5
e.sn	31	34	10.768	0.3758764	5
e.ss	31	34	12.803	0.2348959	5
e.st	31	36	12.549	0.2499916	5
g.ge	31	40	13.024	0.2223330	5
g.no	31	36	14.326	0.1586343	5
g.sg	31	30	14.594	0.1475798	5
g.sn	31	34	14.818	0.1388395	5
g.ss	31	35	11.924	0.2901751	5
g.st	31	33	15.392	0.1184104	5
s.ge	31	36	13.819	0.1814088	5
s.no	31	35	15.496	0.1149977	5
s.sg	31	32	8.676	0.5631034	5
s.sn	31	30	12.516	0.2520049	5
s.ss	31	29	11.457	0.3230384	5
s.st	31	31	13.151	0.2153514	5

Table A.16. Summarized conditional coverage test HS, 2 regimes.

	Exceedance		Test		
mod	expected.exceed	actual.exceed	LRstat	pvalue	Accepted.null.hypotheses
e.ge	31	30	15.077	0.1292797	5
e.sg	31	41	14.107	0.1681667	5
e.sn	31	32	12.946	0.2267067	5
e.ss	31	31	13.305	0.2071153	5
g.ge	31	28	11.256	0.3379242	5
g.sg	31	33	12.549	0.2499916	5
g.ss	31	27	10.494	0.3982722	5
g.st	31	31	16.151	0.0953907	5
s.no	31	37	13.593	0.1923784	5
s.sg	31	36	13.323	0.2061690	5
s.sn	31	28	7.435	0.6838384	5
s.ss	31	31	7.989	0.6299115	5
s.st	31	31	13.151	0.2153514	5

Table A.17. Summarized conditional coverage test HS, 3 regimes.

	Exceedance		Test		
mod	expected.exceed	actual.exceed	LRstat	pvalue	Accepted.null.hypotheses
e.sg	32	39	10.018	0.6143815	6
e.st	32	41	14.568	0.2659152	6
g.sg	32	46	12.586	0.3998356	6
g.ss	32	46	14.611	0.2634019	6
g.st	32	45	14.200	0.2881194	6
s.sg	32	45	12.591	0.3994555	6
s.ss	32	45	11.416	0.4936434	6
s.st	32	45	14.200	0.2881194	6

Table A.18. Summarized conditional coverage test RS, 2 regimes.

	Exceedance		Test		
mod	expected.exceed	actual.exceed	LRstat	pvalue	Accepted.null.hypotheses
e.sg	32	44	14.504	0.2696873	6
g.ge	32	43	13.309	0.3469870	6
g.sg	32	37	10.945	0.5336380	6
g.sn	32	44	13.734	0.3180162	6
g.st	32	46	14.859	0.2492381	6
s.ge	32	46	12.178	0.4314923	6
s.sg	32	46	12.178	0.4314923	6
s.sn	32	37	9.749	0.6379701	6
s.ss	32	47	14.842	0.2501910	6
s.st	32	46	14.859	0.2492381	6

Table A.19. Summarized conditional coverage test RS, 3 regimes.

Table A.10 to A.19 shows the exceedance test results for region NJ, MJ, SD, HS and RS for two and three regimes, respectively. Each table shows the scc test results with different GARCH specifications combined with different distributions.
It is seen in table A.10, that an eGARCH model with skewed normal distribution provides the best results with highest p-value around 0.93 and the lowest Likelihood ratio statistic around 5.79. Table A.11 shows that, the gjrGARCH model has the highest p-value around 0.92 and with the lowest likelihood ratio statistic around 5.96.
Looking at table A.12, the standard GARCH model with Student's t-distribution is the only model that fail to reject the H_0 hypothesis hence it is the best result, and in the case with 3 regimes, table A.13 shows that the standard GARCH with normal distribution provide the highest p-value of 0.7.
From table A.14, the gjrGARCH with generalized error distribution provides the best results with a p-value around 0.7 and with only two observations more in the actual exceed when compared to the expected. In table A.15, the gjrGARCH with normal distributed errors seems to be the best model for 3 regimes with p-value around 0.74
While looking at table A.16, it shows that there are only 31 observations that are expected to exceed the confidence level, which is because there is no observations that exceed the upper confidence level at 99%. The standard GARCH model with generalized error distribution produces the best result for the HS index with a p-value about 0.56, and with only one observation more then the expected exceed. As shown in table A.17, the best model with the highest p-value around 0.68 is the standard GARCH model with skewed normal distribution, and with seven exceeding points more then the expected exceedance.
In table A.18, the eGARCH with skewed generalized error distribution is the best model with a p-value of 0.61 and with Likelihood ration statistic at almost 10, there are seven observations more in the actual exceedance then the expected. In table A.19, standard GARCH with skewed normal distribution is the best model and give the highest p-value around 0.64 and lowest likelihood ratio statics around 9.75.

	Estimate	Std..Error	t_value	p.value
rho	− 0.00958	0.00292	− 3.27653	0.00105
SqrMeter.per.citizen.urban.areas	− 0.000003	0.000001	− 5.37433	0.0000001
lag.lag.log.Relative.growth.rate	0.78675	0.01069	73.58841	0
Vaccinated.pct	− 0.03501	0.00553	− 6.33271	0
Service.concentration.pct	0.00814	0.00212	3.84088	0.00012
Gini.index	− 0.000003	0.00004	− 0.08475	0.93246
Children.institutionalized.pct	0.04252	0.00790	5.38374	0.0000001
Stringency.index.I.Service.concentration.pct	− 0.00072	0.00010	− 6.83651	0
Stringency.index.I.Children.institutionalized.pct	− 0.00340	0.00043	− 7.84218	0

Table A.20. Spatial time fixed effects regression.